A duality construction for interacting quantum Hall systems

by

Johannes Nicolaas Kriel

Dissertation presented for the degree of Doctor of Philosophy in the Faculty of Science at Stellenbosch University

Promoter: Prof. Frederik G. Scholtz

Co-promoter: Prof. Hendrik B. Geyer

March 2011

DECLARATION

By submitting this dissertation electronically, I declare that the entirety of the work contained therein is my own, original work, that I am the sole author thereof (save to the extent explicitly otherwise stated), that reproduction and publication thereof by Stellenbosch University will not infringe any third party rights and that I have not previously in its entirety or in part submitted it for obtaining any qualification.

Date: March 2011

Copyright © 2011 Stellenbosch University
All rights reserved

ABSTRACT

The fractional quantum Hall effect represents a true many-body phenomenon in which the collective behaviour of interacting electrons plays a central role. In contrast to its integral counterpart, the appearance of a mobility gap in the fractional quantum Hall regime is due entirely to the Coulomb interaction and is not the result of a perturbed single particle gap. The bulk of our theoretical understanding of the underlying many-body problem is based on Laughlin's ansatz wave function and the composite fermion picture proposed by Jain. In the latter the fractional quantum Hall effect of interacting electrons is formulated as the *integral* quantum Hall effect of weakly interacting quasiparticles called composite fermions. The composite fermion picture provides a qualitative description of the interacting system's low-energy spectrum and leads to a generalisation of Laughlin's wave functions for the electron ground state. These predictions have been verified through extensive numerical tests.

In this work we present an alternative formulation of the composite fermion picture within a more rigorous mathematical framework. Our goal is to establish the relation between the strongly interacting electron problem and its dual description in terms of weakly interacting quasiparticles on the level of the microscopic Hamiltonian itself. This allows us to derive an analytic expression for the interaction induced excitation gap which agrees very well with existing numerical results. We also formulate a mapping between the states of the free particle and interacting descriptions in which the characteristic Jastrow-Slater structure of the composite fermion ansatz appears naturally. Our formalism also serves to clarify several aspects of the standard heuristic construction, particularly with regard to the emergence of the effective magnetic field and the role of higher Landau levels. We also resolve a long standing issue regarding the overlap of unprojected composite fermion trial wave functions with the lowest Landau level of the free particle Hamiltonian.

OPSOMMING

Die fraksionele kwantum Hall-effek is 'n veeldeeltjie verskynsel waarin die kollektiewe gedrag van wisselwerkende elektrone 'n sentrale rol speel. In teenstelling met die heeltallige kwantum Hall-effek is die ontstaan van 'n energie gaping in die fraksionele geval nie 'n enkeldeeltjie effek nie, maar kan uitsluitlik aan die Coulomb wisselwerking toegeskryf word. Die teoretiese raamwerk waarbinne hierdie veeldeeltjie probleem verstaan word is grootliks gebaseer op Laughlin se proefgolffunksie en die komposiete-fermion beeld van Jain. In laasgenoemde word die fraksionele kwantum Hall-effek van wisselwerkende elektrone geformuleer as die *heeltallige* kwantum Hall-effek van swak-wisselwerkende kwasi-deeljies wat as komposiete-fermione bekend staan. Hierdie beeld lewer 'n kwalitatiewe beskrywing van die wisselwerkende sisteem se lae-energie spektrum en lei tot 'n veralgemening van Laughlin se golffunksies vir die elektron grondtoestand. Hierdie voorspellings is deur verskeie numeriese studies geverifieer.

In hierdie tesis ontwikkel ons 'n alternatiewe formulering van die komposiete-fermion beeld binne 'n strenger wiskundige raamwerk. Ons doel is om die verband tussen die sterk-wisselwerkende elektron sisteem en sy duale beskrywing in terme van swak-wisselwerkende kwasi-deeltjies op die vlak van die mikroskopiese Hamilton-operator self te realiseer. Hierdie konstruksie lei tot 'n analitiese uitdrukking vir die opwekkingsenergie wat baie goed met bestaande numeriese resultate ooreenstem. Ons identifiseer ook 'n afbeelding tussen die vrye-deeltjie en wisselwerkende toestande waarbinne die Jastrow-Slater struktuur van die komposiete-fermion proefgolffunksies op 'n natuurlike wyse na vore kom. Verder werp ons formalisme nuwe lig op kwessies binne die standaard heuristiese konstruksie, veral met betrekking tot die oorsprong van die effektiewe magneetveld en die rol van hoër effektiewe Landau vlakke. Ons lewer ook uitspraak oor die vraagstuk van die oorvleueling van ongeprojekteerde komposiete-fermion golffunksies met die laagste Landau vlak van die vrye-deeltjie Landau probleem.

CONTENTS

LIST OF FIGURES

LIST OF TABLES

CHAPTER 1
Introduction

1.1 The quantum Hall effects

The Hall effects deal with the conductivity properties of two dimensional electron systems subjected to a strong perpendicular magnetic field. In the classical Hall regime [1] the transverse and diagonal resistivities are of the form

$$\rho_{xy} = \frac{-B}{ecn_e} = \frac{h}{\nu e^2} \qquad \text{and} \qquad \rho_{xx} = \frac{m_e}{e^2 \tau n_e} \tag{1.1}$$

where B is the magnetic field strength, n_e the electron density and τ the scattering relaxation time of the electrons. The electron charge is $e < 0$. The filling fraction $\nu \equiv hcn_e/(|e|B)$ serves as a dimensionless measure of the particle density. Classically the transverse (or Hall) resistivity ρ_{xy} therefore increases linearly with B while the diagonal resistivity ρ_{xx} remains constant. These results follow from classical electrodynamics and the Drude conductivity model [2].

In 1980 von Klitzing et al. [3] first observed the integral quantum Hall effect (IQHE) in measurements of the resistivity tensor of a Si-MOSFET system in a strong magnetic field. The Hall resistivity ρ_{xy} was found to exhibit plateaus where it remains constant for a range of magnetic field strengths. At such a plateau the Hall resistivity is extremely accurately quantised to a value of h/ne^2 with n an integer. Comparing this result with the expression for ρ_{xy} in (1.1) suggests that, as far as the Hall resistivity is concerned, the filling fraction ν is effectively pinned at integral values even for a finite range of field strengths. Furthermore, within the plateau regions the diagonal resistivity is found to vanish, suggesting a dissipationless flow of current. The starting point for the theory of the IQHE is the quantum mechanical treatment of a free electron's motion in a magnetic field. This analysis reveals that the electron's kinetic energy is quantised into discrete degenerate Landau levels [4]. It is the energy gap that separates these levels which is ultimately responsible for the vanishing diagonal resistivity. However, explaining the appearance of the plateaus and the extremely accurate quantisation observed in ρ_{xy} requires further insights regarding the interplay between the localised and delocalised states which result from a disorder potential as well as the role of edge state transport.

The Coulomb interaction, which is negligible compared to the disorder potential in the IQHE, plays a central role in the fractional quantum Hall effect (FQHE) which was discovered

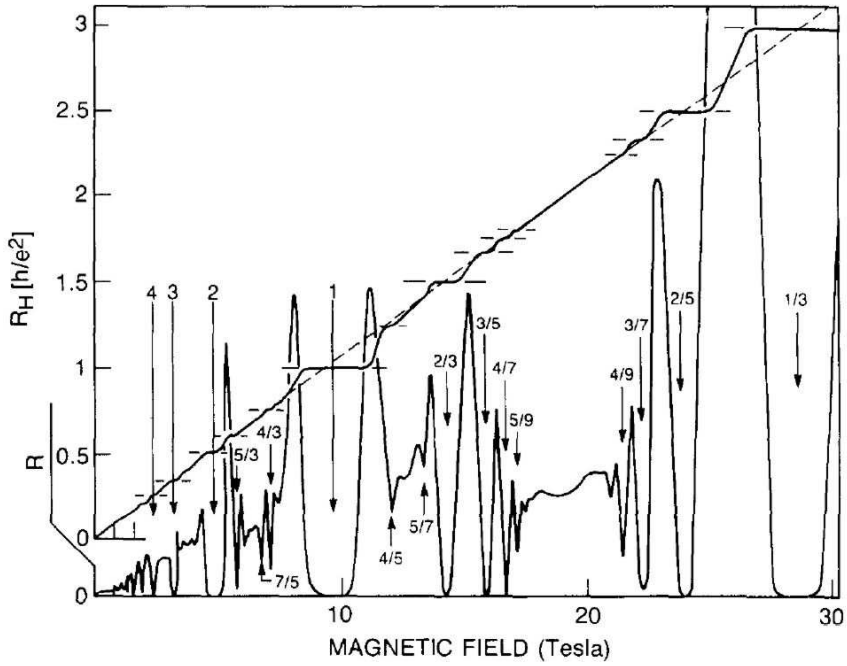

Figure 1.1: The Hall resistance $R_H = \rho_{xy}$ and diagonal resistance $R = \rho_{xx}$ as functions of the magnetic field strength. The filling fractions at which R_H exhibits plateaus and R vanishes are indicated. This figure has been reproduced from [5].

in 1982 by Tsui et al. [6]. They observed further plateaus in ρ_{xy} at fractional values of the filling fraction ν in samples with very weak disorder. As in the integral case the diagonal resistivity was found to vanish in the plateau regions. This is again the result of a mobility gap in the bulk excitation spectrum of the system. The existence of such a gap is therefore common to both the integral and fractional effects but its origin is very different in the two cases. In the IQHE the gap is of a single particle nature and results from the quantisation of the electron's kinetic energy into discrete Landau levels which are separated by the cyclotron energy. In the FQHE regime the electrons are largely confined to the partially filled lowest Landau level. The cyclotron energy which characterises the single particle spectrum now no longer plays a role, and the gap must be due to the interparticle Coulomb interaction. It is with this aspect of the FQHE that our interest lies and which is the focus of what follows. A broader overview of the field can be found in [2, 7, 8, 9] and in the textbooks [10, 11, 12].

1.2 The Landau problem: free particle motion in a magnetic field

We begin with a brief account of the standard quantum mechanical treatment of a free electron in a uniform magnetic field [4]. A detailed derivation using a different formalism appears in the next chapter.

Consider a spinless electron with mass m_e and charge $e < 0$ moving freely in the $x-y$ plane in the presence of a perpendicular magnetic field $\mathbf{B} = B\hat{\mathbf{z}}$ with $B > 0$. The Hamiltonian reads

$$\hat{H}_L = \frac{1}{2m_e}\left(\mathbf{p} - \frac{e}{c}\mathbf{A}\right)^2 \tag{1.2}$$

where $\mathbf{A} = (B/2)\hat{\mathbf{z}}\times\mathbf{r}$ is the magnetic vector potential in the symmetric gauge. The eigenstates of $\hat{H}_L$ are labelled by the integers $n \geq 0$ and $m \geq -n$ which together determine the state's energy and angular momentum[1] as $E_n = \hbar\omega_c(n + 1/2)$ and $L_z \equiv m$. Here $\hbar\omega_c$ is the cyclotron energy and $\omega_c = |e|B/m_e c$ the cyclotron frequency. Since the energy only depends on the n label the spectrum of $\hat{H}_L$ consists of degenerate Landau levels separated by a gap of $\hbar\omega_c$ as shown in Figure 1.2 (a). The unnormalised eigenstates are given by

$$\Psi_{n,m}(z,\bar{z}) = (\bar{z}/2 - 2\partial_z)^n (z/2 - 2\partial_{\bar{z}})^{m+n} e^{-z\bar{z}/4} \tag{1.3}$$

where $z = (x-iy)/\ell$ and $\bar{z} = (x+iy)/\ell$ are dimensionless complex coordinates and $\ell = \sqrt{\hbar c/|e|B}$ is the magnetic length. Note that each eigenstate is the product of an exponential factor $e^{-z\bar{z}/4}$ and a polynomial in z and $\bar{z}$ *of which the degree in* $\bar{z}$ *corresponds to the Landau level label* n. The degeneracy of each Landau level is determined by the total magnetic flux Φ penetrating the system. For a flux of $\Phi = M\phi_0$, with $\phi_0 = hc/|e|$ the flux quantum, each level is then M-fold degenerate. In a system containing N particles the filling fraction $\nu \equiv N/M$ corresponds to the number of filled Landau levels, although this may be a fractional quantity. The filling fraction therefore serves as a dimensionless measure of the particle density. For a N particle system with a uniform bulk density of $\bar{\rho}$ it holds that $\nu = 2\pi\ell^2\bar{\rho}$.

The lowest Landau level (LLL) state with $L_z = m$ has the form

$$\Psi_{0,m}(z) = \frac{1}{\sqrt{2\pi 2^m m!}\ell} z^m e^{-z\bar{z}/4} \tag{1.4}$$

and is localised at a radius of approximately $\sqrt{2m}\ell$ about the origin. The radial profile of $|\Psi_{0,m}(z)|^2$ for a range of m values is shown in Figure 2.2 (a). A general N particle LLL state has the form

$$\Psi(z_1,\ldots,z_N) = \phi(z_1,\ldots,z_N)e^{-\sum_i z_i\bar{z}_i/4} \tag{1.5}$$

[1]Starting from the definition $\hat{L}_z = \hat{\mathbf{z}}\cdot(\mathbf{r}\times\mathbf{p})$ the angular momentum turns out to be $-m\hbar$. Dropping the minus sign and working in units of $\hbar$ provides a convenient labelling scheme without leading to any complications. Alternatively, one could eliminate the minus sign by flipping the orientation of the magnetic field.

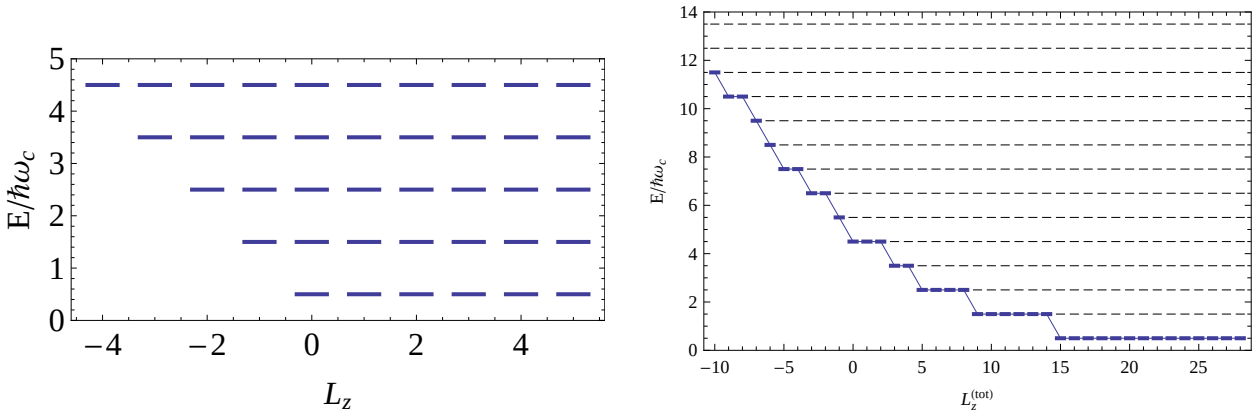

(a) (b)

Figure 1.2: Subsets of the (a) single particle and (b) six particle spectrum of the Landau problem. In (b) the ground states in the various total angular momentum sectors are connected and shown in bold.

where $\phi(z_1, \ldots, z_N) \equiv \phi(\mathbf{z})$ is an antisymmetric polynomial. Note that if $\phi(\mathbf{z})$ is homogeneous in $\mathbf{z} = (z_1, \ldots, z_N)$ with degree d_z then $\Psi(\mathbf{z})$ has a total angular momentum of $L_z^{(\mathrm{tot})} = d_z$.

The spectrum for six free particles appears in Figure 1.2 (b). Let us consider the behaviour of the ground state energy as a function of the total angular momentum $L_z^{(\mathrm{tot})}$. We observe clear jumps, or cusps, in the ground state energy at points where reducing the total angular momentum forces particles into higher Landau levels. For example, at $L_z^{(\mathrm{tot})} = 15$ the LLL single particle states with $m = 0, 1, \ldots, 5$ are occupied and the total angular momentum can only be lowered by moving a particle to the second Landau level. Similarly, at $L_z^{(\mathrm{tot})} = 9$ the $m = 0, 1, \ldots, 4$ states in the LLL are filled, as well as the $m = -1$ in the second LL. Decreasing L_z again requires that a particle be excited to a higher Landau level. These jumps in the ground state energy are also observed in the spectrum of *interacting* system confined to the LLL [13]. This surprising result is one of the main predictions of the composite fermion picture, namely that the low lying spectrum of an interacting system resembles that of the free particle Landau problem. We will also observe this step-like structure in the spectra of operators which at first sight may appear completely unrelated to the Landau problem.

Remark: We will only consider the planar geometry but note that the spherical geometry [14] has also been used extensively to investigate the FQHE. This geometry is particularly convenient for the numerical treatment of finite systems as the lack of boundaries reduce finite size effects and allows for the construction of states with a uniform density. Furthermore, in

this compact geometry each Landau level has a finite degeneracy and the filling of an integer number of levels can therefore be defined unambiguously.

1.3 The interacting problem

Consider a disorder-free two dimensional system of interacting electrons in a perpendicular magnetic field. The Hamiltonian reads

$$\hat{H} = \frac{1}{2m_e}\sum_i \left(\mathbf{p}_i - \frac{e}{c}\mathbf{A}_i\right)^2 + V_{1/r} + g\mu_B B\sum_i S_z^{(i)} \tag{1.6}$$

where the interaction term $V_{1/r}$ has the form

$$V_{1/r} = \sum_{i<j} V(|\mathbf{r}_i - \mathbf{r}_j|) + \sum_i V_{bg}(r_i) + V_{bg-bg} \tag{1.7}$$

with $V(r) = e^2/\epsilon r$. In the presence of a neutralizing background charge the terms $\sum_i V_{bg}(r_i)$ and V_{bg-bg} represent the particle-background and background-background interactions respectively. The final term in (1.6) is the Zeeman interaction.

We follow the standard approach and consider the strong magnetic field limit in which the cyclotron gap $\hbar\omega_c$ and the Zeeman splitting $g\mu_B B$, both of which are linear in B, are assumed to be much greater than the energy scale associated with the Coulomb interaction. In this limit the interaction is too weak to produce spin flips or Landau level mixing. The particles are then completely polarised, which effectively eliminates the spin degree of freedom, and confined to the lowest Landau level. Both the kinetic and Zeeman terms in the Hamiltonian now become trivial constants and we are left with the restriction of the interaction to the LLL which is written as $\mathcal{P}V_{1/r}\mathcal{P}$ where $\mathcal{P}$ is the LLL projection.

Note that the dimensionality of each total angular momentum sector of the LLL is finite, though generally still exponentially large in the number of particles. This fact has spurred a large number of exact numerical studies of finite systems. However, the analytic treatment of the projected interaction $\mathcal{P}V_{1/r}\mathcal{P}$ still poses a formidable technical challenge. At the root of these difficulties is the LLL restriction which eliminates all other competing effects and effectively renders the interaction infinitely strong. The projected interaction therefore represents an inherently non-perturbative problem with *no* sensible weak coupling limit: even setting $V_{1/r}$ to zero does not allow us to identify a suitable LLL basis from which to proceed perturbatively.

1.4 The two-body problem

Valuable insight into the projected interaction can be gained by considering the exactly solvable case of two interacting particles confined to the lowest Landau level. The form of the wave function $\Psi(z_1, z_2)$ is severely restricted by the LLL constraint appearing in (1.5). In fact, for fixed relative and centre of mass angular momenta the state $\Psi(z_1, z_2)$ is uniquely determined as

$$\Psi(z_1, z_2) = (z_1 - z_2)^n (z_1 + z_2)^m e^{-z_1\bar{z}_1/4 - z_2\bar{z}_2/4} \tag{1.8}$$

where n is an odd integer. The average separation of the particles is approximately $\sqrt{2n}\ell$ while $|\Psi(z_1, z_2)|^2$ (and the two particle distribution function) vanishes like $|z_1 - z_2|^{2n}$ when z_1 approaches z_2. Larger relative angular momentum therefore results in stronger interparticle correlations and a reduction of the interaction energy. Since $\Psi(z_1, z_2)$ is the *only* two particle state with relative and centre of mass angular momenta n and m it is automatically an exact eigenstate of $\mathcal{P}V(|\mathbf{r}_1 - \mathbf{r}_2|)\mathcal{P}$. The corresponding eigenvalue V_n is a decreasing function of n for any repulsive interaction $V(r)$. These eigenvalues constitute the so-called pseudopotentials of $V(r)$ and are of fundamental importance as they provide a complete characterisation of the interaction within the LLL even for $N > 2$. We return to this point in Section 2.5.4.

This approach of diagonalizing a two-body interaction by constructing eigenstates of the relative angular momentum cannot be extended beyond $N = 2$ since the various relative angular momenta do not commute. However, the two-body case does suggest the following important guiding principle when dealing with strongly repulsive short-range interactions: It is generally energetically favourable for the system to minimise the average occupation of the lowest ($n = 1$) relative angular momentum orbit. This implies that the low energy wave functions should exhibit, in each coordinate z_i, the maximum allowed number of zeros at the other $N-1$ particle coordinates $z_{j\neq i}$. Such a state will be very effective at keeping particles well separated and minimizing the energy of a strongly repulsive interaction. In the next section we will see how these considerations lead to the identification of Laughlin's quantum liquid states as natural candidates for the ground state at the filling fractions $\nu = 1/3, 1/5, 1/7$.

1.5 Laughlin's state

The Slater determinant obtained by filling the LLL single particle states with angular momenta $m = 0, 1, 2, \ldots, N-1$ is given by[2]

$$\Psi_{\nu=1}(\mathbf{z}) = \prod_{i<j}(z_i - z_j)e^{-\sum_i z_i\bar{z}_i/4} \tag{1.9}$$

and has a filling fraction of $\nu = 1$. In each coordinate z_i this wave function exhibits first order zeroes at the other $N-1$ particle coordinates $z_{j\neq i}$. This is an unavoidable consequence of the antisymmetry of the wave function and therefore represents the weakest correlations permitted by fermion statistics.

In 1983 Laughlin [15] proposed the state

$$\Psi_{1/q}(\mathbf{z}) = \prod_{i<j}(z_i - z_j)^q e^{-\sum_i z_i\bar{z}_i/4} \tag{1.10}$$

as a candidate for the interacting ground state at $\nu = 1/q$ where q is an odd integer. The total angular momentum of this state is $L_z = qN(N-1)/2$. Although $\Psi_{\nu=1}(\mathbf{z})$ and $\Psi_{1/q}(\mathbf{z})$ may appear similar in form the latter represents a very complicated superposition of Slater determinants and exhibits strong interparticle correlations. In fact, $\Psi_{1/q}(\mathbf{z})$ is the *only* state with $L_z \leq qN(N-1)/2$ for which the relative angular momentum of any two particles is at least q. This implies that $\Psi_{1/q}(\mathbf{z})$ is the unique ground state of a model hardcore interaction for which only the pseudopotentials V_n with $n < q$ are non-zero. Any increase in the system's bulk density will therefore involve a finite energy cost due to the non-zero occupation of relative angular momentum orbitals below q. This is essentially the argument for why $\Psi_{1/q}(\mathbf{z})$ represents an incompressible state with gapped excitations.

We have not yet motivated the assertion that $\Psi_{1/q}(\mathbf{z})$ corresponds to a filling of $\nu = 1/q$. A simple argument follows from the observation that the highest occupied single particle state in $\Psi_{1/q}(\mathbf{z})$ is $m = q(N-1)$ which is localised on a radius of approximately $\sqrt{2qN}\ell$. This suggests an average particle density of $\bar{\rho} = 1/(2\pi\ell^2 q)$ and a filling fraction of $\nu = 2\pi\ell^2\bar{\rho} = 1/q$ at large N. To prove that the density is uniform within the bulk requires a more careful argument based on Laughlin's plasma analogy [15]. Finite size numerical studies [16] has shown that

[2] **Proof:** By antisymmetry $\Psi_{\nu=1}(\mathbf{z})$ must contain $J \equiv \prod_{i<j}(z_i - z_j)$ as a factor. However, J already contains terms with z_i up to the power of $N-1$ corresponding to the $m = N-1$ single particle state. The polynomial part of $\Psi_{\nu=1}(\mathbf{z})$ therefore cannot contain any other factors involving the $\mathbf{z}$ variables and must equal J up to a constant.

Laughlin's states are extremely accurate approximations to the true interacting ground state at the filling fractions $\nu = 1/3, 1/5, 1/7$. It is believed that at densities below $\nu = 1/7$ the true ground state is a Wigner Crystal for which $\Psi_{1/q}(\mathbf{z})$ does not provide a good approximation. The estimated density at which this liquid to crystal transition occurs has undergone several refinements in the light of new theoretical and experiment results. See [12] for an overview of these studies.

Laughlin also demonstrated that his states exhibit fractionally charged excitations, the so-called quasiparticles and quasiholes. These are crucial to understanding the origin of the fractionally quantised Hall conductivity. Since these excitations are automatically incorporated in the composite fermion picture we will not go into further detail here.

1.6 The Composite fermion model

1.6.1 Introduction

Laughlin's theory explains the FQHE at filling fractions of the form $\nu = 1/m$ with m an odd integer. However, the FQHE is also observed at numerous other odd-denominator filling fractions belonging to the sequence $\nu = n/(2pn + 1)$ with p and n integers. In 1989 Jain [17] proposed a framework in which the FQHE could be understood as an IQHE of weakly interacting quasiparticles named composite fermions. The basis of this framework is the mapping of the interacting electron system at $\nu = n/(2pn + 1)$ onto a system of weakly interacting composite fermions at an *integral* filling fraction $\nu^* = n$. An introductory overview which emphasises this analogy between the fractional and integral Hall effects appears in [18]. This section summarizes Jain's recent account [11] of this construction.

1.6.2 Definitions

We start by introducing the notion of a vortex in the context of a complex-valued wave function. Let z_0 be a point in the plane and z_i an arbitrary particle coordinate. A wave function $\Psi(\mathbf{z}, \bar{\mathbf{z}})$ is then said to exhibit a vortex of order n at the point z_0 if transporting z_i around z_0 results in $\Psi(\mathbf{z}, \bar{\mathbf{z}})$ undergoing a phase change of $2\pi n$. Two obvious ways in which such a vortex can be realised in $\Psi(\mathbf{z}, \bar{\mathbf{z}})$ are through a factor of $(z_0 - z_i)^n$ or $(z_0 - z_i)^n/|z_0 - z_i|^n$. Note that although these two factors share the same phase structure they produce very different types of correlations in the wave function. A composite fermion is now defined as *the bound state of an electron with an even number of quantised vortices*. The fundamental postulate of the composite fermion model is that the repulsive interparticle interaction is responsible for

the formation of the composite fermions which are themselves only weakly interacting.

1.6.3 Heuristic construction

The following steps provide a heuristic mean-field argument which relates the FQHE of electrons to the IQHE of composite fermions.

Step 1: Consider a system of non-interacting electrons in a uniform magnetic field $B^*\hat{\mathbf{z}}$ with Hamiltonian

$$\hat{H}_L^{(*)} = \frac{1}{2m_e}\sum_i \left(\mathbf{p}_i - \frac{e}{c}\mathbf{A}_i^*\right)^2 \tag{1.11}$$

where $\mathbf{A}_i^* = (B^*/2)\hat{\mathbf{z}} \times \mathbf{r}_i$. At an *integral* filling $\nu^* = n$ the system's ground state $\Phi_n(B^*)$ is non-degenerate and corresponds to completely filling the lowest n Landau levels. A finite gap of $\hbar\omega_c^*$ separates this ground state from the lowest band of excited states obtained through particle-hole excitations. The system is therefore incompressible and should exhibit the IQHE.

Step 2: Next a singular flux tube carrying $2p$ flux quanta is attached to each electron. The magnetic field

$$\mathcal{B}(\mathbf{r}) = 2p\phi_0 \sum_i \delta(\mathbf{r} - \mathbf{r}_i) \tag{1.12}$$

associated with these attachments is generated by the magnetic vector potential [19]

$$\boldsymbol{\mathcal{A}}_i = \hat{\mathbf{z}} \times \frac{2p\phi_0}{2\pi}\sum_{j\neq i}\frac{\mathbf{r}_i - \mathbf{r}_j}{|\mathbf{r}_i - \mathbf{r}_j|^2}. \tag{1.13}$$

The Hamiltonian now reads

$$\hat{H}_{MF} = \frac{1}{2m_e}\sum_i \left(\mathbf{p}_i - \frac{e}{c}\mathbf{A}_i^* - \frac{e}{c}\boldsymbol{\mathcal{A}}_i\right)^2. \tag{1.14}$$

For integer values of p these flux attachments can be expressed as the result of a singular unitary gauge transformation that preserves the fermion statistics of the electrons. $\hat{H}_{MF}$ and $\hat{H}_L^{(*)}$ are then related by

$$\hat{H}_{MF} = U^{2p}\hat{H}_L^{(*)}U^{-2p} \tag{1.15}$$

where

$$U = \prod_{i<j}\frac{z_i - z_j}{|z_i - z_j|}. \tag{1.16}$$

At this stage $\hat{H}_{MF}$ and $\hat{H}_L^{(*)}$ still represent unitarily equivalent free particle problems. The

ground state of $\hat{H}_{MF}$ is therefore

$$\Psi^{MF} = U^{2p}\Phi_n(B^*) = \prod_{i<j}\left(\frac{z_i - z_j}{|z_i - z_j|}\right)^{2p}\Phi_n(B^*) \tag{1.17}$$

where the flux attachments have generated $2p$ quantised vortices at each particle coordinate. This corresponds to one possible realisation of composite fermions. *However, the phase factor U^{2p} containing the vortices does not introduce any interparticle correlations that were not present in the Slater determinant $\Phi_n(B^*)$ originally.* It is for this reason that Ψ^{MF} is said to represent a mean-field approximation to the "true" composite fermion wave functions which will be introduced later. The latter exhibits the same phase structure as Ψ^{MF} but is much more strongly correlated.

Step 3: In the final step the $2p$ flux quanta attached to each electron are "smeared out" adiabatically until they become part of the uniform external field. Assuming a uniform particle density of $\bar{\rho}$ this would result in the external magnetic field increasing in magnitude from B^* to $B = B^* + 2p\phi_0\bar{\rho}$ while the filling fraction is reduced from $\nu^* = n$ to $\nu = n/(2pn+1)$.[3] The crucial assumption is that the *qualitative* features of $\hat{H}_{MF}$'s (and $\hat{H}_L^{(*)}$'s) low energy spectrum are preserved during this adiabatic process. In particular, it is assumed that the excitation gap survives and evolves from $\hbar\omega_c^*$ to Δ, the gap due solely to the interaction. This relates the incompressibility of the FQHE state at $\nu = n/(2pn+1)$ to that of a system of composite fermions filling an integer number of effective Landau levels.[4]

These steps do not amount to a rigorous derivation of composite fermions but only provides a heuristic motivation for the correspondence between the FQHE of electrons and the IQHE of composite fermions. This construction also does not yield the electron ground state directly since keeping track of its evolution during the adiabatic smearing process is not possible. The mean-field composite fermion wave function Ψ^{MF} must therefore be modified "by hand" to produce an approximation to the interacting ground state which is consistent with our physical intuition.

[3] This follows from the relation $\nu B = \nu^* B^* = \phi_0\bar{\rho}$.

[4] At fillings in the sequence $\nu = n/(2pn-1)$ the composite fermions would fill n Landau levels in a *negative* effective magnetic field. The rest of the construction remains unchanged.

1.6.4 Composite fermion wave functions

The wave function Ψ^{MF} exhibits a number of properties that make it an unsuitable candidate for the ground state of the projected interaction. As mentioned the mean-field state Ψ^{MF} is no more strongly correlated than the Slater determinant $\Phi_n(B^*)$ itself. In particular, it lacks the large number of zeros we expect to observe at the various particle coordinates which help minimize the interaction energy. Furthermore, Ψ^{MF} does not reduce to Laughlin's state at $\nu = 1/q$. Instead we obtain

$$\Psi^{MF}_{1/q} = \prod_{i<j} \left(\frac{z_i - z_j}{|z_i - z_j|} \right)^{2p} \prod_{i<j} (z_i - z_j) e^{-\sum_i r_i^2/4\ell^{*2}} \tag{1.18}$$

which has the correct phase structure but lacks the strong interparticle correlations. Finally, Ψ^{MF} generally has a large component in the higher Landau levels of the *original* $\hat{H}_L$ Landau problem. This is due to the factors of $|z_i - z_j|^2 = (z_i - z_j)(\bar{z}_i - \bar{z}_j)$ appearing in the denominator and the fact that the exponential factor contains the magnetic length associated with the *weakened* B^* field. This is clearly not compatible with the strong magnetic field limit.

Surprisingly, most of these issues can be resolved by simply dropping the $\prod_{i<j} |z_i - z_j|^{2p}$ factor appearing in the denominator of Ψ^{MF} and evaluating the Slater determinant Φ_n at a magnetic field strength of B *but still at a filling of* $\nu^* = n$. Both these modifications are necessary to ensure that the size of the system, and the filling fraction ν, remains unchanged. This can be seen by noting that the increase in the system size brought about by dropping $\prod_{i<j} |z_i - z_j|^{2p}$ is exactly cancelled by replacing ℓ^* with ℓ in the exponential. The approximation to the interacting electron ground state now reads

$$\Psi^{\text{unproj}}_{\nu} = \prod_{i<j} (z_i - z_j)^{2p} \Phi_n(B) \tag{1.19}$$

where $\nu = n/(2pn+1)$ and $\Phi_n(B)$ is the Slater determinant of n filled Landau levels evaluated at a magnetic field strength of B. The so-called Jastrow factor $\prod_{i<j}(z_i - z_j)^{2p}$ is responsible for the favourable correlations which help to minimize the interaction energy. For $\nu = 1/(2p+1) = 1/q$ we have $\nu^* = n = 1$ and $\Phi_{\nu^*=1}(B^*)$ therefore corresponds to filling the lowest composite fermion Landau level (CFLL). This implies that $\Phi_{\nu^*=1}(B)$ is precisely the state in (1.9) and so $\Psi^{\text{unproj}}_{1/q}$ indeed reduces to Laughlin's state.

Finally we note that when higher CFLLs in $\Phi_n(B)$ are occupied the polynomial part of $\Psi^{\text{unproj}}_{\nu}$ will still contain $\bar{\mathbf{z}}$ coordinates and therefore some amount of Landau level mixing

remains.[5] This necessitates a projection onto the LLL:

$$\Psi_\nu = \mathcal{P}\prod_{i<j}(z_i - z_j)^{2p}\Phi_n(B). \tag{1.20}$$

An early criticism of this approach was that, prior to projection, Ψ_ν^{unproj} may contain a large component in the higher Landau levels. If this is the case the projection procedure might alter the state to such an extent that the beneficial correlations provided by the Jastrow factor are destroyed. Two measures of the amount of Landau level mixing present in Ψ_ν^{unproj} have been investigated. One is simply the state's average kinetic energy per particle with respect to $\hat{H}_L$. Numerical calculations [20] for $\nu = 1/3, 2/5, 3/7, 4/9$ found the kinetic energy per particle to be in the region of $0.05\hbar\omega_c$ above the ground state. This suggests that the majority of particles are indeed in the LLL. An alternative measure is the overlap of Ψ_ν^{unproj} with the LLL in the inner product sense. Jain [17] provided a heuristic single particle argument for why this overlap is likely to be close to unity. However, the formalism we introduce in the next chapter will allow us to prove that this is in fact *not* the case and that the overlap of Ψ_ν^{unproj} with the LLL may be quite poor. We return to this issue in Section 2.4.

1.6.5 Excitations

The composite fermion model suggests that the incompressible ground state of an interacting electron system can be understood as the non-interacting ground state of free composite fermions filling an integer number of effective Landau levels. A natural extension of this correspondence is to associate the collective excitations of the electron system with the elementary single particle excitations of the free composite fermions. Let $\Phi_n(B^*)$ denote the Slater determinant obtained by filling the lowest n composite fermion Landau levels. Adding a particle to the lowest empty level then produces the state $\Phi_n^{qp}(B^*)$ which is mapped onto the quasiparticle electron state $\Psi_\nu^{qp} = \mathcal{P}\prod_{i<j}(z_i - z_j)^{2p}\Phi_n^{qp}(B)$. Similarly, removing a particle from the top Landau level in $\Phi_n(B^*)$ results in a quasi-hole excitation while a particle-hole excitation in $\Phi_n(B^*)$ generates a so-called composite fermion exciton in the corresponding electron state. These excitations have been studied extensively and shown to either match or closely resemble the quasiparticle and quasihole states proposed by Laughlin. Where differences do occur the composite fermion states provide a better match to the exact results [21]. See [22] for an overview of the wide variety of excitations that follow from the composite fermion picture.

[5] Note that this does *not* describe Landau level mixing in the context of the full Hamiltonian in (1.6). The occupation of higher Landau levels in (1.19) is an artefact of the construction which, up till now, has not enforced the LLL constraint. Extensions of the composite fermion framework to include LL mixing has been investigated. See [11] and the references therein.

For our purposes it is sufficient to have an intuitive understanding of why single particle excitations of composite fermions lead to higher interaction energies for the electron states. Let $\Phi_n^{ex}(B^*)$ denote the Slater determinant obtained from $\Phi_n(B^*)$ through a particle-hole excitation. This excitation necessarily increases the powers of the $\bar{\mathbf{z}}$ variables in the polynomial part of $\Phi_n^{ex}(B^*)$ which result in anti-vortices when two particles have negative relative angular momentum. When the product of $\Phi_n^{ex}(B)$ and $\prod_{i<j}(z_i - z_j)^{2p}$ is projected onto the LLL the anti-vortices and vortices cancel through the fact that $\mathcal{P}(z_i - z_j)^n(\bar{z}_i - \bar{z}_j)^m \propto (z_i - z_j)^{n-m}$. Excitations in $\Phi_n^{ex}(B^*)$ therefore lead to a reduced number of zeros at the particle coordinates in Ψ_ν^{ex}. This results in weaker interparticle correlations and an increased interaction energy.

1.6.6 Comments

The Jastrow factor appearing in Ψ_ν generates strong short-range correlations which are very effective at keeping particles well separated. This suggests a certain measure of universality: the wave function Ψ_ν should provide an accurate approximation to the ground state of *any* projected interaction which is strongly repulsive at short distances. For such interactions the composite fermion model also predicts the existence of an excitation gap at certain filling fractions but provides no direct estimate of its value. In fact, there is a fundamental mismatch between the energy scales governing the cyclotron gap $\hbar\omega_c^*$ of the free composite fermion system and the interaction induced gap Δ. This is seen by noting that the cyclotron gap $\hbar\omega_c^*$ is linear in B and inversely proportional to the electron mass m_e. In contrast, the energy scale of the Coulomb interaction is $e^2/\epsilon\ell$ which scales like $\sim \sqrt{B}$ and is independent of the electron mass. These two energy scales not only depend on different physical parameters but also become infinitely separated in the strong magnetic field limit. This remains the case for non-Coulombic model Hamiltonians since we always have the freedom to change the coupling constant of the interaction independently of the magnetic field strength. This observation highlights the pitfalls of interpreting the free composite fermion picture too literally. The only claim is that the low-energy spectra of $\mathcal{P}V_{1/r}\mathcal{P}$ and $\hat{H}_L^{(*)}$ share the same qualitative features, namely a band structure and excitation gap at particular filling fractions.

The composite fermion model does provide a means of calculating the excitation gap numerically by using Ψ_ν and its various excitations as trial wave functions. A large number of numerical studies have used this approach to produce very accurate estimates of the ground state energies and excitation gaps. We will return to this topic in Section 4.6.

1.7 Questions

There is no doubt that the composite fermion model *works*. It offers a qualitative understanding of the interacting low energy spectrum and provides simple, parameter free expressions for the wave functions of low-lying states. These predictions have been verified through extensive numerical tests. It therefore appears unlikely that any alternative description of the physics underpinning the FQHE will not bear any resemblance to the composite fermion model. Our goal is to provide an alternative formulation of the composite fermion model within a more rigorous mathematical framework. This reformulation should provide new insights into the construction itself and also extend the predictive power of the model. The remainder of this section is dedicated to identifying some of the issues that our formalism will attempt to address.

A heuristic motivation for the assertion that composite fermions experience a weakened magnetic field is that the Berry phases of the bound vortices cancel, in part, the Aharonov-Bohm phase of the uniform external field. Alternatively, if we regard the form of Ψ_ν in (1.19) as a postulate the effective filling fraction ν^* of $\Phi(B)$ can be calculated in terms of ν by keeping track of how the Jastrow factor increases the size of the system. Strangely, the length and energy scales ℓ^* and $\hbar\omega_c^*$ associated with the weakened field appear to play no role at all: we evaluate $\Phi_n(B)$ at the full field strength B and the excitation gap $\Delta \sim e^2/\epsilon\ell$ is seemingly unrelated to $\hbar\omega_c^*$.

Question 1: *Can the origin of the weakened magnetic field and its relation to the wave functions and spectrum be understood at a more fundamental level starting from an interacting Hamiltonian?*

The composite fermion model suggests that there exists a one-to-one correspondence between the low energy states of the free particle and interacting problems. This is clearly true on the level of the *unprojected* states $\Psi_\nu^{\text{unproj}} = \prod_{i<j}(z_i - z_j)^{2p}\Phi_n(B)$ where the Jastrow factor acts as an invertible similarity transformation. However, for a fixed total angular momentum the number of linearly independent LLL states is finite while the same is not true of the free particles states. The one-to-one correspondence therefore cannot hold on the level of the projected states Ψ_ν and there must exist spurious free particle states which have no LLL counterparts. This implies that only a subset of free particle states are physically relevant.

Question 2: *How are the physical free particle states characterised and what are their properties?*

Much has been written regarding the status of the unprojected states $\Psi_\nu^{\rm unproj}$ and their overlap with the LLL. It may appear that the mixing of Landau levels in $\Psi_\nu^{\rm unproj}$ is simply a nuisance which necessitates a further projection step to correct. However, without the additional mathematical structure provided by the $\bar{\mathbf{z}}$ variables the close connection with the single particle picture is lost.

Question 3: *How do we reconcile the need for higher effective Landau levels with the LLL constraint in a way that avoids ad hoc projections or the need to speculate about the overlap of states with the LLL?*

The assumption that underpins the composite fermion model is that it is energetically favourable for the electrons to capture vortices (i.e. zeros) and form weakly interacting composite fermions. This is supported by numerical evidence which proves that the Jastrow-Slater wave function Ψ_ν is very effective at minimizing the interaction energy. Despite this, a derivation of this Jastrow-Slater structure starting from the projected interaction itself is still lacking. The mismatch between the energy scales governing the projected interaction and free particle picture also results in a further conceptual barrier between the composite fermion model and the actual interacting Hamiltonian.

Question 4: *Can the mapping between the interacting and free particle problems be performed on the level of the microscopic Hamiltonian itself? Can such a construction provide analytic approximations to both the wave functions and excitation gaps?*

1.8 Outline of strategy

We conclude this chapter by outlining the construction with which we hope to address these questions. We shall focus exclusively on the polynomial part of the wave functions and treat these as representing the state of the system. The relevant Hilbert spaces are therefore function spaces of polynomials where the exponential factor $\exp[-\sum_i z_i\bar{z}_i/4]$ has been absorbed into the inner product. We consider filling fractions in the range $1/3 \leq \nu < 1/2$.

1.8.1 Preliminaries

The isomorphic spaces Λ and $\mathcal{L}$ **(Section 3.1)**

Our goal is to study the interaction $V_{1/r}$ within the LLL subspace $\mathcal{L}$ of translationally invariant (polynomial) states. Fermion statistics require that any $\psi(\mathbf{z}) \in \mathcal{L}$ be factorizable as $\psi(\mathbf{z}) = \sigma(\mathbf{z})J$ where $J = \prod_{i<j}(z_i - z_j)$ and $\sigma(\mathbf{z})$ is a symmetric polynomial. Applying the unitary transformation $U^{-2} = \bar{J}/J$ to $\psi(\mathbf{z})$ produces $U^{-2}\psi(\mathbf{z}) = \sigma(\mathbf{z})\bar{J}$ and we denote the

space of such states by $\Lambda = U^{-2}\mathcal{L}$. Whereas the elements of $\mathcal{L}$ are holomorphic polynomials in $\mathbf{z}$ alone the states in Λ contain *both* $\mathbf{z}$ and $\bar{\mathbf{z}}$ coordinates. However, the $\bar{\mathbf{z}}$ dependence of these states is severely restricted and occurs only through a factor of $\bar{J}$. This introduction of the $\bar{\mathbf{z}}$ coordinates is a crucial technical step, though no connection with a free particle spectrum is yet apparent.

The $su(1,1)$ representation **(Section 2.2)**

Next we define a representation of the Lie algebra $su(1,1)$ in terms of differential operators acting on the Hilbert space of polynomials states. The corresponding Casimir operator is denoted by $\hat{K}^{(r)}$. We explore the connection between the generators of this algebra and the free particle Landau Hamiltonian and obtain an algebraic reformulation of the LLL projection procedure. This allows us to resolve the long standing issue regarding the LLL overlap of the unprojected Ψ_ν^{unproj} states.

1.8.2 Detour: The projected Casimir operator

The operator $\hat{K}^{(r)}$ in Λ and $\mathcal{I}$ **(Sections 3.1-3.3)**

Next we turn our attention to a seemingly unrelated problem and study the *projected* Casimir operator $\hat{K}^{(r)}_\Lambda \equiv \mathcal{P}_\Lambda \hat{K}^{(r)} \mathcal{P}_\Lambda$. This turns out to be a highly non-trivial problem; on par with the projected interaction itself. The source of these difficulties is the fact that $\hat{K}^{(r)}$ does not leave the space Λ invariant and the spectrum of $\hat{K}^{(r)}_\Lambda$ is therefore not simply a subset of that of $\hat{K}^{(r)}$ itself. As an aid we introduce the space $\mathcal{I}$ of so-called irreducible states which *is* invariant under $\hat{K}^{(r)}$ and is therefore spanned by a subset of $\hat{K}^{(r)}$'s eigenstates. Due to the algebraic properties of these irreducible states any eigenstate of $\hat{K}^{(r)}$ in $\mathcal{I}$ is automatically also an eigenstate of the free particle Landau problem. In fact, the elements of $\mathcal{I}$ have all the properties we require of the physical free particle states. We also show that $\mathcal{I}$ and Λ are isomorphic which guarantees a one-to-one relation between the irreducible states and those of the LLL subspace $\mathcal{L}$.

The spectrum and eigenstates of $\hat{K}^{(r)}_\Lambda$ **(Sections 3.4-3.5)**

We are now confronted with the unsolvable problem $\hat{K}^{(r)}_\Lambda$ and a simpler, solvable problem $\hat{K}^{(r)}_\mathcal{I} \equiv \hat{K}^{(r)}|_\mathcal{I}$ which involves the same operator restricted to different, though isomorphic, subspaces. Our goal is to use the known eigenstates and eigenvalues of $\hat{K}^{(r)}_\mathcal{I} = \hat{K}^{(r)}|_\mathcal{I}$ to obtain approximations for those of $\hat{K}^{(r)}_\Lambda$. We construct a mapping $\mathcal{A}_{\bar{z}}$ from $\mathcal{I}$ to Λ which maps the low-lying eigenstates of $\hat{K}^{(r)}_\mathcal{I}$ onto low-lying states of $\hat{K}^{(r)}_\Lambda$. The result is a basis for Λ of states which resemble the composite fermion states of Jain very closely. Numerical calculations are

used to verify the accuracy of these results. Furthermore, we show that the low energy states in $\mathcal{I}$ that map onto a LLL state with $\nu = n/(2n+1)$ will have a filling fraction of $\nu^* = n$, as is the case in the composite fermion picture.

Next we investigate the spectrum of $\hat{K}_\Lambda^{(r)}$. Motivated by numerical evidence we introduce a conjecture which relates the spectra of $\hat{K}_\Lambda^{(r)}$ and $\hat{K}_\mathcal{I}^{(r)}$. This eventually leads to an analytic expression for the excitation gap for any strongly repulsive short-range interaction.

1.8.3 Relating $\hat{K}_\Lambda^{(r)}$ to the inverse quadratic interaction (Chapter 4)

The preceding study of $\hat{K}_\Lambda^{(r)}$ provides a clear picture of its low-lying spectrum and eigenstates. However, these results are of little use unless a connection between $\hat{K}_\Lambda^{(r)}$ and the projected interaction can be established. We show that $\hat{K}_\Lambda^{(r)}$ is indeed equivalent to an interacting system in the LLL, but one which involves both two- and three-body interactions. A careful analysis shows that the two-body interaction, which has an inverse quadratic form, dominates the low energy physics and that the three-body interaction may be treated as a perturbation. The results obtained for $\hat{K}_\Lambda^{(r)}$ are now directly applicable to the problem of particles in the LLL interacting via a $V(r) \sim 1/r^2$ potential. In particular, we obtain an analytic expression for the excitation gap which compares well with existing numerical results.

1.8.4 Establishing the link with the Coulomb interaction (Section 4.6.3)

Of course, our true interest lies with the Coulomb interaction. The fact that the excitation gap is governed by the short-range behaviour of the interaction suggests a natural analytic ansatz for the excitation gap of any strongly repulsive short-range interaction. The unknown density dependence appearing in this ansatz is fixed by our knowledge of the inverse quadratic interaction which in turn followed from the study of $\hat{K}_\Lambda^{(r)}$. This leads to an analytic expression for the excitation gap of the Coulomb interaction which compares very well with numerical results. For example, at $\nu = 1/3$ we obtain a value of $\Delta = 1/\sqrt{96} \approx 0.10206$ while the best numerical estimate is $\Delta = 0.1012$ [23]. To our knowledge this is the only construction that provides an analytic estimate of the gap without the use of any free parameters.

CHAPTER 2
Mathematical background

This chapter provides an overview of the mathematical formalism on which our construction is based. The investigation will focus on the algebraic properties of the polynomial parts of the wave functions and their relation to the Landau problem and LLL projection. In this spirit we begin by solving the Landau problem a second time, now using the language of differential operators acting on polynomial function spaces.

2.1 The free particle Landau problem

Consider a system of N non-interacting spinless electrons moving in the $x-y$ plane in the presence of a uniform magnetic field $B\hat{z}$ with $B > 0$. The Hamiltonian reads

$$\hat{H}_L = \frac{1}{2m_e} \sum_i \left(\mathbf{p}_i - \frac{e}{c} \mathbf{A}_i \right)^2 \tag{2.1}$$

where $\mathbf{A}_i = (B/2)\hat{\mathbf{z}} \times \mathbf{r}_i$ is the magnetic vector potential in the symmetric gauge. We also define the magnetic length $\ell = \sqrt{(\hbar c)/(|e|B)}$ and cyclotron frequency $\omega_c = (|e|B)/(m_e c)$. The eigenstates of $\hat{H}_L$ are square integrable functions on $\mathbb{R}^2$ of the form

$$\Psi(\mathbf{z}, \bar{\mathbf{z}}) = \phi(\mathbf{z}, \bar{\mathbf{z}}) e^{-\sum_i z_i \bar{z}_i / 4} \tag{2.2}$$

where $\phi(\mathbf{z}, \bar{\mathbf{z}})$ is an antisymmetric polynomial and $(\mathbf{z}, \bar{\mathbf{z}}) \equiv (z_1, \ldots, z_N, \bar{z}_1, \ldots, \bar{z}_N)$ denotes the set of dimensionless complex coordinates $z_j = (x_j - iy_j)/\ell$ and $\bar{z}_j = (x_j + iy_j)/\ell$. The polynomial part $\phi(\mathbf{z}, \bar{\mathbf{z}})$ of the eigenstates may be isolated through a similarity transformation which eliminates the exponential factor. Applying this transformation to the Hamiltonian itself produces the differential operator $\hat{H}_L^{\mathbb{P}}$ which acts directly on $\phi(\mathbf{z}, \bar{\mathbf{z}})$:

$$\begin{aligned}
\hat{H}_L^{\mathbb{P}} = e^{+\sum_i z_i \bar{z}_i / 4} \hat{H}_L e^{-\sum_i z_i \bar{z}_i / 4} &= \frac{1}{2m_e} \sum_j \left(\mathbf{p}_j + \frac{i\hbar}{2\ell^2} \mathbf{r}_j - \frac{e}{c} \mathbf{A}_j \right)^2 && (2.3) \\
&= \frac{\hbar\omega_c}{2} \sum_j \left(-\ell^2 \nabla_j^2 + \mathbf{r}_j \cdot \nabla_j - i\hat{\mathbf{z}} \cdot (\mathbf{r}_j \times \nabla_j) + 1 \right) && (2.4) \\
&= \hbar\omega_c \sum_i \left([\bar{z}_i - 2\partial_{z_i}] \, \partial_{\bar{z}_i} + 1/2 \right). && (2.5)
\end{aligned}$$

Also of interest is the z component of the total angular momentum. The corresponding operator $\hat{L}_z$ is unaffected by this similarity transformation and may be defined, in units of $-\hbar$, as[6]

$$\hat{L}_z \equiv \frac{-1}{\hbar}\sum_i \hat{\mathbf{z}}\cdot(\mathbf{r}_i \times \mathbf{p}_i) = \sum_i (z_i\partial_{z_i} - \bar{z}_i\partial_{\bar{z}_i}). \tag{2.6}$$

Since $\hat{H}_L^{\mathbb{P}}$ and $\hat{L}_z$ commute we can proceed to characterise their simultaneous eigenstates. For this purpose we employ the similarity transformation

$$\hat{S} = \exp\left[-2\sum_i \partial_{z_i}\partial_{\bar{z}_i}\right] \tag{2.7}$$

which shifts the z_i ($\bar{z}_i$) coordinate by $\partial_{\bar{z}_i}$ (∂_{z_i}) as in

$$\hat{S}^{-1} z_i \hat{S} = z_i + 2\partial_{\bar{z}_i} \qquad \text{and} \qquad \hat{S}^{-1}\bar{z}_i\hat{S} = \bar{z}_i + 2\partial_{z_i}. \tag{2.8}$$

Applying $\hat{S}$ to $\hat{H}_L^{\mathbb{P}}$ then produces

$$\hat{S}^{-1}\hat{H}_L^{\mathbb{P}}\hat{S} = \hbar\omega_c\sum_i \bar{z}_i\partial_{\bar{z}_i} + \frac{\hbar\omega_c N}{2} \tag{2.9}$$

where $\sum_i \bar{z}_i\partial_{\bar{z}_i}$ acts as a counting operator for the total degree of $\bar{\mathbf{z}}$. The simultaneous eigenstates of $\hat{H}_L^{\mathbb{P}}$ and $\hat{L}_z$ are therefore of the form

$$\phi(\mathbf{z},\bar{\mathbf{z}}) = \hat{S}\tilde{\phi}(\mathbf{z},\bar{\mathbf{z}}) = e^{-2\sum_i \partial_{z_i}\partial_{\bar{z}_i}}\tilde{\phi}(\mathbf{z},\bar{\mathbf{z}}) \tag{2.10}$$

where $\tilde{\phi}(\mathbf{z},\bar{\mathbf{z}})$ is a homogeneous polynomial in $\mathbf{z} = (z_1,\ldots,z_N)$ and $\bar{\mathbf{z}} = (\bar{z}_1,\ldots,\bar{z}_N)$ *individually*. If d_z and $d_{\bar{z}}$ are the degrees of $\tilde{\phi}(\mathbf{z},\bar{\mathbf{z}})$ in $\mathbf{z}$ and $\bar{\mathbf{z}}$ we say that $\tilde{\phi}(\mathbf{z},\bar{\mathbf{z}})$ has bidegree $(d_z, d_{\bar{z}})$. The energy and angular momentum of $\phi(\mathbf{z},\bar{\mathbf{z}})$ are fixed by the bidegree as $E = \hbar\omega_c(d_{\bar{z}} + N/2)$ and $L_z = d_z - d_{\bar{z}}$.

2.1.1 Single particle states

Each single particle eigenstate $\phi(z,\bar{z})$ of $\hat{H}_L^{\mathbb{P}}$ and $\hat{L}_z$ is associated with a unique monomial $\tilde{\phi}(z,\bar{z}) = z^n\bar{z}^{\bar{n}}$ through equation (2.10). Since the energy only depends on $\bar{n}$ the single particle spectrum of $\hat{H}_L^{\mathbb{P}}$ consists of degenerate Landau levels of states with different angular momenta. Each combination of n and $\bar{n}$ determines a unique set of eigenvalues for $\hat{H}_L^{\mathbb{P}}$ and $\hat{L}_z$ and different monomials are therefore mapped onto distinct orthogonal polynomials by $\hat{S}$. In the standard

[6] This convention results in LLL states always being associated with positive values of L_z. In particular, L_z is identical to the homogeneous degree of a LLL polynomial state.

treatment of the Landau problem the single particle wave functions are often given in terms of the Laguerre polynomials. This result can be obtained by rewriting (2.10) as

$$\begin{aligned}\phi(z,\bar{z}) = e^{-2\partial_z\partial_{\bar{z}}} z^n \bar{z}^{\bar{n}} &= (z-2\partial_{\bar{z}})^n(\bar{z}-2\partial_z)^{\bar{n}}\cdot 1 \\ &= e^{z\bar{z}/2}(-2\partial_{\bar{z}})^n(-2\partial_z)^{\bar{n}}e^{-z\bar{z}/2} \\ &= (-2)^{\bar{n}}\bar{z}^{-n}e^{z\bar{z}/2}\partial_z^{\bar{n}}(z\bar{z})^n e^{-z\bar{z}/2} \\ &= (-2)^{\bar{n}}z^{n-\bar{n}}\left[s^{\bar{n}-n}e^s\partial_s^{\bar{n}}s^n e^{-s}\right]_{s=z\bar{z}/2} \\ &= (-2)^{\bar{n}}\bar{n}!z^{n-\bar{n}}L_{\bar{n}}^{n-\bar{n}}\left(z\bar{z}/2\right) \end{aligned} \tag{2.11}$$

where the Rodrigues formula [24] was used to produce the associated Laguerre polynomial in the final line.

2.1.2 N particle states

For N particles the natural basis for the space of antisymmetric homogeneous polynomials of bidegree $(d_z, d_{\bar{z}})$ are Slater determinants constructed from a set of N monomials

$$\tilde{\phi}_{d_z^{(i)},d_{\bar{z}}^{(i)}}(z,\bar{z}) = z^{d_z^{(i)}}\bar{z}^{d_{\bar{z}}^{(i)}} \quad \text{with} \quad i=1,\ldots,N \tag{2.12}$$

for which $\sum_i d_z^{(i)} = d_z$ and $\sum_i d_{\bar{z}}^{(i)} = d_{\bar{z}}$. Distinct Slater determinants of these monomials are then mapped onto orthogonal eigenstates of $\hat{H}_L^{\mathbb{P}}$ by $\hat{S}$. The degenerate subspace of lowest energy states are spanned by homogeneous polynomials in $\mathbf{z}$ alone, i.e. holomorphic functions of which the total degree equals the state's angular momentum. This is the so-called lowest Landau level (LLL). In contrast, the excited eigenstates of $\hat{H}_L^{\mathbb{P}}$ are generally not homogeneous.

2.1.3 Symmetries

Central to our construction are the simultaneous eigenstates of $\hat{H}_L^{\mathbb{P}}$ and $\hat{L}_z$ which exhibit translation and scaling invariance. It should be kept in mind that these are symmetries of the *polynomial* states $\phi(\mathbf{z},\bar{\mathbf{z}})$ which do not extend to the full wave function $\Psi(\mathbf{z},\bar{\mathbf{z}})$. For eigenstates of $\hat{L}_z$ rotational invariance of the average particle density $\rho(\mathbf{r}) = \langle\hat{\rho}(\mathbf{r})\rangle$ is guaranteed.

For $\phi(\mathbf{z},\bar{\mathbf{z}})$ to be scale invariant while also having a well-defined angular momentum it must be homogeneous in both $\bar{\mathbf{z}}$ and $\mathbf{z}$ separately. The form of $\hat{H}_L^{\mathbb{P}}$ in (2.5) then suggests that for such a state to be an eigenstate of $\hat{H}_L^{\mathbb{P}}$ it has to lie in the kernel of $\sum_i \partial_{z_i}\partial_{\bar{z}_i}$. Such scale invariant states contain no dependence on the particular magnetic length ℓ except through trivial prefactors and are therefore valid polynomial factors of eigenstates of the Landau problem with *any* non-zero magnetic field strength. This is in contrast to, for example, the single particle states

in (2.11) where the magnetic length features explicitly in the (generally non-homogeneous) Laguerre polynomial.

For $\phi(\mathbf{z}, \bar{\mathbf{z}})$ to be both translationally invariant and a polynomial it cannot have any dependence on the centre of mass coordinates $Z = N^{-1/2} \sum_i z_i$ and $\bar{Z}$ and must therefore lie in the kernels of both ∂_Z and $\partial_{\bar{Z}}$.

Generally we do not expect the states which exhibit these symmetries to be pure Slater determinants. Those which *are* will play an important role in what follows and can be characterised in a simple way. To see this, first consider the action of $\sum_i \partial_{z_i} \partial_{\bar{z}_i}$ on a Slater-determinant of monomials $\tilde{\phi}(\mathbf{z}, \bar{\mathbf{z}})$. Each term in the second quantised representation of $\sum_i \partial_{z_i} \partial_{\bar{z}_i}$ would amount to annihilating a particle in some state $(d_z, d_{\bar{z}})$ and creating a particle in the state $(d_z - 1, d_{\bar{z}} - 1)$. However, if $(d_z - 1, d_{\bar{z}} - 1)$ is already occupied the antisymmetry of $\tilde{\phi}(\mathbf{z}, \bar{\mathbf{z}})$ guarantees a zero result. Referring to Figure 2.1 it is clear that any monomial Slater determinant in which each column is either empty or completely filled up to some highest state will lie in the kernel of $\sum_i \partial_{z_i} \partial_{\bar{z}_i}$. Since $\hat{S}$ leaves these states invariant we have $\phi(\mathbf{z}, \bar{\mathbf{z}}) = \tilde{\phi}(\mathbf{z}, \bar{\mathbf{z}})$ and we may continue to think in terms of monomial single particle states instead of the complicated form given in (2.11). In a similar picture applying ∂_Z amounts to shifting particles one position to the left within a fixed Landau level while $\partial_{\bar{Z}}$ moves particles one position downward and to the right, as shown in Figure 2.1. We conclude that any Slater-determinant of monomials with the property that if $(d_z, d_{\bar{z}})$ is filled then so too is $(d_z - 1, d_{\bar{z}})$, $(d_z, d_{\bar{z}} - 1)$ and $(d_z - 1, d_{\bar{z}} - 1)$ will exhibit all three these symmetries. In the notation of [13] we denote such a state by $[N_0, N_1, N_2, \ldots, N_s]$ where s is the label of the highest non-empty Landau level and N_k is the number of particles filling the k'th Landau level starting from the left most state with $L_z = -k$. To ensure translational and scaling invariance we require that $N_{k+1} \leq N_k$ for $k = 0, \ldots, s-1$. These states represent a subset of the so-called compact states introduced by Jain in [13] which are subject to the weaker constraint that $N_{k+1} \leq N_k + 1$.

Finally, we return to the discussion in Section 1.2 regarding the behaviour of the ground state energy as a function of the total angular momentum as depicted in Figure 1.2 (b). We observed jumps in the ground state energy at those values of L_z (denoted $L_z^{(\mathrm{tot})}$ previously) where lowering the total angular momentum forces particles into higher Landau levels. It is now clear that whenever such a jump occurs the lower energy (higher L_z) ground state is a compact state.

2.1.4 Polynomial function space

Having found the eigenstates of $\hat{H}_L^{\mathbb{P}}$ the original similarity transformation may be inverted to restore the exponential factor and obtain the square integrable wave functions $\Psi(\mathbf{z}, \bar{\mathbf{z}})$ of (2.2). We will not follow this route, but instead proceed in the spirit of [25] and focus on the polynomials $\phi(\mathbf{z}, \bar{\mathbf{z}})$ which we take to represent the physical states of the system. Differential operators involving $\mathbf{z}$ and $\bar{\mathbf{z}}$ will be assumed to act directly on $\phi(\mathbf{z}, \bar{\mathbf{z}})$ while the exponential factor now only appears in the measure of the inner product on the space of polynomial states:

$$\langle \Psi_1(\mathbf{z}, \bar{\mathbf{z}}) | \Psi_2(\mathbf{z}, \bar{\mathbf{z}}) \rangle \equiv \langle \phi_1(\mathbf{z}, \bar{\mathbf{z}}) | \phi_2(\mathbf{z}, \bar{\mathbf{z}}) \rangle \equiv \int \mathrm{d}\mathbf{z}\, \mathrm{d}\bar{\mathbf{z}}\, e^{-\sum_i z_i \bar{z}_i / 2}\, \bar{\phi}_1(\mathbf{z}, \bar{\mathbf{z}})\, \phi_2(\mathbf{z}, \bar{\mathbf{z}}). \tag{2.13}$$

The adjoints of ∂_{z_i} and $\partial_{\bar{z}_i}$ with respect to this inner product are

$$\partial_{z_i}^\dagger = -\partial_{\bar{z}_i} + z_i/2 \qquad \text{and} \qquad \partial_{\bar{z}_i}^\dagger = -\partial_{z_i} + \bar{z}_i/2. \tag{2.14}$$

Henceforth we will drop the $\mathbb{P}$ superscript for operators acting on the polynomial part of the wave function. It should be clear from the context on which space the operators act.

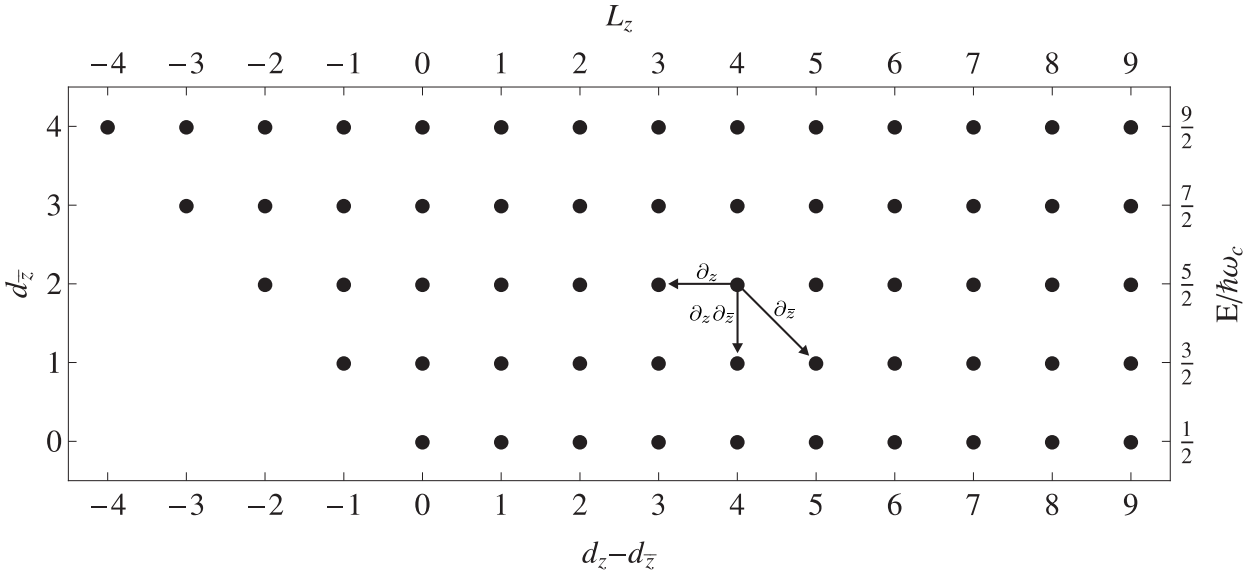

Figure 2.1: The single particle spectrum of $\hat{H}_L$. Top and right axis give the angular momentum and energy of the eigenstates which follow from applying $\hat{S}$ to the monomial $z^{d_z} \bar{z}^{d_{\bar{z}}}$ as in (2.11). Left and bottom axis refer to the degrees in z and $\bar{z}$ of the corresponding monomial states. Each row corresponds to a degenerate Landau level while states in a single column share the same angular momentum. Arrows indicate the action of partial derivatives on the monomials.

2.2 The $su(1,1)$ representation

The space of antisymmetric polynomials in $\mathbf{z}$ and $\bar{\mathbf{z}}$ carries a representation of the $su(1,1)$ Lie algebra given by the differential operators

$$\hat{A}_+ = \sum_i \bar{z}_i z_i, \qquad \hat{A}_- = \sum_i \partial_{z_i}\partial_{\bar{z}_i} \qquad \text{and} \qquad \hat{A}_0 = \frac{1}{2}\sum_i (z_i\partial_{z_i} + \bar{z}_i\partial_{\bar{z}_i} + 1) \tag{2.15}$$

which satisfy the $su(1,1)$ commutation relations

$$[\hat{A}_-, \hat{A}_+] = 2\hat{A}_0 \qquad \text{and} \qquad [\hat{A}_0, \hat{A}_\pm] = \pm\hat{A}_\pm. \tag{2.16}$$

This is a reducible representation which decomposes as the direct sum of irreducible representation from the positive discrete series [26]. It follows from expression (2.14) that the adjoints of $\hat{A}_{\pm,0}$ are

$$\hat{A}_+^\dagger = \hat{A}_+, \qquad \hat{A}_-^\dagger = \hat{A}_- - \hat{A}_0 + \frac{1}{4}\hat{A}_+ \qquad \text{and} \qquad \hat{A}_0^\dagger = -\hat{A}_0 + \frac{1}{2}\hat{A}_+. \tag{2.17}$$

Although this is not a unitary representation the Casimir operator $\hat{K} = \hat{A}_0(\hat{A}_0 - 1) - \hat{A}_+\hat{A}_-$ turns out to be Hermitian. It can be shown that this representation is equivalent to a unitary representation. All the irreps appearing in its decomposition are therefore infinite dimensional since $SU(1,1)$ is a non-compact Lie group.

Next we define the basis of simultaneous eigenstates of $\hat{K}$, $\hat{A}_0$ and $\hat{L}_z$. For the moment we suppress state labels relating to angular momentum as well as any multiplicity labels required to distinguish states belonging to different copies of the same $su(1,1)$ irrep. For the remainder of this section we only consider states with well-defined angular momentum. Consider an irreducible subspace on which $\hat{K} = k(k-1)\hat{\mathbb{I}}$ with k either an integer or half-integer. A non-orthogonal basis for this subspace is provided by the states $\{|k,n\rangle \;:\; n = 0,1,2,\ldots\}$ which satisfy

$$\begin{aligned}
&\hat{K}\,|k,n\rangle = k(k-1)\,|k,n\rangle && \hat{A}_0\,|k,n\rangle = (k+n)\,|k,n\rangle \\
&\hat{A}_+\,|k,n\rangle = c_{k,n}^{(+)}\,|k,n+1\rangle && \hat{A}_-\,|k,n\rangle = c_{k,n}^{(-)}\,|k,n-1\rangle \\
&|k,n\rangle = d_{k,n}\hat{A}_+^n\,|k,0\rangle && \hat{A}_-^n\hat{A}_+^m\,|k,0\rangle = (c_{k,m}/c_{k,m-n})\hat{A}_+^{m-n}\,|k,0\rangle
\end{aligned} \tag{2.18}$$

where $m \geq n$ and the values of the various constants are

$$c_{k,n} = n!\Gamma(2k+n)/\Gamma(2k) \qquad d_{k,n} = 2^{-n}\left(\Gamma(2k)/\Gamma(2n+2k)\right)^{1/2}$$
$$c^{(+)}_{k,n} = (8(2k+2n+1)(k+n))^{1/2} \qquad c^{(-)}_{k,n} = n(2k+n-1)\left(8(k+n-1)(2k+2n-1)\right)^{-1/2} \tag{2.19}$$

Any two states $|k,n\rangle$ and $|k,n'\rangle$ belonging to the same representation will have a non-zero overlap, but the Hermiticity of $\hat{K}$ ensures that states with different k values are orthogonal. Being simultaneous eigenstates of $\hat{A}_0$ and $\hat{L}_z$ each $|k,n\rangle$ is necessarily homogeneous in $\mathbf{z}$ and $\bar{\mathbf{z}}$ with degrees $d_z = (2(n+k) + L_z - N)/2$ and $d_{\bar{z}} = (2(n+k) - L_z - N)/2$ respectively. We also note that the kernel of $\hat{A}_-$ is just the subspace spanned by the lowest weight states. These are precisely the homogeneous scale invariant eigenstates of the free particle Landau problem discussed in Section 2.1.

Any homogeneous polynomial $\phi(\mathbf{z},\bar{\mathbf{z}})$ with bidegree $(d_z, d_{\bar{z}})$ can now be expanded in terms of the eigenstates of $\hat{K}$, $\hat{A}_0$ and $\hat{L}_z$ as

$$\phi(\mathbf{z},\bar{\mathbf{z}}) = \sum_{k=k_0}^{m} \alpha_k |k, m-k\rangle = \sum_{k=k_0}^{m} \alpha_k d_{k,m-k} \hat{A}_+^{m-k} |k,0\rangle \tag{2.20}$$

where $m = (d_z + d_{\bar{z}} + N)/2$ and $k_0 = (|d_z - d_{\bar{z}}| + N)/2$ are the absolute upper and lower bounds on the values of k that can appear in the expansion. The former is simply the eigenvalue of $\phi(\mathbf{z},\bar{\mathbf{z}})$ (and indeed of each term in the expansion) with respect to $\hat{A}_0$. The value of k_0 follows from the observation that any polynomial of bidegree $(d_z, d_{\bar{z}})$ is mapped to zero by the operator $\hat{A}_-^{\min(d_z,d_{\bar{z}})+1}$. This implies that $m - k_0 = \min(d_z, d_{\bar{z}})$, or equivalently that

$$k_0 = (d_z + d_{\bar{z}} - 2\min(d_z, d_{\bar{z}}) + N/2) = (|d_z - d_{\bar{z}}| + N)/2. \tag{2.21}$$

The values of k appearing in the expansion are either all integers or all half-integers depending on whether $d_z + d_{\bar{z}}$ is odd or even respectively. The state $|k_0, 0\rangle$ is proportional to $\hat{A}_-^{\min(d_z,d_{\bar{z}})}\phi(\mathbf{z},\bar{\mathbf{z}})$ and, if non-zero, is either completely holomorphic ($d_z > d_{\bar{z}}$) or anti-holomorphic ($d_z < d_{\bar{z}}$). At the filling fractions we consider only the $d_z > d_{\bar{z}}$ case will be relevant. Whenever it is non-zero the $|k_0, 0\rangle$ state is therefore holomorphic and, as we will show in Section 2.4.1, proportional to the projection of $\phi(\mathbf{z},\bar{\mathbf{z}})$ onto the space of holomorphic polynomials, i.e. the lowest Landau level.

The $k = k_0 + n$ term is constructed from the lowest weight state $|k_0 + n, 0\rangle$ which has bidegree $(d_z - d_{\bar{z}} + n, n)$. As we move to higher k values the homogeneous degree of $\bar{\mathbf{z}}$ in $|k,0\rangle$

therefore increases linearly with k. In Section 2.1 we identified these lowest weight states as the homogeneous eigenstates of the free particle Landau problem and in this sense (2.20) is a representation of a general homogeneous state $\phi(\mathbf{z},\bar{\mathbf{z}})$ in terms of this particular class of scale invariant $\hat{H}_L$ eigenstates. However, we stress that this representation is quite different from an expansion in the eigenstates of $\hat{H}_L$. In appendix A we show how, given $\phi(\mathbf{z},\bar{\mathbf{z}})$, the set of states $\{|k,m-k\rangle : k=k_0,\ldots,m\}$ and corresponding coefficients $\{\alpha_k : k=k_0,\ldots,m\}$ may be calculated.

Finally we take note of an identity concerning the matrix elements of powers of $\hat{A}_+$ between two arbitrary homogeneous states $\phi_1(\mathbf{z},\bar{\mathbf{z}})$ and $\phi_2(\mathbf{z},\bar{\mathbf{z}})$ with eigenvalues m_1 and m_2 with respect to $\hat{A}_0$. It follows from induction on n and the expressions in (2.17), (2.19) and (2.18) that

$$\langle\phi_1(\mathbf{z},\bar{\mathbf{z}})|\hat{A}_+^n|\phi_2(\mathbf{z},\bar{\mathbf{z}})\rangle = \frac{2^n\Gamma(n+m_1+m_2)}{\Gamma(m_1+m_2)}\langle\phi_1(\mathbf{z},\bar{\mathbf{z}})|\phi_2(\mathbf{z},\bar{\mathbf{z}})\rangle. \tag{2.22}$$

2.3 Relative and centre of mass coordinates

In a system with rotational symmetry the total angular momentum $\hat{L}_z = \sum_i (z_i\partial_{z_i} - \bar{z}_i\partial_{\bar{z}_i})$ is a conserved quantity. For a translationally invariant system where particles interact via a two-body interaction the angular momentum due to the centre of mass motion and the relative motion of particles are independently conserved. It is then convenient to express $\hat{L}_z$ as the sum of these two contributions as

$$\hat{L}_z = \frac{1}{N}\sum_{i<j}\left(z_{ij}\partial_{z_{ij}} - \bar{z}_{ij}\partial_{\bar{z}_{ij}}\right) + \left(Z\partial_Z - \bar{Z}\partial_{\bar{Z}}\right) = \hat{L}_z^{(r)} + \hat{L}_z^{(c)} \tag{2.23}$$

where $z_{ij} = z_i - z_j$ and $Z = N^{-1/2}\sum_i z_i$ are the interparticle and centre of mass coordinates. Applying the same procedure to the three generators of the $su(1,1)$ representation yields

$$\hat{A}_+ = \frac{1}{N}\sum_{i<j}\bar{z}_{ij}z_{ij} + \bar{Z}Z = \hat{A}_{r+} + \hat{A}_{c+} \tag{2.24}$$

$$\hat{A}_- = \frac{1}{N}\sum_{i<j}\partial_{\bar{z}_{ij}}\partial_{z_{ij}} + \partial_{\bar{Z}}\partial_Z = \hat{A}_{r-} + \hat{A}_{c-} \tag{2.25}$$

$$\hat{A}_0 = \frac{1}{2N}\sum_{i<j}\left(\bar{z}_{ij}\partial_{\bar{z}_{ij}} + z_{ij}\partial_{z_{ij}} + 2\right) + \frac{1}{2}\left(Z\partial_Z + \bar{Z}\partial_{\bar{Z}} + 1\right) = \hat{A}_{r0} + \hat{A}_{c0} \tag{2.26}$$

The two mutually commuting sets of operators $\{\hat{A}_{r0},\hat{A}_{r+},\hat{A}_{r-}\}$ and $\{\hat{A}_{c0},\hat{A}_{c+},\hat{A}_{c-}\}$ are themselves $su(1,1)$ representations with Casimir operators $\hat{K}^{(r)}$ and $\hat{K}^{(c)}$. In this sense the original representation $\{\hat{A}_0,\hat{A}_+,\hat{A}_-\}$ is the direct sum of two $su(1,1)$ representations realised in terms

of the relative and centre of mass coordinates respectively. All the results obtained in Section 2.2 can clearly be adapted to apply to either of these two representations.

2.4 Projection onto the lowest Landau level

2.4.1 Representations of the LLL projection

Let $\mathcal{P}$ denote the projection operator onto the degenerate subspace of lowest energy eigenstates of $\hat{H}_L$ known as the lowest Landau level (LLL). In Section 2.1 it was shown that a general eigenstate of $\hat{H}_L$ has the form

$$\phi(\mathbf{z},\bar{\mathbf{z}}) = e^{-2\sum_i \partial_{z_i}\partial_{\bar{z}_i}}\tilde{\phi}(\mathbf{z},\bar{\mathbf{z}}) = e^{-2\hat{A}_-}\tilde{\phi}(\mathbf{z},\bar{\mathbf{z}}) = \hat{S}\tilde{\phi}(\mathbf{z},\bar{\mathbf{z}}) \tag{2.27}$$

where $\tilde{\phi}(\mathbf{z},\bar{\mathbf{z}})$ is homogeneous with bidegree $(d_z, d_{\bar{z}})$. The energy of the state $\phi(\mathbf{z},\bar{\mathbf{z}})$ is then determined by $d_{\bar{z}}$ as $E = \hbar\omega_c(d_{\bar{z}} + N/2)$ and the LLL therefore coincides with the subspace of holomorphic polynomials for which $d_{\bar{z}} = 0$. In terms of $\tilde{\phi}(\mathbf{z},\bar{\mathbf{z}})$ the LLL projection therefore simply amounts to setting the $\bar{\mathbf{z}}$ variables to zero. This suggests the following representation of the projection operator:

$$\mathcal{P}\phi(\mathbf{z},\bar{\mathbf{z}}) = \hat{S}([\hat{S}^{-1}\phi(\mathbf{z},\bar{\mathbf{z}})]_{\bar{\mathbf{z}}=0}) = [\hat{S}^{-1}\phi(\mathbf{z},\bar{\mathbf{z}})]_{\bar{\mathbf{z}}=0} = [\phi(\mathbf{z}+2\partial_{\bar{\mathbf{z}}},\bar{\mathbf{z}}+2\partial_{\mathbf{z}})\cdot 1]_{\bar{\mathbf{z}}=0} \tag{2.28}$$

where the final step follows from (2.8). Since $z_i + 2\partial_{\bar{z}_i}$ and $\bar{z}_i + 2\partial_{z_i}$ commute no ambiguities arise from the ordering of operators in the expression $\phi(\mathbf{z}+2\partial_{\bar{\mathbf{z}}},\bar{\mathbf{z}}+2\partial_{\mathbf{z}})$. Now consider the *ordered* polynomial $\phi[\bar{\mathbf{z}},\mathbf{z}]$ obtained from $\phi(\mathbf{z},\bar{\mathbf{z}})$ by ordering the $\bar{\mathbf{z}}$ variables to the left of the $\mathbf{z}$'s. As polynomials in commuting variables $\phi[\bar{\mathbf{z}},\mathbf{z}]$ and $\phi(\mathbf{z},\bar{\mathbf{z}})$ are identical, but for non-commutative arguments the ordering convention present in $\phi[\cdot,\cdot]$ is necessary to produce an unambiguous result. With this in mind (2.28) can be written as

$$\mathcal{P}\phi(\mathbf{z},\bar{\mathbf{z}}) = [\phi[\bar{\mathbf{z}}+2\partial_{\mathbf{z}},\mathbf{z}+2\partial_{\bar{\mathbf{z}}}]\cdot 1]_{\bar{\mathbf{z}}=0} = \phi[2\partial_{\mathbf{z}},\mathbf{z}]. \tag{2.29}$$

The LLL projection of a state $\phi(\mathbf{z},\bar{\mathbf{z}})$ therefore amounts to ordering the $\bar{z}_i$'s to the left of the z_i's and then replacing each $\bar{z}_i$ by the derivative $2\partial_{z_i}$ acting to the right. This agrees with the result of obtained in [25] by considering the inner product of $\phi(\mathbf{z},\bar{\mathbf{z}})$ with a general LLL state. In the special case where $\phi(\mathbf{z},\bar{\mathbf{z}})$ is homogeneous with bidegree $(d_z, d_{\bar{z}})$ an alternative form of the projection follows from (2.28) as

$$\mathcal{P}\phi(\mathbf{z},\bar{\mathbf{z}}) = \left[e^{2\hat{A}_-}\phi(\mathbf{z},\bar{\mathbf{z}})\right]_{\bar{\mathbf{z}}=0} = \frac{2^{d_{\bar{z}}}}{d_{\bar{z}}!}\hat{A}_-^{d_{\bar{z}}}\phi(\mathbf{z},\bar{\mathbf{z}}). \tag{2.30}$$

Returning to the discussion that followed (2.20) we see that the claimed proportionality of the lowest weight state $|k_0, 0\rangle$ and the LLL projection is a direct consequence of this form of the projection. An immediate application of this result is presented in Section 2.4.4.

2.4.2 Projection of product states

In this section we consider the LLL projection of product states with the form $\phi(\mathbf{z}, \bar{\mathbf{z}})\sigma(\mathbf{z})$ of which composite fermion states is one example. From (2.29) it follows that

$$\mathcal{P}\phi(\mathbf{z}, \bar{\mathbf{z}})\sigma(\mathbf{z}) = \phi[2\partial_{\mathbf{z}}, \mathbf{z}]\sigma(\mathbf{z}) \tag{2.31}$$

where the derivatives in $\phi[2\partial_{\mathbf{z}}, \mathbf{z}]$ stand to the left and act on the $\mathbf{z}$ variables in $\phi[2\partial_{\mathbf{z}}, \mathbf{z}]$ itself as well as those in $\sigma(\mathbf{z})$. Next we define the polynomial $\tilde{\phi}(\mathbf{z}, \bar{\mathbf{z}})$ by $\tilde{\phi}(\mathbf{z}, \bar{\mathbf{z}}) = \exp[2A_-]\phi(\mathbf{z}, \bar{\mathbf{z}})$ and note that

$$\phi(\mathbf{z}, \bar{\mathbf{z}}) = e^{-2A_-}\tilde{\phi}(\mathbf{z}, \bar{\mathbf{z}}) = \tilde{\phi}(\mathbf{z} - 2\partial_{\bar{\mathbf{z}}}, \bar{\mathbf{z}} - 2\partial_{\mathbf{z}}) \cdot 1 = \tilde{\phi}[\mathbf{z} - 2\partial_{\bar{\mathbf{z}}}, \bar{\mathbf{z}}] \cdot 1 \tag{2.32}$$

where the first argument of $\tilde{\phi}[\mathbf{z} - 2\partial_{\bar{\mathbf{z}}}, \bar{\mathbf{z}}]$ is ordered to the left of the second. The projected state in (2.31) can be expressed in terms of $\tilde{\phi}$ as

$$\begin{aligned}
\mathcal{P}\phi(\mathbf{z}, \bar{\mathbf{z}})\sigma(\mathbf{z}) = \phi[2\partial_{\mathbf{z}}, \mathbf{z}]\sigma(\mathbf{z}) &= e^{2A_-}\phi(\mathbf{z}, \bar{\mathbf{z}})\sigma(\mathbf{z})\big|_{\bar{\mathbf{z}}=0} && (2.33)\\
&= e^{2A_-}\tilde{\phi}[\mathbf{z} - 2\partial_{\bar{\mathbf{z}}}, \bar{\mathbf{z}}]\sigma(\mathbf{z})\Big|_{\bar{\mathbf{z}}=0} && (2.34)\\
&= \tilde{\phi}[\mathbf{z}, \bar{\mathbf{z}} + 2\partial_{\mathbf{z}}]\sigma(\mathbf{z})\Big|_{\bar{\mathbf{z}}=0} && (2.35)\\
&= \tilde{\phi}[\mathbf{z}, 2\partial_{\mathbf{z}}]\sigma(\mathbf{z}). && (2.36)
\end{aligned}$$

It follows that $\phi[2\partial_{\mathbf{z}}, \mathbf{z}]$ and $\tilde{\phi}[\mathbf{z}, 2\partial_{\mathbf{z}}]$ are identical differential operators derived from the polynomials $\phi(\mathbf{z}, \bar{\mathbf{z}})$ and $\tilde{\phi}(\mathbf{z}, \bar{\mathbf{z}})$ using two different ordering conventions. In the special case where $\phi(\mathbf{z}, \bar{\mathbf{z}})$ is a lowest weight state we have

$$\mathcal{P}\phi(\mathbf{z}, \bar{\mathbf{z}})\sigma(\mathbf{z}) = \phi[2\partial_{\mathbf{z}}, \mathbf{z}]\sigma(\mathbf{z}) = \phi[\mathbf{z}, 2\partial_{\mathbf{z}}]\sigma(\mathbf{z}). \tag{2.37}$$

The result of the substitution $\bar{\mathbf{z}} \to 2\partial_{\mathbf{z}}$ is therefore independent of whether the $\bar{\mathbf{z}}$'s are first ordered to the left or the right of the $\mathbf{z}$'s. Since this result only applies to lowest weight $\phi(\mathbf{z}, \bar{\mathbf{z}})$ it may appear to be of little general interest. In the next section we prove that the opposite is in fact true: this is the *only* case we will ever need to consider.

2.4.3 Spurious product states

In general there are infinitely many states $\phi(\mathbf{z},\bar{\mathbf{z}})$ which produce the same LLL state $\mathcal{P}\phi(\mathbf{z},\bar{\mathbf{z}})\sigma(\mathbf{z})$. In our construction, as in the composite fermion picture, this redundancy gives rise to spurious states which have no counterpart in the lowest Landau level. We can now identify and eliminate at least one source of such spurious states. Suppose $\phi(\mathbf{z},\bar{\mathbf{z}})$ is a simultaneous eigenstate of the set of commuting operators $\{\hat{K}^{(r)},\hat{A}_{r0},L_z^{(r)},\hat{K}^{(c)},\hat{A}_{c0},L_z^{(c)}\}$. It follows that $\phi(\mathbf{z},\bar{\mathbf{z}})$ can be factorised into relative and centre of mass coordinates as

$$\phi(\mathbf{z},\bar{\mathbf{z}}) = \left(\hat{A}_{r+}^n\phi_r(\mathbf{z},\bar{\mathbf{z}})\right)\times\left(\hat{A}_{c+}^m\phi_c(Z,\bar{Z})\right) \tag{2.38}$$

where $\phi_r(\mathbf{z},\bar{\mathbf{z}})$ has no Z or $\bar{Z}$ dependence and $\hat{A}_{r-}\phi_r(\mathbf{z},\bar{\mathbf{z}}) = \hat{A}_{c-}\phi_c(Z,\bar{Z}) = 0$. If $\sigma(\mathbf{z})$ is translationally invariant we have

$$\begin{aligned}\mathcal{P}\phi(\mathbf{z},\bar{\mathbf{z}})\sigma(\mathbf{z}) &= \left[e^{2\hat{A}_-}\phi(\mathbf{z},\bar{\mathbf{z}})\sigma(\mathbf{z})\right]_{\bar{\mathbf{z}}=0} &(2.39)\\ &= \left[e^{2\hat{A}_{r-}}\hat{A}_{r+}^n\phi_r(\mathbf{z},\bar{\mathbf{z}})\sigma(\mathbf{z})\right]_{\bar{\mathbf{z}}=0}\times\left[e^{2\hat{A}_{c-}}\hat{A}_{c+}^m\phi_c(Z,\bar{Z})\right]_{\bar{Z}=0}. &(2.40)\end{aligned}$$

As pointed out in the discussion following equation (2.30) only the lowest $\hat{K}^{(r)}$ and $\hat{K}^{(c)}$ components of $\phi_r(\mathbf{z},\bar{\mathbf{z}})\sigma(\mathbf{z})$ and $\phi_c(Z,\bar{Z})$ contribute to the projection. The presence of $\hat{A}_{r+}^n$ and $\hat{A}_{c+}^m$ therefore just result in $\hat{A}_{r-}$ and $\hat{A}_{c-}$ having to act a larger number of times to strip away any $\bar{\mathbf{z}}$ or $\bar{Z}$ dependence before these coordinates are set to zero. It follows that $\mathcal{P}\phi(\mathbf{z},\bar{\mathbf{z}})\sigma(\mathbf{z})$ and $\mathcal{P}\phi_r(\mathbf{z},\bar{\mathbf{z}})\phi_c(Z,\bar{Z})\sigma(\mathbf{z})$ are equal up to a constant. When considering projections of the form $\mathcal{P}\phi(\mathbf{z},\bar{\mathbf{z}})\sigma(\mathbf{z})$ with translationally invariant $\sigma(\mathbf{z})$ we can therefore restrict ourselves to $\phi(\mathbf{z},\bar{\mathbf{z}})$ states which are lowest weight states with respect to *both* $\hat{A}_{r-}$ and $\hat{A}_{c-}$. In particular, to produce translationally invariant LLL states only translationally invariant $\phi(\mathbf{z},\bar{\mathbf{z}})$ need to be considered. We will continue this process of eliminating spurious states in Section 3.3.

2.4.4 Overlap of composite fermion states with the lowest Landau level

The representation of the LLL projection in (2.30) and the $\hat{K}$ basis expansion given in (2.20) now allows us to derive the following result.

Proposition 2.4.1 *Consider a normalised homogeneous state $\phi(\mathbf{z},\bar{\mathbf{z}})$ with bidegree $(d_z,d_{\bar{z}})$ where $d_{\bar{z}}$ is at most of order $\mathcal{O}(N)$ and d_z is at least of order $\mathcal{O}(N^2)$. The overlap of $\phi(\mathbf{z},\bar{\mathbf{z}})$ with the LLL is then bounded from above in the sense that*

$$\langle\phi(\mathbf{z},\bar{\mathbf{z}})\,|\mathcal{P}|\,\phi(\mathbf{z},\bar{\mathbf{z}})\rangle \leq \frac{\Gamma^2(2k_0+d_{\bar{z}})}{\Gamma(2k_0)\Gamma(2k_0+2d_{\bar{z}})} = e^{-d_{\bar{z}}^2/(2k_0)+\mathcal{O}(1/N)} \tag{2.41}$$

where $k_0 = (d_z - d_{\bar{z}} + N)/2$.

Proof: Consider the expansion of $\phi(\mathbf{z}, \bar{\mathbf{z}})$ in the eigenstates of $\hat{K}$ as in equation (2.20). Since states with different k values are orthogonal we have

$$\langle \phi(\mathbf{z}, \bar{\mathbf{z}}) | \phi(\mathbf{z}, \bar{\mathbf{z}}) \rangle = \sum_{k=k_0}^{m} |\alpha_k|^2 = 1. \tag{2.42}$$

and so $|\alpha_{k_0}|^2 \leq 1$. Applying the LLL projection in the form of (2.30) and using (2.18) yields

$$\mathcal{P}\phi(\mathbf{z}, \bar{\mathbf{z}}) = \frac{2^{d_{\bar{z}}}}{d_{\bar{z}}!} \hat{A}_-^{d_{\bar{z}}} \phi(\mathbf{z}, \bar{\mathbf{z}}) = \frac{\alpha_{k_0} d_{k_0, d_{\bar{z}}} 2^{d_{\bar{z}}} c_{k_0, d_{\bar{z}}}}{d_{\bar{z}}!} |k_0, 0\rangle . \tag{2.43}$$

Finally we take the inner product with $\phi(\mathbf{z}, \bar{\mathbf{z}})$ in both sides and use (2.22) to obtain

$$\langle \phi(\mathbf{z}, \bar{\mathbf{z}}) | \mathcal{P}\phi(\mathbf{z}, \bar{\mathbf{z}}) \rangle = |\alpha_{k_0}|^2 \frac{\Gamma^2(2k_0 + d_{\bar{z}})}{\Gamma(2k_0)\Gamma(2k_0 + 2d_{\bar{z}})} \leq \frac{\Gamma^2(2k_0 + d_{\bar{z}})}{\Gamma(2k_0)\Gamma(2k_0 + 2d_{\bar{z}})} \tag{2.44}$$

By applying Stirling's approximation to the logarithm of the upper bound we find

$$\log \left[\frac{\Gamma^2(2k_0 + d_{\bar{z}})}{\Gamma(2k_0)\Gamma(2k_0 + 2d_{\bar{z}})} \right] = -\frac{d_{\bar{z}}^2}{2k_0} + \mathcal{O}(1/N) \tag{2.45}$$

from which the desired result follows. ■

Let us consider the implications of this upper bound for the unprojected composite fermion state[7]

$$\phi(\mathbf{z}, \bar{\mathbf{z}}) = \phi_0(\mathbf{z}, \bar{\mathbf{z}}) J^2 \tag{2.46}$$

where $J = \prod_{i<j}(z_i - z_j)$ is the Vandermonde polynomial (see Section 2.5.3) and $\phi_0(\mathbf{z}, \bar{\mathbf{z}})$ is the Slater determinant corresponding to the complete filling of n Landau levels. According to composite fermion theory $\mathcal{P}\phi(\mathbf{z}, \bar{\mathbf{z}})$ approximates the ground state of N interacting electrons in the LLL at a filling of $\nu = n/(2n+1)$. Since the introduction of the composite fermion picture it has been widely believed that, prior to projection, $\phi(\mathbf{z}, \bar{\mathbf{z}})$ already lies predominantly within the lowest Landau level [17, 27, 28, 11]. This assumption was based on the following heuristic single particle argument. First $\phi_0(\mathbf{z}, \bar{\mathbf{z}})J^2$ is expanded as a polynomial and a single monomial term identified. The coordinates of the i'th particle would appear in the monomial in the form $z_i^d \bar{z}_i^{\bar{d}}$ where $\bar{d} < n$. In a typical term the power d of z_i is expected to be of order $\mathcal{O}(N)$. The

[7] In the notation of (1.19) we have $\phi(\mathbf{z}, \bar{\mathbf{z}})$ and $\phi_0(\mathbf{z}, \bar{\mathbf{z}})$ representing the polynomial parts of Ψ_ν^{unproj} and $\Phi_n(B)$ respectively.

overlap of $\phi_i = z_i^d \bar{z}_i^{\bar{d}}$ with the lowest Landau level is then easily seen to be

$$\frac{\langle\phi_i|\mathcal{P}|\phi_i\rangle}{\langle\phi_i|\phi_i\rangle} = \frac{d!\,d!}{(d-\bar{d})!(\bar{d}+d)!} = e^{-\alpha^2+\mathcal{O}(1/d)} \tag{2.47}$$

where $\alpha = \bar{d}/\sqrt{d}$. For a single particle α^2 is clearly of order $1/N$ and ϕ_i will indeed lie almost entirely in the LLL if $N >> 1$. However, care must be taken when trying to extend this result to the N particle wave function for which the analog of (2.47) is now given by (2.41). The crucial difference is that $d_{\bar{z}}$, the total degree in *all* the $\bar{z}$ variables, has now taken the place of $\bar{d}$ while k_0 has replaced d. While $\bar{d}$ is always much smaller than a typical $\sqrt{d}$ it is not generally true that $d_{\bar{z}} << \sqrt{k_0}$ since $d_{\bar{z}} = \mathcal{O}(N)$ and $k_0 = \mathcal{O}(N^2)$ whenever more than one Landau level in $\phi_0(\mathbf{z}, \bar{\mathbf{z}})$ is filled. Generalizing the single particle result to the N particle case is therefore not valid and there is no reason to expect that $\phi(\mathbf{z}, \bar{\mathbf{z}})$ will lie predominantly in the lowest Landau level, as has been widely assumed in the literature. The underlying reason for why extending the single particle picture fails can be traced back to the expansion of $\phi(\mathbf{z}, \bar{\mathbf{z}})$ in $\hat{K}$ eigenstates as in (2.20). First note that only the $k = k_0$ term has a non-zero LLL overlap and that it contains $\mathcal{O}(N)$ powers of a *single* $\bar{z}_i$ coordinate. So even though the power of a single $\bar{z}_i$ in $\phi(\mathbf{z}, \bar{\mathbf{z}}) = \phi_0(\mathbf{z}, \bar{\mathbf{z}})J^2$ is bounded by $n-1$ this is *not* true of its k_0 component. The single particle argument therefore cannot be applied to the k_0 term, which is the *only* part of $\phi(\mathbf{z}, \bar{\mathbf{z}}) = \phi_0(\mathbf{z}, \bar{\mathbf{z}})J^2$ that can contribute to its LLL projection. Of course, in the full expansion these high powers of $\bar{z}_i$ must cancel between the various terms, but under projection none of the $k > k_0$ terms survive. This does not occur for a single particle since here each angular momentum sector carries only a single $su(1,1)$ representation with $k = k_0 = (L_z + 1)/2$. As noted by Jain in his original paper [17] the single particle case may imply the N particle result barring "*some very strange cancellations*". It seems that these cancellations are indeed present, and occur in the projections of the $k > k_0$ components of $\phi(\mathbf{z}, \bar{\mathbf{z}})$. An alternative measure of how close $\phi(\mathbf{z}, \bar{\mathbf{z}})$ is to being a LLL state is its average kinetic energy per particle $\langle\phi|\hat{H}_L|\phi\rangle/N$. Monte-Carlo calculations [20] have shown this to be fairly small, of the order of $0.05\hbar\omega_c$ above the ground state energy. This implies that most of the particles are indeed in the LLL. However, this has little bearing on the actual overlap of $\phi(\mathbf{z}, \bar{\mathbf{z}})$ with the LLL and certainly does not contradict the results derived here. In fact, it is not difficult to imagine states for which both the kinetic energy per particle as well as the overlap with the LLL vanish in the thermodynamic limit.

We conclude this section with a calculation of numeric values for the upper bound in the large N limit. In Section 2.1 the Slater determinant $\phi_0(\mathbf{z}, \bar{\mathbf{z}})$ was shown to be homogeneous. The same is true for J and therefore also for $\phi(\mathbf{z}, \bar{\mathbf{z}})$. First we determine the bidegree of $\phi_0(\mathbf{z}, \bar{\mathbf{z}})$. In the k'th Landau level all the monomial states have degree $k-1$ in $\bar{z}$ while the degrees of z range from zero up to $N/n + \mathcal{O}(1)$. The degrees of $\mathbf{z}$ and $\bar{\mathbf{z}}$ in $\phi_0(\mathbf{z}, \bar{\mathbf{z}})$ are therefore $d_z^{(0)} = N^2/(2n) + \mathcal{O}(N)$ and $d_{\bar{z}}^{(0)} = N(n-1)/2 + \mathcal{O}(1)$. Multiplication by J^2 raises the degree of $\mathbf{z}$ by a further $N(N-1)$ and the bidegree of $\phi(\mathbf{z}, \bar{\mathbf{z}})$ is therefore

$$(N^2/(2n) + N^2 + \mathcal{O}(N), N(n-1)/2 + \mathcal{O}(1))$$

which implies an upper bound of $\exp[-d_{\bar{z}}^2/(2k_0)] = \exp[-n(n-1)^2/(2+4n)]$ in the limit of large N. For the filling of $n = 1, \ldots, 6$ Landau levels the corresponding upper bounds are 1, 0.819, 0.424, 0.135, 0.026, 0.003. This illustrates the rapid decrease in the LLL overlap of the composite fermion state as higher Landau levels in $\phi_0(\mathbf{z}, \bar{\mathbf{z}})$ are filled.

2.5 Properties of the lowest Landau level

We end this chapter by highlighting some important features of lowest Landau level states.

2.5.1 Single particles states and the filling fraction

The full wave function of the LLL single particle state with angular momentum $L_z = m$ is

$$\Psi_m(z) = \frac{1}{\sqrt{2\pi 2^m m! \ell}} z^m e^{-|z|^2/4}. \tag{2.48}$$

This state is localised at a radius of approximately $\sqrt{2m}\ell$ about the origin and has an r^2 expectation value of $2(m+1)\ell^2$. The surface area of $2\pi(m+1)\ell^2$ that this state encloses is penetrated by a total flux of $\phi_0(m+1)$ and in this sense each LLL state is associated with one flux quantum $\phi_0 = hc/|e|$. The total flux penetrating the system therefore determines the degeneracy of the lowest Landau level. For a system containing N particles and penetrated by a total flux of $\Phi = M\phi_0$ the LLL is M-fold degenerate and the ratio $\nu = N/M$ is called the filling fraction. In the spherical geometry [14] a perfectly uniform particle density $\bar{\rho}$ can be realised for finite systems, in which case the filling fraction is given by $\nu = 2\pi\ell^2\bar{\rho}$. For a finite system in the plane, such as a quantum dot centered at the origin, the precise definition of the filling fraction is less clear. The difficulty lies with the way in which the system size should be defined and enforced. Requiring that the wave functions vanish at the system boundary or introducing an angular momentum cut-off results in a breaking of translation symmetry within

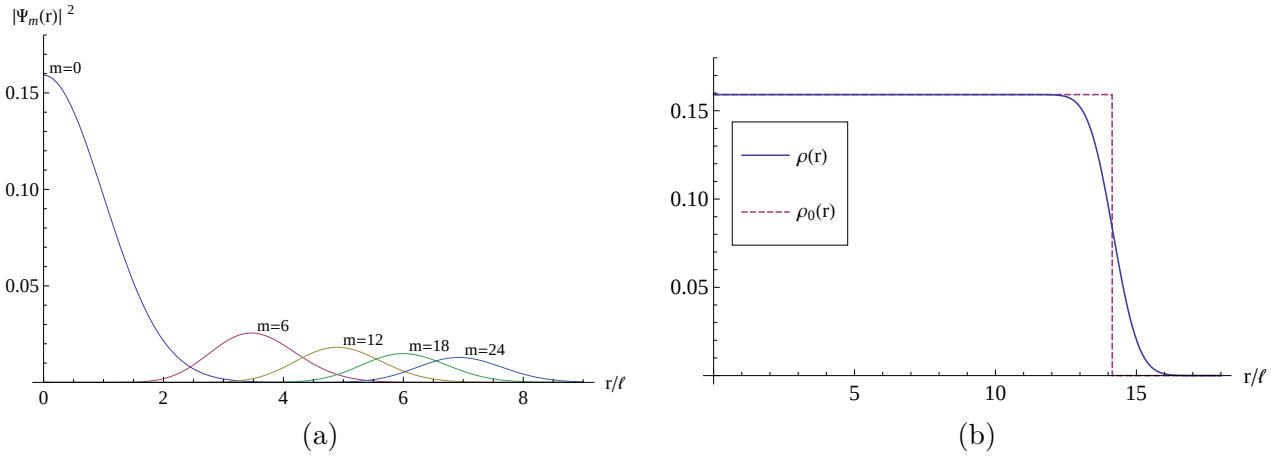

Figure 2.2: (a) The radial dependence of the probability densities associated with the single particle LLL states with angular momenta $m = 0, 6, 12, 18, 24$. (b) The exact radial particle density $\rho(r)$ for $N = 100$ particles, as well as the step-function approximation $\rho_0(r)$ of Section 2.5.2.

the polynomial parts of the wave functions as well. To avoid this complication we instead fix the total angular momentum and thereby also the root-mean-square distance of particles from the origin. The filling fraction is then given by $\nu = N(N-1)/(2L_z)$ (see next section) up to corrections of order $\mathcal{O}(1/N)$. For states with a uniform particle density $\bar{\rho}$ in the bulk region the relation $\nu = 2\pi\ell^2\bar{\rho}$ will again hold in the thermodynamic limit.

2.5.2 Large N scaling behaviour of L_z

Let $\hat{\rho}(\mathbf{r}) = \sum_i \delta(\mathbf{r} - \mathbf{r}_i)$ denote the particle density operator and consider its expectation value $\rho(r) = \langle\psi(\mathbf{z})|\hat{\rho}(\mathbf{r})|\psi(\mathbf{z})\rangle$ with respect to a LLL state $\psi(\mathbf{z})$ with well-defined angular momentum. For an interacting state at a filling fraction ν the density profile $\rho(r)$ is expected to describe a droplet with radius $R = \sqrt{2N/\nu}$ and a constant average density $\bar{\rho} = \nu/(2\pi\ell^2)$ within the bulk. In the edge region around $r = R$ the average density may deviate from $\bar{\rho}$ but should decay to zero quickly at $r > R$. A simple approximation to $\rho(r)$ which reflects its bulk properties is then given by $\rho_0(r) = \bar{\rho}\,\Theta(r - R)$ with $\Theta(r)$ the step function. From this we can

infer the large N scaling behaviour of the angular momentum as follows:

$$\begin{aligned} L_z = d_z &= \langle\psi| \sum_i z_i \partial_{z_i} |\psi\rangle && (2.49)\\ &= \langle\psi| 2^{-1} \sum_i \bar{z}_i z_i - N |\psi\rangle \qquad \text{(from eq. 2.29)} && (2.50)\\ &= \frac{1}{2\ell^2} \int \mathrm{d}\mathbf{r} \langle\psi|\hat{\rho}(\mathbf{r})|\psi\rangle r^2 - N && (2.51)\\ &= \frac{\pi\bar{\rho}R^4}{4} - N + \frac{1}{2\ell^2} \int \mathrm{d}\mathbf{r} \delta\rho(r) r^2 && (2.52)\\ &= \frac{N^2}{2\nu} + \delta L_z && (2.53) \end{aligned}$$

where $\delta\rho(r) = \rho(r) - \rho_0(r)$ and δL_z represents the final two terms in line (2.52). If $\rho_0(r)$ approximates $\rho(r)$ well within the bulk we expect δL_z to be at most of order $\mathcal{O}(N)$, in which case

$$L_z = d_z = \frac{N^2}{2\nu} + \mathcal{O}(N). \tag{2.54}$$

Let us consider two examples for which analytic results are known. The state $\psi_1(\mathbf{z}) = J$ has $\nu = 1$ and for large N the average particle density is given by

$$\rho(r) = \frac{1}{4\pi\ell^2} \left(1 - \mathrm{erf}\left[(r - R)/\ell\right]\right) \tag{2.55}$$

where $R = \sqrt{2N}\ell$ and $\mathrm{erf}(x)$ is the error function. As shown in Figure 2.2 (b) $\rho(r)$ is well suited to the step function approximation. Since $L_z = N(N-1)/2$ we indeed find that $\delta L_z = -N/2$. Similarly for the $\nu = 1/3$ Laughlin state $\psi_2(\mathbf{z}) = J^3$ we have $L_z = 3N(N-1)/2$ which implies that $\delta L_z = -3N/2$. The average particle density of this state is also uniform within the bulk but is known to fluctuate within a range of about five magnetic lengths of the edge [29, 30].

We shall assume that the scaling behaviour of L_z in (2.54) is sufficiently robust to hold for all the low energy states at the filling fractions associated with incompressibility.

2.5.3 The Vandermonde polynomial

The Vandermonde polynomial J is an antisymmetric homogeneous polynomial in $\mathbf{z}$ with degree

$$d_J = \frac{N(N-1)}{2} \tag{2.56}$$

which is the lowest permitted by antisymmetry. These properties fix J (up to constants) as

$$J = \prod_{i<j}(z_i - z_j). \tag{2.57}$$

As a Slater determinant the Vandermonde polynomial corresponds to filling the N LLL single particle states with the lowest angular momentum (i.e. lowest degree), namely $z^0, z^1, z^2, \ldots, z^{N-1}$. The antisymmetry of a general LLL state $\psi(\mathbf{z})$ implies that it has, in each z_i coordinate, $N-1$ zeros at the coordinates $z_{j\neq i}$. It follows that $\psi(\mathbf{z})$ must contain J as a factor, and we may write

$$\psi(\mathbf{z}) = \sigma(\mathbf{z})J \tag{2.58}$$

where $\sigma(\mathbf{z})$ is a symmetric polynomial. In fact, if $\psi(\mathbf{z})$ is a Slater determinant then $\sigma(\mathbf{z})$ is a Schur polynomial [31].

Also note that the Jastrow factor $\prod_{i<j}(z_i - z_j)^{2p}$ appearing in the composite fermion wave functions (1.19) and (1.20) is just an even power of the Vandermonde polynomial.

2.5.4 Pseudopotentials

Consider the matrix elements of a two-body interaction $\sum_{i<j} V(|\mathbf{r}_i - \mathbf{r}_j|)$ between two arbitrary many-body LLL states. It is well known that these matrix elements are completely determined by the so-called pseudopotentials [14] of $V(r)$ which are defined as

$$V_n = \frac{1}{2^{2n+1}\ell^{n+1}n!}\int_0^\infty \mathrm{d}r e^{-r^2/4} r^{2n+1} V(r) \qquad \text{with} \quad n = 1, 3, 5, 7, \ldots \tag{2.59}$$

This can be understood by considering the matrix element of a single term, say $V(|\mathbf{r}_1 - \mathbf{r}_2|)$, and noting that the polynomial part $\phi(\mathbf{z})$ of any LLL state may be written in the form

$$\phi(\mathbf{z}) = \sum_{\substack{m \\ \text{odd } n}} (z_1 - z_2)^n (z_1 + z_2)^m P_{n,m}(z_3, z_4, \ldots, z_N). \tag{2.60}$$

Since $V(|\mathbf{r}_1 - \mathbf{r}_2|)$ leaves the relative angular momentum of particles 1 and 2 unchanged the only way in which the potential can enter in $\langle\phi_1|V(|\mathbf{r}_1 - \mathbf{r}_2|)|\phi_2\rangle$ is through *diagonal* matrix elements with respect to two particle states of the form $(z_1 - z_2)^n$. Introducing $r = |z_1 - z_2|$ along with appropriate normalisation factors then leads to the form of the pseudopotentials given in (2.59).

CHAPTER 3
The projected Casimir operator

In this chapter we investigate the projection of the $su(1,1)$ Casimir operator $\hat{K}^{(r)}$ into the space Λ which is isomorphic to the translationally invariant sector of the lowest Landau level. This problem turns out to be closely related to the interacting quantum Hall system; a connection we will establish in the next chapter. *At present it is sufficient to regard $\mathcal{P}_\Lambda \hat{K}^{(r)} \mathcal{P}_\Lambda$ and the projected interaction as being equivalent problems.* In particular, results obtained for $\mathcal{P}_\Lambda \hat{K}^{(r)} \mathcal{P}_\Lambda$ can be translated to apply to the projected interaction. We will see how the study of $\mathcal{P}_\Lambda \hat{K}^{(r)} \mathcal{P}_\Lambda$ naturally leads to a framework which is strongly reminiscent of the composite fermion picture. Section 3.6 serves as a quick reference for the various spaces and mappings encountered in this chapter. Henceforth we will deal with filling fractions in the range $1/3 \leq \nu < 1/2$.

3.1 Introduction

Let $\mathcal{L}$ denote the space of translationally invariant LLL states. We will restrict our construction to $\mathcal{L}$ as this eliminates the trivial degeneracies associated with the centre of mass motion of a system with pairwise interactions.

Now consider the unitary transformation $U^2 = J/\bar{J}$ which first appeared in Section 1.6.3 as a singular gauge transformation used to generate the $\boldsymbol{\mathcal{A}}_i$ vector potential [19] in the Landau Hamiltonian. Since no kinetic term is present in the projected interaction interpreting U^2 as a gauge transformation no longer seems appropriate and we will simply regard it as a useful unitary transformation. Our interest in U^2 stems from the observation that if a state $\psi(\mathbf{z}) \in \mathcal{L}$ describes free composite fermions it should be possible to remove the bound vortices by applying U^{-2} and thereby expose the underlying free particle state. This approach has been used to arrive at mean-field descriptions of composite fermions similar to that of Section 1.6.3. Here it serves as the first step of a more precise formalism.

Recall that any state $\psi(\mathbf{z}) \in \mathcal{L}$ can be factorised as $\psi(\mathbf{z}) = \sigma(\mathbf{z})J$. Applying U^{-2} to $\psi(\mathbf{z})$ then produces

$$\phi(\mathbf{z}, \bar{\mathbf{z}}) = U^{-2}\psi(\mathbf{z}) = \sigma(\mathbf{z})\bar{J} \tag{3.1}$$

and we denote the space of these transformed states by $\Lambda \equiv U^{-2}\mathcal{L}$. An element of $\mathcal{L}$ with angular momentum L_z is therefore mapped onto an antisymmetric homogeneous polynomial of

bidegree $(L_z - d_J, d_J)$ where $d_J = N(N-1)/2$ is the total degree of the Vandermonde polynomial J. *In what follows we will always denote the angular momentum of $\mathcal{L}$ states by L_z and write $L_z^* = L_z - 2d_J$ for the angular momentum of its Λ counterpart.*

Next we consider the action of the $su(1,1)$ generators defined in Section 2.3 on Λ. Since the elements of Λ do not depend on the centre of mass coordinates Z and $\bar{Z}$ the operators $\hat{A}_{c0}$ and $\hat{K}^{(c)}$ are constant on Λ with values of $1/2$ and $-1/4$ respectively. $\hat{A}_{r0}$ also acts on Λ in a simple way since a state with angular momentum $L_z^* = L_z - 2d_J$ is automatically an eigenstate of $\hat{A}_{r0}$ with eigenvalue $m_r = (L_z + N - 1)/2$. The action of $\hat{K}^{(r)}$ is far less trivial. In fact, Λ is generally not invariant under the action of $\hat{K}^{(r)}$ and this rules out the possibility of constructing exact eigenstates of $\hat{K}^{(r)}$ in Λ. This follows from the observation that the elements of Λ possess both symmetric and antisymmetric exchange symmetries in the $\mathbf{z}$ and $\bar{\mathbf{z}}$ variables respectively. These symmetries are not preserved by $\hat{K}^{(r)}$ which is only symmetric with respect to the exchange of particle labels, i.e. the simultaneous exchange of both $z_i \leftrightarrow z_j$ and $\bar{z}_i \leftrightarrow \bar{z}_j$.

Our aim is to study the projection of $\hat{K}^{(r)}$ onto Λ, written $\hat{K}^{(r)}_\Lambda \equiv \mathcal{P}_\Lambda \hat{K}^{(r)} \mathcal{P}_\Lambda$, and relate its low-lying eigenstates and eigenvalues to those of the *unprojected* Casimir operator $\hat{K}^{(r)}$. Using the expansion in (2.20) an arbitrary state $\phi(\mathbf{z}, \bar{\mathbf{z}}) \in \Lambda$ with angular momentum $L_z^* = L_z - 2d_J$ may be expressed in terms of the simultaneous eigenstates of $\hat{K}^{(r)}$ and $\hat{A}_{r0}$ as[8]

$$\phi(\mathbf{z}, \bar{\mathbf{z}}) = \sum_{k=k_0}^{m_r} \alpha_k \, |k, m_r - k\rangle \tag{3.2}$$

where $|k, m_r - k\rangle = d_{k,m_r-k} \hat{A}_{r+}^{m_r-k} \, |k, 0\rangle$, $m_r = (L_z + N - 1)/2$ and $k_0 = m_r - d_J$. The set of expansion coefficients $\{\alpha_k\}$ and states $\{|k, m_r - k\rangle\}$ are constrained in a complex manner to ensure that the linear superposition is an element of Λ. These constraints do not allow for the construction of exact eigenstates of $\hat{K}^{(r)}$ in Λ, or possibly even of states which are well localised in k-space. This appears to cast doubt on the existence of any simple correspondence between the eigenvalues and eigenstates of $\hat{K}^{(r)}$ and $\hat{K}^{(r)}_\Lambda$. Despite these difficulties such a correspondence will indeed be found, but this requires a more precise formulation of the problem. We will continue this discussion in Section 3.3, but first we revisit one of the four questions posed in Section 1.7.

[8] Angular momentum and multiplicity labels are still suppressed.

3.2 Question 1: The origin of the effective magnetic field

In Section 1.7 we posed the question: *Can the origin of the weakened magnetic field and its relation to the wave functions and spectrum be understood at a more fundamental level starting from an interacting Hamiltonian?*

Issues regarding the spectrum will be investigated later, but the origin of the effective magnetic field, and the effective filling fraction in particular, can already be identified. Let us consider the expansion of a state $\phi(\mathbf{z},\bar{\mathbf{z}}) = U^{-2}\psi(\mathbf{z}) \in \Lambda$ in the basis of $\hat{K}^{(r)}$ and $\hat{A}_{r0}$ eigenstates as it appears in (3.2). Following the composite fermion picture one may be tempted to interpret this as an expansion in the eigenstates of the Landau problem with a weakened effective magnetic field. However, two observations appear to negate such an interpretation. First, we note that each term has bidegree $(L_z - d_J, d_J)$ and therefore a total degree of L_z, which is identical to that of $\psi(\mathbf{z})$ itself. All terms therefore represent states of the same physical size and filling fraction ν as $\psi(\mathbf{z})$. Secondly, any link with low energy free particle states appears tenuous in light of the extremely high powers of $\bar{\mathbf{z}}$ appearing in each term. At this point it may appear that transforming from $\mathcal{L}$ to Λ has not provided any link to the free particle picture.

Luckily, all these difficulties are the result of spurious properties of the individual terms which turn out to be mathematically irrelevant. Specifically, the problematic features of a typical term $|k, m_r - k\rangle$ result from the high powers of $\hat{A}_{r+}$ that relate it to the lowest weight state $|k, 0\rangle$. However, the Casimir operator $\hat{K}^{(r)}$ is *only* concerned with the k-label of $|k, m_r - k\rangle$ and all relevant physical information is therefore also contained in the lowest weight states. It is the lowest weight states that turn out to have all the desired features we require of the free particle picture.[9] The algebraic properties of the Casimir operator therefore results in a significant simplification: the enormously high powers of $\mathbf{z}$ and $\bar{\mathbf{z}}$ contained in each $\hat{A}_{r+}^{m_r-k}$ factor become harmless spectators while the focus shifts to the lowest weight states. The latter are automatically eigenstates of the free particle Landau problem at a higher filling fraction. *The physics contained in the projected Casimir operator, and therefore also the projected interaction, at a filling ν are governed by the behaviour of particles at a higher effective filling fraction.*

These observations provide a conceptual understanding of how the effective filling fraction emerges on a mathematical level. What remains is to determine its value, or possibly range of values, in terms of the filling fraction ν of $\psi(\mathbf{z})$. We first consider the lowest weight state $|k, 0\rangle$

[9] In fact, we could have mapped each state $\phi(\mathbf{z},\bar{\mathbf{z}}) = \sum_{k=k_0}^{m_r} \alpha_k |k, m_r - k\rangle$ in Λ onto the state $\sum_{k=k_0}^{m_r} \alpha_k |k, 0\rangle$ and diagonalised $\hat{K}^{(r)}$ in the resulting subspace. This represents a completely equivalent problem in which the connection to the free particle picture is clear from the outset.

associated with a single term in the expansion and try to determine its filling fraction ν^*. Since $|k,0\rangle$ is an eigenstate of $\hat{A}_0$ with eigenvalue $k+1/2$ it follows from (2.22) that $\langle k,0|\hat{A}_+|k,0\rangle = 4k+2$. The average squared distance of a single particle from the origin is therefore given by $\langle k,0|r_i^2|k,0\rangle = 4k\ell^2/N$. On the other hand, if we approximate the average particle density by a uniform disk we are led to conclude that $\langle k,0|r_i^2|k,0\rangle = N/(2\pi\bar{\rho}^*) = N\ell^2/\nu^*$. Equating these two expressions and dropping $\mathcal{O}(1/N)$ corrections lead to

$$\nu^* = \frac{N^2}{4k}. \tag{3.3}$$

However, in expansion (3.2) k ranges from k_0 up to m_r which implies a corresponding range of filling fractions for the lowest weight states. We are interested in the *average* effective filling fraction $\langle\nu^*\rangle$ when $\phi(\mathbf{z},\bar{\mathbf{z}})$ is a low-lying eigenstate of $\hat{K}_\Lambda^{(r)}$. This is equivalent to calculating the expectation value of $\hat{k}$ in $\phi(\mathbf{z},\bar{\mathbf{z}})$ of which we only need the $\mathcal{O}(N^2)$ behaviour to determine $\langle\nu^*\rangle$ up to $\mathcal{O}(1/N)$ corrections. Proposition 4.2.1 in the next chapter proves that if $\phi(\mathbf{z},\bar{\mathbf{z}})$ has a uniform density then the expectation value of $\hat{k}$ satisfies $\langle\hat{k}\rangle = N^2/(4n) + \mathcal{O}(N)$ where n is related to the filling fraction of $\psi(\mathbf{z}) = U^2\phi(\mathbf{z},\bar{\mathbf{z}})$ by $\nu = n/(2n+1)$. Here we give a more heuristic derivation of this result. If $\phi(\mathbf{z},\bar{\mathbf{z}})$ represent a low-lying eigenstate of $\hat{K}_\Lambda^{(r)}$ we expect the terms with low k values to carry the largest weight in expansion (3.2). Since minimizing k at a fixed angular momentum amounts to minimizing the state's degree in $\bar{\mathbf{z}}$ we expect the low-k terms to mimic low energy eigenstates of the Landau problem. In particular, the effective Landau levels will be filled from the bottom up to minimize the total degree in $\bar{\mathbf{z}}$. We know that the angular momentum of $|k,0\rangle$ is $L_z^* = L_z - 2d_J = N^2/(2\nu) - N^2 + \mathcal{O}(N)$ which can also be expressed in terms of the bidegree $(d_z^{(0)}, d_{\bar{z}}^{(0)})$ of $|k,0\rangle$ as $d_z^{(0)} - d_{\bar{z}}^{(0)}$. For low-$k$ states we expect $d_{\bar{z}}^{(0)}$ to be at most of order $\mathcal{O}(N)$, and therefore $d_z^{(0)} = N^2/(2\nu) - N^2 + \mathcal{O}(N)$. Since $k = (d_z^{(0)} + d_{\bar{z}}^{(0)} + N - 1)/2$ we conclude that $\langle\hat{k}\rangle = N^2/(4\nu) - N^2/2 + \mathcal{O}(N) = N^2/(4n) + \mathcal{O}(N)$.

Returning to (3.3) we see that the average filling fraction, which we henceforth denote just by ν^*, is given by $\nu^* = n$. This is exactly the same result as in the composite fermion picture. In conclusion, if $\phi(\mathbf{z},\bar{\mathbf{z}})$ is a low-lying uniform density eigenstate of $\hat{K}_\Lambda^{(r)}$ then the average filling fraction of the lowest weight states appearing in its expansion is $\nu^* = n$ where $\nu = n/(2n+1)$. In particular, if n is an integer then the lowest weight states which dominate the expansion resemble the filling of n Landau levels.

Finally, we note that since the lowest weight states are homogeneous polynomials they are scale invariant and not explicitly dependent on any particular magnetic length. This neatly

resolves any questions regarding the "correct" magnetic field strength at which these states should be evaluated.

Returning to the problem of diagonalizing $\hat{K}^{(r)}_{\Lambda}$ we note that the task would be greatly simplified if Λ was invariant under $\hat{K}^{(r)}$. This would allow us to construct exact eigenstates of $\hat{K}^{(r)}$ in Λ of which the associated lowest weight states would resemble free particle eigenstates of the Landau problem. The $\mathcal{L}$ constraint, now transformed into the Λ constraint, makes this impossible: the expansion of $\phi(\mathbf{z},\bar{\mathbf{z}})$ always contains a complicated superposition of different $\hat{K}^{(r)}$ eigenstates. If we were to ignore this fact, as is done implicitly in the heuristic mean-field derivation of the composite fermion picture, we will have to resort to ad hoc projection procedures at a later stage. We therefore return to the general question posed at the end of Section 3.1 and investigate the possibility of relating the spectra and eigenvalues of $\hat{K}^{(r)}_{\Lambda}$ to that of $\hat{K}^{(r)}$.

3.3 Irreducible states

No sensible comparison between $\hat{K}^{(r)}_{\Lambda}$ and $\hat{K}^{(r)}$ is possible unless the domain of the latter is restricted to a subspace with the same dimensionality as Λ. In this section we define the notion of an irreducible state and argue that the subspace of such states should be taken as the domain of $\hat{K}^{(r)}$ if its relation to $\hat{K}^{(r)}_{\Lambda}$ is to become clear. Furthermore, these irreducible states will be seen to posses all the properties required of the physical free particle states described in Question 2 of Section 1.7.

Let $\mathcal{S}_k$ denote the space of translationally invariant lowest weight eigenstates of $\hat{K}^{(r)}$ with eigenvalue $k(k-1)$. We also define $\mathcal{S}_{<k} \equiv \bigoplus_{k'<k} \mathcal{S}_{k'}$ and refer to the elements of $\mathcal{S}_k$ as k-states. A k-state $\phi_k(\mathbf{z},\bar{\mathbf{z}}) \in \mathcal{S}_k$ is said to be *reducible* if $\mathcal{P}\phi_k(\mathbf{z},\bar{\mathbf{z}})J$ is zero or if there exists a state $\tilde{\phi}(\mathbf{z},\bar{\mathbf{z}}) \in \mathcal{S}_{<k}$ such that

$$\mathcal{P}\phi_k(\mathbf{z},\bar{\mathbf{z}})J = \mathcal{P}\tilde{\phi}(\mathbf{z},\bar{\mathbf{z}})J. \tag{3.4}$$

A state is therefore reducible if there exists a state with a lower degree which yields the same LLL state under the projection in (3.4). Note that only lowest weight states are considered in this definition since, by the discussion in Section 2.4.3, states with non-lowest weights are trivially reducible. The set of reducible k-states constitutes the subspace $\mathcal{R}_k$ of $\mathcal{S}_k$. *Irreducible* k-states are defined as those belonging to $\mathcal{I}_k$, the orthogonal complement of $\mathcal{R}_k$ in $\mathcal{S}_k$ and we denote the space of all such irreducible states by $\mathcal{I} = \bigoplus_k \mathcal{I}_k$. The following proposition proves that Λ and $\mathcal{I}$ are isomorphic and that $\mathcal{P}_{\Lambda}$ provides a one-to-one map from $\mathcal{I}$ onto Λ.

Proposition 3.3.1 *The kernel of $\mathcal{P}_\Lambda$ in $\mathcal{I}$ is trivial and $\Lambda \subseteq \mathcal{P}_\Lambda\mathcal{I}$. Therefore $\mathcal{P}_\Lambda : \mathcal{I} \to \Lambda$ is a bijection.*

Proof: First we make an observation regarding the projection of states onto Λ. Let

$$\{\psi_i(\mathbf{z}) = \sigma_i(\mathbf{z})\bar{J} \,:\, i = 1, 2, \ldots, \mathrm{Dim}(\Lambda)\}$$

be an arbitrary orthogonal basis for Λ. The projection of a $\phi(\mathbf{z}, \bar{\mathbf{z}}) \in \mathcal{I}$ then reads

$$\begin{aligned}\mathcal{P}_\Lambda\phi(\mathbf{z}, \bar{\mathbf{z}}) = \sum_i \left|\sigma_i(\mathbf{z})\bar{J}\right\rangle \left\langle\sigma_i(\mathbf{z})\bar{J}|\phi(\mathbf{z}, \bar{\mathbf{z}})\right\rangle &= \sum_i \left|\sigma_i(\mathbf{z})\bar{J}\right\rangle \left\langle\sigma_i(\mathbf{z})|\phi(\mathbf{z}, \bar{\mathbf{z}})J\right\rangle \\ &= \sum_i \left|\sigma_i(\mathbf{z})\bar{J}\right\rangle \left\langle\sigma_i(\mathbf{z})|\mathcal{P}\phi(\mathbf{z}, \bar{\mathbf{z}})J\right\rangle. \qquad (3.5)\end{aligned}$$

Note that the set $\{\sigma_i(\mathbf{z})\}$ forms a basis for the space of translationally invariant symmetric polynomials in $\mathbf{z}$; a space of which $\mathcal{P}\phi(\mathbf{z}, \bar{\mathbf{z}})J$ is a member. For $\mathcal{P}_\Lambda\phi(\mathbf{z}, \bar{\mathbf{z}})$ to be zero $\mathcal{P}\phi(\mathbf{z}, \bar{\mathbf{z}})J$ must therefore be zero.

With this in mind we can proceed to show that $\mathcal{P}_\Lambda\phi(\mathbf{z}, \bar{\mathbf{z}}) = 0$ implies $\phi(\mathbf{z}, \bar{\mathbf{z}}) = 0$ for any $\phi(\mathbf{z}, \bar{\mathbf{z}}) \in \mathcal{I}$. Suppose this was *not* the case, and that there exists a non-zero state $\phi(\mathbf{z}, \bar{\mathbf{z}}) = \sum_k \beta_k\phi_k(\mathbf{z}, \bar{\mathbf{z}})$ in $\mathcal{I}$ which lies in the kernel of $\mathcal{P}_\Lambda$. By the observation above this implies that $\mathcal{P}\phi(\mathbf{z}, \bar{\mathbf{z}})J = 0$. Since $\phi(\mathbf{z}, \bar{\mathbf{z}})$ is assumed to be non-zero its expansion in k-states must contain a unique non-zero highest k term $\beta_{k'}\phi_{k'}(\mathbf{z}, \bar{\mathbf{z}})$. However, from $\mathcal{P}_\Lambda\phi(\mathbf{z}, \bar{\mathbf{z}})J = 0$ we see that $\phi_{k'}(\mathbf{z}, \bar{\mathbf{z}})$ would then be reducible since

$$\phi_{k'}(\mathbf{z}, \bar{\mathbf{z}})J \overset{\mathcal{P}}{=} \frac{-1}{\beta_{k'}} \sum_{k<k'} \beta_k\phi_k(\mathbf{z}, \bar{\mathbf{z}})J \qquad (3.6)$$

where $\frac{-1}{\beta_{k'}} \sum_{k<k'} \beta_k\phi_k(\mathbf{z}, \bar{\mathbf{z}})$ is an element of $\mathcal{S}_{<k'}$. This contradicts the fact that $\phi_{k'}(\mathbf{z}, \bar{\mathbf{z}})$ is a non-zero element of $\mathcal{I}_k$. The kernel of $\mathcal{P}_\Lambda$ in $\mathcal{I}$ is therefore trivial.

Next we show that the projections of $\mathcal{I}$ states span Λ. If this was not the case there would exist a state

$$\phi(\mathbf{z}, \bar{\mathbf{z}}) = \sigma(\mathbf{z})\bar{J} = \sum_{k=k_0}^{m_r} \alpha_k d_{k,m_r-k} \hat{A}_+^{m_r-k}\phi_k(\mathbf{z}, \bar{\mathbf{z}}) \qquad (3.7)$$

with angular momentum $L_z^* = L_z - 2d_J$ in Λ which is orthogonal to the subspace $\mathcal{P}_\Lambda\mathcal{I}$. This is only possible if each $\phi_k(\mathbf{z}, \bar{\mathbf{z}})$ appearing in (3.7) is orthogonal to the corresponding space $\mathcal{I}_k$, i.e. each $\phi_k(\mathbf{z}, \bar{\mathbf{z}})$ must be an element of $\mathcal{R}_k$ and therefore be reducible. Suppose

$\alpha_{k'} d_{k',m_r-k'} \hat{A}_+^{m_r-k'} \phi_{k'}(\mathbf{z},\bar{\mathbf{z}})$ is the non-zero term with the lowest value of k appearing in (3.7). It follows that there must exist a state $\tilde{\phi}(\mathbf{z},\bar{\mathbf{z}}) \in \mathcal{S}_{<k'}$ such that

$$\phi_{k'}(\mathbf{z},\bar{\mathbf{z}})J \stackrel{\mathcal{P}}{=} \tilde{\phi}(\mathbf{z},\bar{\mathbf{z}})J \tag{3.8}$$

But this would imply that

$$\langle\phi(\mathbf{z},\bar{\mathbf{z}})|\phi_{k'}(\mathbf{z},\bar{\mathbf{z}})\rangle = \langle\sigma(\mathbf{z})\bar{J}|\phi_{k'}(\mathbf{z},\bar{\mathbf{z}})\rangle = \langle\sigma(\mathbf{z})|\phi_{k'}(\mathbf{z},\bar{\mathbf{z}})J\rangle = \langle\sigma(\mathbf{z})|\tilde{\phi}(\mathbf{z},\bar{\mathbf{z}})J\rangle = \langle\phi(\mathbf{z},\bar{\mathbf{z}})|\tilde{\phi}(\mathbf{z},\bar{\mathbf{z}})\rangle = 0 \tag{3.9}$$

where the final equality follows from the fact $\phi(\mathbf{z},\bar{\mathbf{z}})$ does not contain any k-components with $k < k'$. However, from (3.7) we also see that $\langle\phi(\mathbf{z},\bar{\mathbf{z}})|\phi_{k'}(\mathbf{z},\bar{\mathbf{z}})\rangle \propto \alpha_{k'}$ which immediately contradicts the assumption that the k' term in (3.7) is nonzero. It follows that such a non-zero $\phi(\mathbf{z},\bar{\mathbf{z}})$ cannot exist and that the projections of irreducible states indeed span Λ. ■

The projection $\mathcal{P}_\Lambda$ therefore provides a bijective map from the space of irreducible states $\mathcal{I}$ onto Λ and, through the unitary transformation U^2, also to $\mathcal{L}$. Let us summarize the properties of the irreducible states:

- By definition these states are translationally invariant and therefore contain no dependence on the centre of mass coordinates Z and $\bar{Z}$. This also implies that the centre of mass angular momentum $L_z^{(c)}$ of these states is zero.
- Each fixed angular momentum sector of $\mathcal{I}_k$ consists of degenerate eigenstates of the Landau problem with an energy of $d_{\bar{z}}$ units of cyclotron energy above the ground state. These states are homogeneous and scale invariant and are (the polynomial parts of) eigenstates of *any* Landau problem with a finite magnetic field.[10]
- The k-value of a state $\phi_k(\mathbf{z},\bar{\mathbf{z}}) \in \mathcal{I}_k$ is related to its bidegree $(d_z, d_{\bar{z}})$ by $k = (d_z + d_{\bar{z}} + N - 1)/2$ while its angular momentum is given by $L_z^* = L_z - 2d_J = d_z - d_{\bar{z}}$. For a fixed angular momentum minimizing k is therefore equivalent to minimizing $d_{\bar{z}}$ and states with low k values will resemble low energy Landau states in which Landau levels are filled from the bottom up. As shown in Section 3.2 this implies that $k = N^2/(4n) + \mathcal{O}(N^2)$ and the filling fraction of these low-k states are therefore $\nu^* = n$ where $\nu = n/(2n+1)$ is the filling fraction of the $\mathcal{L}$ states with angular momentum $L_z = L_z^* + 2d_J$. This is exactly

[10] Although the algebraic properties of the irreducible states allow for an interpretation in terms of free particle eigenstates of the Landau problem, this picture is not forced on us. It is largely a matter of convenience and serves to highlight the connection with the composite fermion framework. There is as yet no Landau Hamiltonian associated with these states.

the relation between ν and ν^* found in the composite fermion picture.

- We expect the number of such low k states to be severely limited by antisymmetry, i.e. the requirement that particles occupy different single particle states may by itself almost exhaust the total degree available to the many-body state, resulting in very little freedom as to which single particle states are occupied. For some values of the angular momentum we expect that, at least in the thermodynamic limit, there should exist a unique lowest k state which corresponds to an integer number of filled Landau levels. States of this form have already been identified as lowest weight states in Section 2.1.

Let us return to the problem of diagonalizing $\hat{K}^{(r)}_{\Lambda}$. It has been shown that Λ is isomorphic to the space of irreducible states $\mathcal{I}$ and that the latter is invariant under $\hat{K}^{(r)}$. Diagonalizing the restriction of $\hat{K}^{(r)}$ to $\mathcal{I}$, denoted by $\hat{K}^{(r)}_{\mathcal{I}} \equiv \hat{K}^{(r)}|_{\mathcal{I}}$, is therefore almost trivial: its eigenstates and eigenvalues are simply a subset of those of the unrestricted operator $\hat{K}^{(r)}$. A simple, intuitive characterisation of the irreducible states is still lacking, and generally we can only rely on the constraints imposed by the exclusion principle to identify the ground state of $\hat{K}^{(r)}_{\mathcal{I}}$ with a particular angular momenta.

In summary, we are confronted with an unsolvable problem $\hat{K}^{(r)}_{\Lambda}$ and a simpler, semi-solvable problem $\hat{K}^{(r)}_{\mathcal{I}}$ which involves the same operator restricted to different, though isomorphic, subspaces. Two separate questions now arise:

- Does there exist a procedure that allows accurate estimates of the low-lying eigenstates of $\hat{K}^{(r)}_{\Lambda}$ to be derived from those of $\hat{K}^{(r)}_{\mathcal{I}}$?
- What is the relation, if any, between the spectra of $\hat{K}^{(r)}_{\Lambda}$ and $\hat{K}^{(r)}_{\mathcal{I}}$? In particular, to what extent can the spectrum of $\hat{K}^{(r)}_{\Lambda}$ be considered as a perturbed version of that of $\hat{K}^{(r)}_{\mathcal{I}}$?

The rest of this chapter is devoted to investigating these questions.

3.4 The low lying eigenstates of $\hat{K}^{(r)}_{\Lambda}$

We wish to establish a mapping between the low-lying eigenstates of $\hat{K}^{(r)}_{\mathcal{I}}$ and those of $\hat{K}^{(r)}_{\Lambda}$. It has been shown that the projection $\mathcal{P}_{\Lambda}$ is a bijection from $\mathcal{I}$ to Λ and one may ask to what extent the projections of low-k $\hat{K}^{(r)}_{\mathcal{I}}$ eigenstates provide estimates for the low-lying eigenstates of $\hat{K}^{(r)}_{\Lambda}$. To formulate this question more precisely we first focus on a fixed angular momentum. Let $\mathcal{I}_{k^*}$ denote the lowest (smallest k) non-empty eigenspace of $\hat{K}^{(r)}_{\mathcal{I}}$ in the $L^*_z = L_z - 2d_J$ sector of $\mathcal{I}$. We are asking whether $\mathcal{P}_{\Lambda}\mathcal{I}_{k^*}$ provides an accurate basis for the subspace spanned by

the lowest $\mathrm{Dim}(\mathcal{I}_{k^*})$ eigenstates of $\hat{K}_\Lambda^{(r)}$ with angular momentum L_z^*. The numerical results presented later will show that this simple procedure indeed produces surprisingly accurate approximations to the true low-lying eigenstates of $\hat{K}_\Lambda^{(r)}$. However, this approach suffers from a number of serious drawbacks. Firstly, we have no simple expression for the projected state $\mathcal{P}_\Lambda\phi(\mathbf{z},\bar{\mathbf{z}})$ from which to gauge its qualitative properties or to compare with the composite fermions states in (1.20). Applying the projection also appears to require the calculation of all the inner products appearing in (3.5) which has to be done numerically and yields little insight into the nature of the projected state. Finally, projection using $\mathcal{P}_\Lambda$ fails to reproduce important special cases such as Laughlin's state for $\nu = 1/3$ which we will show is an *exact* eigenstate of $\hat{K}_\Lambda^{(r)}$. This motivates us to abandon this approach and seek an alternative mapping from $\mathcal{I}$ to Λ which is free of these drawbacks but still provides an equally good, or possibly better, description of the low lying eigenstates of $\hat{K}_\Lambda^{(r)}$.

3.4.1 Projection through antisymmetrisation

3.4.1.1 Characterising Λ

The first step in identifying this new mapping is to find an appropriate characterisation of the space Λ onto which $\mathcal{I}$ will be mapped. Recall that each element of Λ is the result of applying U^{-2} to a state in the LLL subspace $\mathcal{L}$. A natural approach is therefore to transform the defining property of lowest Landau level states, namely their independence of $\bar{\mathbf{z}}$, into a characterisation of Λ. The LLL constraint

$$\psi(\mathbf{z},\bar{\mathbf{z}}) \in \mathrm{LLL} \quad \Leftrightarrow \quad \partial_{\bar{z}_i}\psi(\mathbf{z},\bar{\mathbf{z}}) = 0 \qquad i = 1,2,\ldots,N \tag{3.10}$$

then translates into

$$\phi(\mathbf{z},\bar{\mathbf{z}}) \in \Lambda \quad \Leftrightarrow \quad U^{-2}\partial_{\bar{z}_i}U^2\phi(\mathbf{z},\bar{\mathbf{z}}) = \left[\partial_{\bar{z}_i} + \sum_{j\neq i}\frac{1}{\bar{z}_i - \bar{z}_j}\right]\phi(\mathbf{z},\bar{\mathbf{z}}) = 0 \qquad i = 1,2,\ldots,N. \tag{3.11}$$

Unfortunately this straightforward approach yields a result of little practical value since reconciling these rational expressions with our polynomial-state formalism poses technical difficulties. We therefore abandon this approach and instead seek a characterisation the states in Λ based solely on their symmetries and polynomial properties.

The form of a state $\phi(\mathbf{z},\bar{\mathbf{z}}) \in \Lambda$ with angular momentum $L_z^* = L_z - 2d_J$ is given by (3.1) as

$$\phi(\mathbf{z},\bar{\mathbf{z}}) = U^{-2}\psi(\mathbf{z}) = \sigma(\mathbf{z})\bar{J} \tag{3.12}$$

where $\sigma(\mathbf{z})$ is a symmetric polynomial and $\phi(\mathbf{z}, \bar{\mathbf{z}})$ has bidegree $(L_z - d_J, d_J)$. In Section 2.5.3 it was noted that the Vandermonde polynomial J is the unique antisymmetric polynomial in N variables with degree $d_J = N(N-1)/2$. *The subspace of* Λ *with angular momentum* $L_z^* = L_z - 2d_J$ *is therefore completely characterised by the bidegree* $(L_z - d_J, d_J)$ *and the fact that the states are respectively symmetric and antisymmetric in the* $\mathbf{z}$ *and* $\bar{\mathbf{z}}$ *variables.* In fact, we expect that antisymmetrisation in the $\bar{\mathbf{z}}$ variables of a polynomial with $d_{\bar{z}} = d_J$ will produce an element of Λ while Λ itself will be invariant under this procedure. The remainder of this section is dedicated to formalizing these ideas.

3.4.1.2 The antisymmetriser $\mathcal{A}_{\bar{z}}$

For each permutation $\rho \in S_N$ we define the operator $P_\rho^{(\bar{z})}$ which acts on a polynomial in $\mathbf{z}$ and $\bar{\mathbf{z}}$ by permuting the $\bar{\mathbf{z}} = (\bar{z}_1, \bar{z}_2, \ldots, \bar{z}_N)$ variables to $\rho(\bar{\mathbf{z}}) = (\bar{z}_{\rho(1)}, \bar{z}_{\rho(2)}, \ldots, \bar{z}_{\rho(N)})$ while leaving the $\mathbf{z}$'s unchanged. The antisymmetriser of the $\bar{\mathbf{z}}$ variables then reads

$$\mathcal{A}_{\bar{z}} = \frac{1}{N!} \sum_{\rho \in S_N} \mathrm{sgn}(\rho) P_\rho^{(\bar{z})}. \tag{3.13}$$

We note that $\mathcal{A}_{\bar{z}}$ preserves the existing symmetry or antisymmetry of a state with respect to the exchange of particle labels. In other words, $\mathcal{A}_{\bar{z}}$ does not alter the fermionic of bosonic nature of the states on which it acts. This implies that if $\phi(\mathbf{z}, \bar{\mathbf{z}})$ is symmetric (antisymmetric) with respect to particle exchange then $\mathcal{A}_{\bar{z}}\phi(\mathbf{z}, \bar{\mathbf{z}})$ must be antisymmetric (symmetric) in $\mathbf{z}$. The following three propositions lead to an analytic expression for the antisymmetrised state. We begin by identifying the correct domain of $\mathcal{A}_{\bar{z}}$.

Proposition 3.4.1 *Let* $\phi(\mathbf{z}, \bar{\mathbf{z}})$ *be a translationally invariant homogeneous polynomial with bidegree* $(d_z, d_{\bar{z}})$*. If* $d_{\bar{z}} < d_J$ *then* $\mathcal{A}_{\bar{z}}\phi(\mathbf{z}, \bar{\mathbf{z}}) = 0$*, while* $d_{\bar{z}} = d_J$ *guarantees that* $\mathcal{A}_{\bar{z}}\phi(\mathbf{z}, \bar{\mathbf{z}}) \in \Lambda$*.*

Proof: The first claim follows from the fact that d_J is the lowest possible degree of an antisymmetric polynomial in N variables. For the second we note that $\mathcal{A}_{\bar{z}}\phi(\mathbf{z}, \bar{\mathbf{z}})$ must contain $\bar{J}$ as a factor and that this already exhausts the total degree $d_{\bar{z}} = d_J$ in $\bar{\mathbf{z}}$. $\mathcal{A}_{\bar{z}}\phi(\mathbf{z}, \bar{\mathbf{z}})$ must therefore be the product of $\bar{J}$ and a translationally invariant symmetric polynomial in $\mathbf{z}$. This proves that $\mathcal{A}_{\bar{z}}\phi(\mathbf{z}, \bar{\mathbf{z}})$ is indeed an element of Λ. ■

Based on this proposition we will only consider the action of $\mathcal{A}_{\bar{z}}$ on states with $d_{\bar{z}} = d_J$. In particular, it is not sensible to apply $\mathcal{A}_{\bar{z}}$ directly to $\mathcal{I}$ since all the states for which $d_{\bar{z}} < d_J$ will simply be projected to zero. To identify the correct domain of $\mathcal{A}_{\bar{z}}$ we consider a basis of $\mathcal{I}$ consisting of eigenstates of $\hat{A}_{r0}$ with well-defined angular momentum. Each element of

such a basis is a homogeneous polynomial with a bidegree $(d_z, d_{\bar{z}})$ where $d_{\bar{z}} \leq d_J$. Applying $\hat{A}_{r+}$ to each element of this basis an appropriate number of times to raise its degree in $\bar{\mathbf{z}}$ to d_J yields a basis for the space we denote by $\bar{\mathcal{I}}$. Clearly $\mathcal{I}$ and $\bar{\mathcal{I}}$ are isomorphic and $\hat{K}^{(r)}$ has an identical spectrum in both. The natural domain of $\mathcal{A}_{\bar{z}}$ is therefore $\bar{\mathcal{I}}$. This technical point does not change the fact that we are considering mappings of exact eigenstates of $\hat{K}^{(r)}$ to Λ, nor the interpretation attached to the lowest weight states from which the elements of $\bar{\mathcal{I}}$ are constructed. The following two propositions lead to a simple analytic expression for the action of $\mathcal{A}_{\bar{z}}$ on an element of $\bar{\mathcal{I}}$. This will eventually also allow us to *define* $\mathcal{A}_{\bar{z}}$ directly on $\mathcal{I}$, making $\bar{\mathcal{I}}$ redundant.

Proposition 3.4.2 *If $\hat{A}_{r+}^{d_J}$ and $\hat{A}_{+}^{d_J}$ are treated as homogeneous polynomials in $\mathbf{z}$ and $\bar{\mathbf{z}}$ then their images under $\mathcal{A}_{\bar{z}}$ are*

$$\mathcal{A}_{\bar{z}}\hat{A}_{r+}^{d_J} = \mathcal{A}_{\bar{z}}\hat{A}_{+}^{d_J} = \frac{1}{N!}\binom{d_J}{0\ 1\ 2\ 3\ \cdots\ N-1} J\bar{J}. \tag{3.14}$$

Proof: The first equality follows from Proposition 3.4.1 and the fact that $\hat{A}_{r+}$ and $\hat{A}_{+}$ differ by $\hat{A}_{c+}$ which is completely symmetric in both $\mathbf{z}$ and $\bar{\mathbf{z}}$. The fact that $\hat{A}_{+}^{d_J}$ is symmetric with respect to particle exchange and has bidegree (d_J, d_J) immediately implies that $\mathcal{A}_{\bar{z}}\hat{A}_{+}^{d_J}$ must be proportional to $J\bar{J}$. The prefactor follows from a multinomial expansion of $\hat{A}_{+}^{d_J}$. See Section B.1 of the appendix for details. ■

The next result uses the antisymmetrised form of $\hat{A}_{r+}^{d_J}$ in (3.14) as a generating function to obtain a simple analytic expression for the action of $\mathcal{A}_{\bar{z}}$ on an element of $\mathcal{I}$.

Proposition 3.4.3 *If $\phi(\mathbf{z}, \bar{\mathbf{z}})$ is homogeneous with bidegree $(d_z, d_{\bar{z}})$ where $d_{\bar{z}} < d_J$ then*

$$\mathcal{A}_{\bar{z}}\left[\hat{A}_{r+}^{d_J - d_{\bar{z}}}\phi(\mathbf{z}, \bar{\mathbf{z}})\right] = \lambda(d_{\bar{z}})\bar{J}\phi[\mathbf{z}, \partial_{\mathbf{z}}]J \tag{3.15}$$

where

$$\lambda(d_{\bar{z}}) = \frac{(d_{\bar{z}} - d_J)!}{d_J!\, N!}\binom{d_J}{0\ 1\ 2\ 3\ \cdots\ N-1} \tag{3.16}$$

and $\phi[\mathbf{z}, \partial_{\mathbf{z}}]$ is derived from $\phi(\mathbf{z}, \bar{\mathbf{z}})$ by ordering the $\bar{\mathbf{z}}$ variables to the right before replacing them by derivatives acting on J.

Proof: Let $i_1, i_2, \ldots, i_{d_{\bar{z}}}$ be an arbitrary sequence of particle indices. Taking the derivatives to the corresponding $\mathbf{z}$ variables on both sides of (3.14) then yields

$$\mathcal{A}_{\bar{z}}\left[\hat{A}_{r+}^{d_J-d_{\bar{z}}}\bar{z}_{i_1}\bar{z}_{i_2}\cdots\bar{z}_{i_{d_{\bar{z}}}}\right] = \lambda(d_{\bar{z}})\bar{J}\prod_{n=1}^{d_{\bar{z}}}\partial_{z_{i_n}}J. \tag{3.17}$$

The expression in (3.15) now follows by first expanding $\phi(\mathbf{z},\bar{\mathbf{z}})$ in monomials and then applying $\mathcal{A}_{\bar{z}}$ to each term in $\hat{A}_{r+}^{d_J-d_{\bar{z}}}\phi(\mathbf{z},\bar{\mathbf{z}})$ before applying the identity above. ■

Note that (3.15) allows us to *define* $\mathcal{A}_{\bar{z}}$ directly on $\mathcal{I}$ as $\mathcal{A}_{\bar{z}}\phi(\mathbf{z},\bar{\mathbf{z}}) \equiv \lambda(d_{\bar{z}})\bar{J}\phi[\mathbf{z},\partial_{\mathbf{z}}]J$ for all homogeneous $\phi(\mathbf{z},\bar{\mathbf{z}}) \in \mathcal{I}$. Also note that since $\phi(\mathbf{z},\bar{\mathbf{z}})$ is a lowest weight state it follows from (2.37) that $\phi[\mathbf{z},\partial_{\mathbf{z}}]J = \phi[\partial_{\mathbf{z}},\mathbf{z}]J$. Up to a factor of $2^{d_{\bar{z}}}$ this is just $\mathcal{P}\phi(\mathbf{z},\bar{\mathbf{z}})J$, the projection of $\phi(\mathbf{z},\bar{\mathbf{z}})J$ onto the (bosonic) lowest Landau level.

Proposition 3.4.4 *$\mathcal{A}_{\bar{z}}$ is a bijective map from $\mathcal{I}$ to Λ.*

Proof: From 3.3.1 it is known that $\mathrm{Dim}(\mathcal{I}) = \mathrm{Dim}(\Lambda)$, and all that remains is to show that the kernel of $\mathcal{A}_{\bar{z}}$ on $\mathcal{I}$ is trivial. If this was not the case there would exist a nonzero $\phi(\mathbf{z},\bar{\mathbf{z}}) \in \mathcal{I}$ such that $\mathcal{A}_{\bar{z}}\phi(\mathbf{z},\bar{\mathbf{z}}) = 0$. This would imply the existence of a $\tilde{\phi}(\mathbf{z},\bar{\mathbf{z}}) \in \mathcal{I}$ for which $\mathcal{P}\tilde{\phi}(\mathbf{z},\bar{\mathbf{z}})J = 0$ and, through the same argument used to prove Proposition 3.3.1, would lead to the contradictory conclusion that $\mathcal{I}$ contains reducible states. The kernel of $\mathcal{A}_{\bar{z}}$ in $\mathcal{I}$ is therefore trivial and $\mathcal{A}_{\bar{z}}$ is a bijective map between $\mathcal{I}$ and Λ. ■

The representation of the symmetric group in terms of permutations of the $\bar{\mathbf{z}}$ variables is not unitary and the antisymmetrisation operator $\mathcal{A}_{\bar{z}}$ is therefore not Hermitian. The following result relates the matrix elements of $\mathcal{A}_{\bar{z}}$ to that of its adjoint $\mathcal{A}_{\bar{z}}^\dagger$.

Proposition 3.4.5 *Consider two lowest weight states $\phi_k(\mathbf{z},\bar{\mathbf{z}})$ and $\phi_{k'}(\mathbf{z},\bar{\mathbf{z}})$ with eigenvalues $k(k-1)$ and $k'(k'-1)$ with respect to $\hat{K}^{(r)}$ and degrees $d_{\bar{z}} \leq d_J$ and $d'_{\bar{z}} \leq d_J$ in $\bar{\mathbf{z}}$ respectively. Both $\phi_k(\mathbf{z},\bar{\mathbf{z}})$ and $\phi_{k'}(\mathbf{z},\bar{\mathbf{z}})$ have angular momentum $L_z^* = L_z - 2d_J$. The matrix elements of $\mathcal{A}_{\bar{z}}$ and its adjoint $\mathcal{A}_{\bar{z}}^\dagger$ are then related by*

$$\frac{\langle\hat{A}_{r+}^{m_r-k'}\phi_{k'}(\mathbf{z},\bar{\mathbf{z}})|\mathcal{A}_{\bar{z}}|\hat{A}_{r+}^{m_r-k}\phi_k(\mathbf{z},\bar{\mathbf{z}})\rangle}{\Gamma(m_r+k)\Gamma(m_r-k+1)} = \frac{\langle\hat{A}_{r+}^{m_r-k'}\phi_{k'}(\mathbf{z},\bar{\mathbf{z}})|\mathcal{A}_{\bar{z}}^\dagger|\hat{A}_{r+}^{m_r-k}\phi_k(\mathbf{z},\bar{\mathbf{z}})\rangle}{\Gamma(m_r+k')\Gamma(m_r-k'+1)} \tag{3.18}$$

where $m_r - k = d_J - d_{\bar{z}}$ and $m_r - k' = d_J - d'_{\bar{z}}$ with $m_r = (L_z + N - 1)/2$.

Proof: See Section B.2 of the appendix.

3.4.1.3 Discussion

Let us summarize the state of affairs. Early in the chapter we considered the projection $\mathcal{P}_\Lambda$ which provided a bijective mapping from $\mathcal{I}$ to Λ. However, as outlined in Section 3.4, the usefulness of $\mathcal{P}_\Lambda$ is limited by the lack of an explicit analytic expression for the images of the irreducible states under projection. This led us introduce the antisymmetrisation operator $\mathcal{A}_{\bar{z}} : \mathcal{I} \to \Lambda$ for which the action on a $\mathcal{I}$ state had a simple algebraic form analogous to that of composite fermion states. This is encouraging, but a fundamental question remains: *why do we expect $\mathcal{A}_{\bar{z}}$ to produce better estimates of the low-lying eigenstates of $\hat{K}^{(r)}_\Lambda$ than the conceptually simpler mapping $\mathcal{P}_\Lambda$?* The equivalence between $\hat{K}^{(r)}_\Lambda$ and the projected interaction suggests that this question can also be phrased as: *why is the Jastrow-Slater structure observed in the composite fermion wave functions and in (3.15) so successful at minimizing the energy of the projected interaction?*

The key to answering these questions is provided by Proposition 3.4.5 and is most easily understood in the context of the space $\mathcal{K}$ of states with $d_{\bar{z}} = d_J$ and a fixed angular momentum $L^*_z = L_z - 2d_J$. Note that $\mathcal{K}$ contains the L^*_z sectors of both Λ and $\bar{\mathcal{I}}$ and that $\hat{A}_{r0}$ takes a constant value of $m_r = (L_z + N - 1)/2$ on $\mathcal{K}$. Next we define $\hat{k}$ through $\hat{K}^{(r)} \equiv \hat{k}(\hat{k} - 1)$ and introduce the operator

$$\hat{\eta}(\hat{k}) = [(m_r - \hat{k})!\Gamma(m_r + \hat{k})] \tag{3.19}$$

which acts on $\mathcal{K}$. The result of Proposition 3.4.5 implies that $\mathcal{A}_{\bar{z}}$ and $\mathcal{A}^\dagger_{\bar{z}}$ are related by

$$\mathcal{A}^\dagger_{\bar{z}} = \hat{\eta}(\hat{k})\mathcal{A}_{\bar{z}}\hat{\eta}^{-1}(\hat{k}) \tag{3.20}$$

and the operator $\mathcal{A}_{\bar{z}}$ is therefore Hermitian with respect to the inner product

$$\langle \phi_1(\mathbf{z}, \bar{\mathbf{z}}) | \phi_2(\mathbf{z}, \bar{\mathbf{z}}) \rangle_\eta \equiv \langle \phi_1(\mathbf{z}, \bar{\mathbf{z}}) | \hat{\eta}(\hat{k}) | \phi_2(\mathbf{z}, \bar{\mathbf{z}}) \rangle \tag{3.21}$$

defined on $\mathcal{K}$. We conclude that antisymmetrisation in $\bar{\mathbf{z}}$ is equivalent to the projection of states from $\bar{\mathcal{I}}$ onto Λ using the modified inner product $\langle \cdot | \cdot \rangle_\eta$. What distinguished $\langle \cdot | \cdot \rangle_\eta$ from the original $\langle \cdot | \cdot \rangle$ which appear in (2.13) are the different weights it attaches to the various eigenspaces of $\hat{K}^{(r)}$. The relative weights associated with two consecutive eigenspaces corresponding to k and $k + 1$ is given by

$$\frac{\eta(k+1)}{\eta(k)} = \frac{(m_r - k - 1)!\,\Gamma(m_r + k + 1)}{(m_r - k)!\,\Gamma(m_r + k)}. \tag{3.22}$$

From the discussion in Section 3.2 we have, to highest order in N, that $m_r = N^2/(4\nu) + \mathcal{O}(N)$

while $k = N^2/(4\nu) - N^2/2 + \mathcal{O}(N)$ and therefore $k/m_r = 1 - 2\nu + \mathcal{O}(1/N)$. Applying Stirling's approximation to (3.22) produces, in the large N limit,

$$\frac{\eta(k+1)}{\eta(k)} = \frac{1}{\nu} - 1 > 1. \tag{3.23}$$

The weights that $\langle\cdot|\cdot\rangle_\eta$ attaches to the eigenstates of $\hat{K}^{(r)}$ therefore increase exponentially with k.

Let us consider the implications of this measure for the projection of $\mathcal{I}$ states onto Λ. In general the projection of some vector v onto a subspace S is equivalent to finding the subspace element $s \in S$ which minimizes $||s - v|| = \sqrt{(s - v, s - v)}$, where the particular inner product features explicitly in the definition of the distance metric. The inner product therefore determines the "cost function" $||s - v||$ which is to be minimized by the choice of $s \in S$. Since the measure of $\langle\cdot|\cdot\rangle_\eta$ is an exponentially increasing function of $\hat{k}$ using $\mathcal{A}_{\bar{z}}$ to project $\phi_{k'}(\mathbf{z}, \bar{\mathbf{z}}) \in \mathcal{I}$ onto Λ amounts to a minimisation procedure where a very large penalty is placed on non-zero k-components with $k > k'$ appearing in $\mathcal{A}_{\bar{z}}\phi_{k'}(\mathbf{z}, \bar{\mathbf{z}})$. Projecting $\phi_{k'}(\mathbf{z}, \bar{\mathbf{z}})$ onto Λ using $\mathcal{A}_{\bar{z}}$ therefore produces a state in which accuracy in the low k-sectors has been sacrificed in order to suppress the appearance of higher $k > k'$ components. This is precisely what we require to construct an approximate basis for the subspace of low lying eigenstates of $\hat{K}^{(r)}_\Lambda$. Just as finding the ground state of $\hat{K}^{(r)}_\Lambda$ represents a non-trivial minimisation problem so too does finding the projection of $\phi_{k'}(\mathbf{z}, \bar{\mathbf{z}}) \in \mathcal{I}$ onto Λ in the $\eta(k)$ metric. However, whereas the former problem has no analytic solution we *do* have an explicit expression for the latter in the form of (3.15). It will be clear from numerical results that this procedure is indeed superior to using the standard projection $\mathcal{P}_\Lambda$.

We also note the similarity between the procedure

$$\phi(\mathbf{z}, \bar{\mathbf{z}}) \xrightarrow{\mathcal{A}_{\bar{z}}} \bar{J}\phi[\mathbf{z}, \partial_{\mathbf{z}}]J \xrightarrow{U^2} J\phi[\mathbf{z}, \partial_{\mathbf{z}}]J \tag{3.24}$$

which yields a LLL state, and its analogue in the composite fermion picture

$$\phi(\mathbf{z}, \bar{\mathbf{z}}) \to \mathcal{P}\phi(\mathbf{z}, \bar{\mathbf{z}})J^2 = \phi[\mathbf{z}, 2\partial_{\mathbf{z}}]J^2. \tag{3.25}$$

In fact, if $\phi(\mathbf{z}, \bar{\mathbf{z}})$ is at most linear in $\bar{\mathbf{z}}$ these two constructions yield the same LLL state up to a constant.

Next we consider the important special case of $\nu = 1/3$ before returning to two of the questions posed in Section 1.7.

3.4.1.4 Laughlin's state for $\nu = 1/3$

Consider a system in the LLL with $\nu = 1/3$ and $L_z = 3d_J$. The corresponding angular momentum in Λ and $\mathcal{I}$ is $L_z^* = L_z - 2d_J = d_J$ and the unique lowest k state in $\mathcal{I}$ is therefore the Vandermonde polynomial J. The result of projecting J onto Λ using the $\langle\cdot|\cdot\rangle_\eta$ inner product is proportional to $J^2\bar{J}$. This is a Λ state in which the higher k-components are suppressed and which should be a good approximation to the lowest eigenstate of $\hat{K}_\Lambda^{(r)}$. In fact, applying U^2 to recover the corresponding LLL state yields $\psi(\mathbf{z}) = J^3$ which is precisely the Laughlin state for $\nu = 1/3$. Surprisingly, $J^2\bar{J}$ also turns out to be an *exact* eigenstate of $\hat{K}_\Lambda^{(r)}$ in the $L_z^* = d_J$ sector. A proof of this fact appears in Section 4.2.4 of the next chapter.

3.4.2 Question 2: Physical free particle states

In Section 1.7 we posed the question: *How are the physical free particle states characterised and what are their properties?* Based on the properties listed in Section 3.3 it is natural to identify $\mathcal{I}$ as the space of physical free particle states. It is both isomorphic to Λ and spanned by eigenstates of the free particle Landau Hamiltonian with the low-lying states exhibiting an effective filling fraction of $\nu^* = n$. Since the elements of $\mathcal{I}$ are also lowest weight states each irrep of $su(1,1)$ contributes *at most* one physical state. This eliminates a huge number of spurious states since all the elements of an irreducible subspace would have been mapped, up to constant factors, onto the *same* LLL state by $\mathcal{A}_{\bar{z}}$.

These observations suggest a classification scheme in which physical states are identified with $su(1,1)$ irreps constructed on the space of antisymmetric polynomial states. However, not all lowest weight states are irreducible and therefore not all irreps correspond to physical states. A complete classification scheme phrased in representation theory language requires further investigation of the connections between the representations of $su(1,1)$ and symmetry group acting on the $\bar{\mathbf{z}}$ variables.

3.4.3 Question 3: Effective Landau levels and the LLL constraint

In Section 1.7 we posed the question: *How do we reconcile the need for higher effective Landau levels with the LLL constraint in a way that avoids ad hoc projections or the need to speculate about the overlap of states with the LLL?* The $\bar{\mathbf{z}}$ coordinates, which are the mathematical signature of higher Landau levels, were introduced through the unitary transformation

$U^{-2} = \bar{J}/J$ which mapped $\mathcal{L}$ onto Λ. The LLL constraint itself is transformed into the restriction that Λ states may only depend on $\bar{\mathbf{z}}$ through a factor of $\bar{J}$. At first, the $\mathcal{O}(N^2)$ powers of $\bar{\mathbf{z}}$ contained in $\bar{J}$ appeared to rule out a simple connection to free particles occupying low-lying effective Landau levels. However, as explained in Section 3.2 the free particle states appear as the lowest weight states in the expansion (3.2). Motivated by this we introduced the space $\mathcal{I}$ of physical free particle states. Antisymmetrisation in $\bar{\mathbf{z}}$ was used to define a mapping from $\mathcal{I}$ back to Λ by restoring the $\bar{J}$ factor. This procedure suppresses higher-k components and automatically generates two Vandermonde polynomial factors which are reminiscent of the Jastrow factor. The $\bar{\mathbf{z}}$ variables are then removed by applying the inverse transformation U^2. The fact that Vandermonde polynomial factors are generated by a mapping which produces low-lying eigenstates of $\hat{K}^{(r)}_{\Lambda}$ already hints the central theme of the next chapter: *the projected Casimir operator is equivalent to an interacting system with strongly repulsive interactions.*

The irreducible states in $\mathcal{I}$ are guaranteed to have a non-zero overlap[11] with Λ, but the actual magnitude of this overlap does not appear to be relevant to the construction. The $\mathcal{A}_{\bar{z}}$ projection maps low-k states in $\mathcal{I}$ onto approximations to the low-lying eigenstates of $\hat{K}^{(r)}_{\Lambda}$ regardless of the $\mathcal{I}$-state's overlap with Λ prior to projection. In the composite fermion construction there are concerns regarding the LLL projection and the possibly destructive effect it may have on the favourable Jastrow correlations. In contrast, the anti-symmetrisation projection actually *generates* these correlations automatically in our approach.

3.4.4 Numerical Results

Exact numerical calculations for a system of six particles allows the results obtained using the projection procedures $\mathcal{A}_{\bar{z}}$ and $\mathcal{P}_{\Lambda}$ to be compared with those of the composite fermion picture. In each angular momentum sector we project the elements of the lowest non-empty eigenspace of $\hat{K}^{(r)}_{\mathcal{I}}$ (denoted $\mathcal{I}_{k^*}$) onto Λ using either $\mathcal{A}_{\bar{z}}$ or $\mathcal{P}_{\Lambda}$ and then diagonalise $\hat{K}^{(r)}_{\Lambda}$ within the resulting subspace. In the composite fermion case we start with the lowest eigenspace of $\hat{K}^{(r)}$ in $\mathcal{S} = \oplus_k \mathcal{S}_k$ and apply (3.25) followed by U^{-2} to obtain the subspace in which $\hat{K}^{(r)}_{\Lambda}$ is diagonalised[12].

As before we use L_z to denote the angular momentum of a LLL state and $L^*_z = L_z - 2d_J$ for that of its Λ or $\mathcal{I}$ counterpart. For comparison with later results it is convenient to rep-

[11] If $\mathcal{P}_{\Lambda}\phi(\mathbf{z}, \bar{\mathbf{z}}) = 0$ then $\mathcal{P}\phi(\mathbf{z}, \bar{\mathbf{z}})J = 0$ and $\phi(\mathbf{z}, \bar{\mathbf{z}})$ is reducible by definition.

[12] Actually, the alternative representations of $\hat{K}^{(r)}_{\Lambda}$ derived in the next chapter allow us to skip the last step and work directly with the LLL states.

resent quantities as functions of $L_z = L_z^* + 2d_J$ rather than L_z^*. Figure 3.1 (a) shows the exact spectrum of $\hat{K}_\Lambda^{(r)}$ together with the approximations obtained by diagonalizing $\hat{K}_\Lambda^{(r)}$ in the subspace obtained using $\mathcal{A}_{\bar{z}}$. The agreement with exact results is clearly very good with errors of a fraction of a percent. Table 3.1 summarizes the percentage errors in the ground state eigenvalues as well as the overlaps with the true ground state in each angular momentum sector. For $L_z \geq 39$ and $L_z \neq 46$ the ground states of $\hat{K}_\mathcal{I}^{(r)}$ are at most linear in $\bar{\mathbf{z}}$ and the results constructed using $\mathcal{A}_{\bar{z}}$ are identical to those of the composite fermion construction. For L_z below 39 the two approaches differ and while both produce very good results neither appear to gain a clear advantage. It is not known whether this trend continues as N increases or if one of the two eventually gains the upper hand. The ground state itself is also reproduced with a very high degree of accuracy by both methods, with overlaps never dropping below 0.99. Finally we note that in the majority of cases the standard projection $\mathcal{P}_\Lambda$ fares markedly worse than the other two methods. This is due to the standard projection measure not weighing the higher k-sectors more heavily. Also note the low dimensionality of the fixed angular momentum sectors in $\mathcal{I}_{k^*}$ compared to that in Λ.

Applying $\mathcal{A}_{\bar{z}}$ to the bases of the lowest *two* eigenspaces of $\hat{K}_\mathcal{I}^{(r)}$ in each L_z sector provides an enlarged subspace in which to diagonalise $\hat{K}_\Lambda^{(r)}$ and will yield a better description of its low-lying spectrum. The results of this calculation appear in Figure 3.1 (b). Percentage errors in the ground state energy decrease by about an order of magnitude while overlaps with the true ground states are found to be consistently larger than 0.9996.

			GSEV Percentage Error			Overlap with exact GS		
L_z	Dim(Λ)	Dim($\mathcal{I}_{k^*}$)	$\mathcal{A}_{\bar{z}}$	CF	$\mathcal{P}_\Lambda$	$\mathcal{A}_{\bar{z}}$	CF	$\mathcal{P}_\Lambda$
19	5	1	0.0250	0	0.0421	0.99936	1.00000	0.99892
20	7	1	0.0351	0.3143	0.2079	0.99931	0.99378	0.99589
21	11	1	0.0195	0.4449	0.2135	0.99974	0.99428	0.99725
22	14	3	0.0302	0	0.0024	0.99950	1.00000	0.99995
23	20	2	0.0601	0.0162	0.0081	0.99893	0.99982	0.99992
24	26	1	0.0785	0.7676	0.5052	0.99869	0.98605	0.99117
25	35	1	0.2046	0.4367	0.3717	0.99714	0.99372	0.99506
26	44	3	0.1092	0.1060	0.3135	0.99808	0.99852	0.99515
27	58	2	0.2703	0.3352	0.3588	0.99501	0.99636	0.99457
28	71	5	0.1020	0.0819	0.1319	0.99826	0.99801	0.99749
29	90	2	0.1303	0.4521	0.4192	0.99811	0.99311	0.99335
30	110	1	0.3436	0.2670	0.1481	0.99535	0.99698	0.99853
31	136	3	0.2000	0.4237	1.3860	0.99655	0.99354	0.97645
32	163	7	0.1325	0.1722	0.5223	0.99739	0.99657	0.97643
33	199	2	0.3687	0.3476	0.5990	0.99315	0.99490	0.99133
34	235	4	0.1947	0.2497	0.7388	0.99615	0.99566	0.98867
35	282	1	0.1193	0.1853	0.8238	0.99839	0.99738	0.98877
36	331	2	0.1621	0.2076	1.6140	0.99665	0.99621	0.97041
37	391	5	0.0852	0.1287	0.8226	0.99871	0.99791	0.98472
38	454	9	0.0525	0.0768	0.5174	0.99916	0.99868	0.99132
39	532	1	0.1151	0.1151	1.0210	0.99798	0.99798	0.98415
40	612	2	0.0904	0.0904	1.4500	0.99803	0.99803	0.97674
41	709	4	0.0835	0.0835	1.1320	0.99815	0.99815	0.97926
42	811	7	0.0579	0.0579	0.6990	0.99883	0.99883	0.98545
43	931	12	0.0566	0.0566	0.3605	0.99870	0.99870	0.99171
44	1057	18	0.0422	0.0422	0.3800	0.99908	0.99908	0.99210
45	1206	1	0	0	1.1270	1.00000	1.00000	0.98026
46	1360	39	0.0087	0.0087	0.2300	0.99978	0.99978	0.99459
47	1540	2	0.0125	0.0125	1.3120	0.99962	0.99962	0.97328
48	1729	3	0.0217	0.0217	1.1090	0.99936	0.99936	0.97344
49	1945	5	0.0194	0.0194	0.5858	0.99946	0.99946	0.98482
50	2172	7	0.0192	0.0192	0.6268	0.99945	0.99945	0.98273
51	2432	11	0.0080	0.0080	0.2420	0.99979	0.99979	0.99399

Table 3.1: Comparison of exact diagonalisation results for $N = 6$ particles with the predictions of the three methods described in the text. The angular momentum of the Λ states are $L_z^* = L_z - 2d_J$.

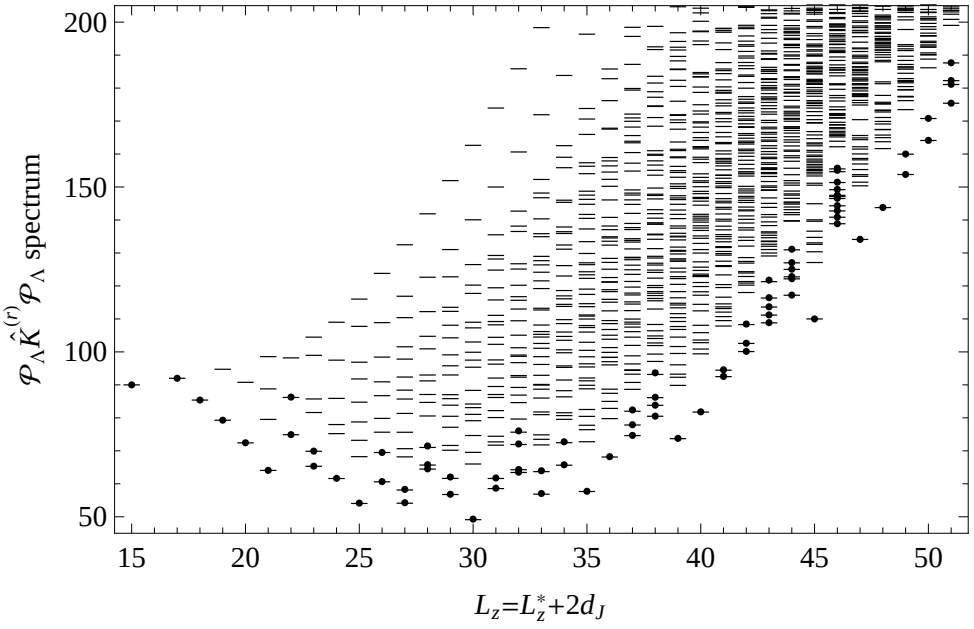

(a)

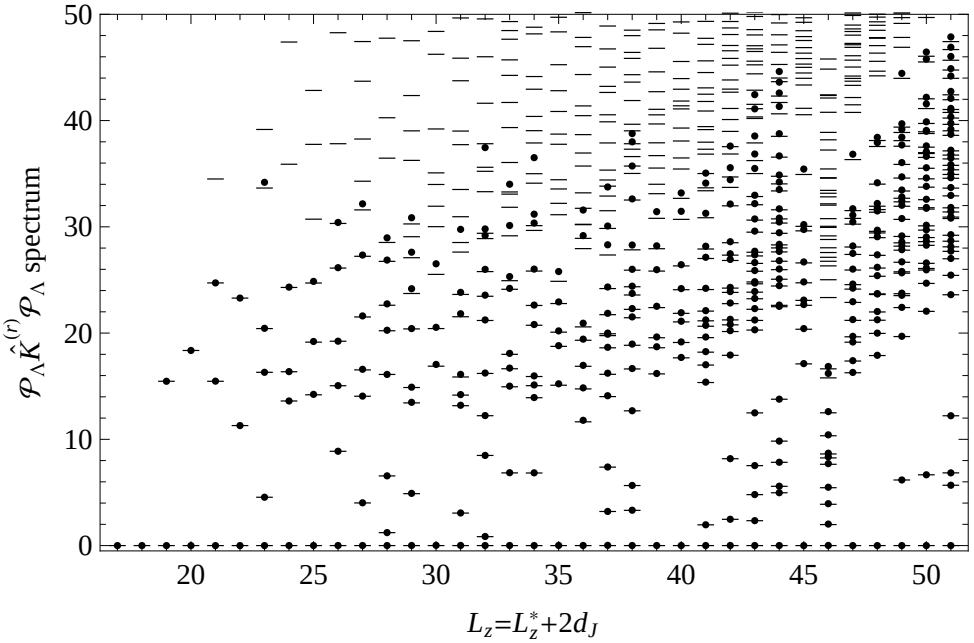

(b)

Figure 3.1: (a) The exact spectrum of $\hat{K}_\Lambda^{(r)}$ (bars) together with the estimates (dots) obtained by diagonalizing $\hat{K}_\Lambda^{(r)}$ in the $\mathcal{A}_{\bar{z}}$ projection of the lowest eigenspace of $\hat{K}_\mathcal{I}^{(r)}$ in each angular momentum sector. (b) As in (a) but where the lowest two non-empty $\hat{K}_\mathcal{I}^{(r)}$ eigenspaces are used. For clarity the eigenvalues in each sector has been shifted downward by the corresponding exact ground state eigenvalue. In the $L_z^* = 16$ ($L_z = 46$) sector only the lowest non-empty $\mathcal{I}_k$ was used.

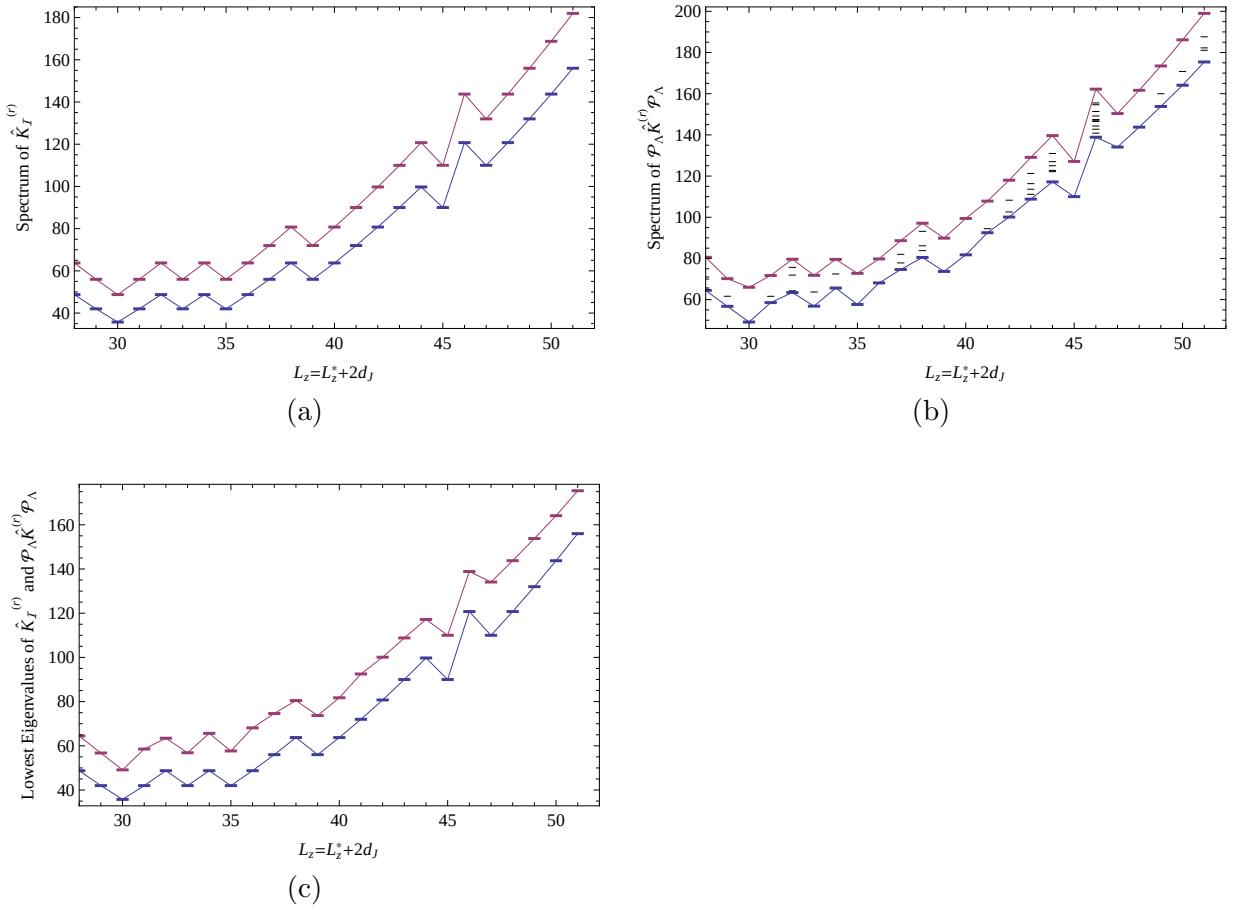

Figure 3.2: (a) The lowest two eigenvalues of $\hat{K}_{\mathcal{I}}^{(r)}$ in each angular momentum sector. Each bar represents a set of degenerate states. (b) The first $\mathrm{Dim}(\mathcal{I}_{k*})+1$ eigenvalues of $\hat{K}_{\Lambda}^{(r)}$ in each angular momentum sector. The largest and smallest eigenvalue in each sector are shown in bold. (c) The lowest eigenvalues of $\hat{K}_{\mathcal{I}}^{(r)}$ (bottom) and $\hat{K}_{\Lambda}^{(r)}$ (top) for each L_z sector. We see that the difference between the two sets of eigenvalues varies slowly amongst neighbouring sectors.

3.5 The spectrum of $\hat{K}_{\Lambda}^{(r)}$

The projection scheme set out in the previous section provides very accurate estimates of the low-lying eigenstates of $\hat{K}_{\Lambda}^{(r)}$. In contrast, systematic approximations to the eigenvalues are still lacking, a situation mirrored in the composite fermion approach. The aim of this section is to arrive at a conjecture regarding the low-lying spectrum of $\hat{K}_{\Lambda}^{(r)}$ which will allow us to make predictions regarding the excitation gaps of interacting quantum Hall systems. These predictions can be verified through comparison with the results of extensive numerical studies.

The question posed at the beginning of the chapter is whether there exists any relation between the spectra of $\hat{K}_{\Lambda}^{(r)}$ and $\hat{K}_{\mathcal{I}}^{(r)}$. In particular, we are interested in the extent to which

the spectrum of $\hat{K}^{(r)}_{\Lambda}$ may be regarded as a perturbed version of that of $\hat{K}^{(r)}_{\mathcal{I}}$. Recall that since $\hat{K}^{(r)}$ leaves $\mathcal{I}$ invariant the spectrum of $\hat{K}^{(r)}_{\mathcal{I}}$ is simply a subset of that of the unrestricted $\hat{K}^{(r)}$. However, although $\mathcal{I}$ only contains lowest weight states the spectrum of $\hat{K}^{(r)}_{\mathcal{I}}$ will still contain degeneracies since the space of anti-symmetric polynomials carries multiple copies of the same $su(1,1)$ irrep. A priori there is little reason to expect the spectrum of $\hat{K}^{(r)}_{\Lambda}$ to bear any resemblance to that of $\hat{K}^{(r)}_{\mathcal{I}}$ since the constraint to Λ may enforce a large amount of mixing between the different eigenspaces of $\hat{K}^{(r)}$. In particular, quantities such as the difference between the eigenvalues of two states should be treated with care, since they are of a lower order in N than the eigenvalues themselves. To proceed we must therefore introduce a conjecture which relates these two spectra. For this purpose numerical results provide some guidance. Figure 3.2 (a) shows the lowest two distinct eigenvalues of $\hat{K}^{(r)}_{\mathcal{I}}$ in each angular momentum sector. Each bar therefore represents a set of degenerate eigenstates. Figure 3.2 (b) is the analogous picture for the spectrum of $\hat{K}^{(r)}_{\Lambda}$ where the lowest $\mathrm{Dim}(\mathcal{I}_{k*}) + 1$ eigenvalues per sector are shown. We associate the first $\mathrm{Dim}(\mathcal{I}_{k*})$ states with the "broadened" set of degenerate states belonging to $\mathcal{I}_{k*}$. The $\mathrm{Dim}(\mathcal{I}_{k*}) + 1$'st state is taken to be the state at the bottom of the band formed by the "broadened" set of $\mathcal{I}_{k*+1}$ states. The states at the bottom of each band is shown in bold and are connected amongst the different angular momentum sectors. When compared in this way there is a striking similarity between the spectrum of $\hat{K}^{(r)}_{\mathcal{I}}$ and the lowest states in each of the first two bands of $\hat{K}^{(r)}_{\Lambda}$. The restriction to Λ therefore appears to shift the spectrum of neighbouring angular momentum sectors by a constant and cause an *upwards* broadening of the degenerate levels. Put differently, it appears that the "cost of constraint", i.e. by how much the ground state eigenvalue of $\hat{K}^{(r)}_{\Lambda}$ is greater than that of $\hat{K}^{(r)}_{\mathcal{I}}$, varies slowly from one angular momentum sector to the next. Based on these observations we introduce the following conjecture:

Conjecture: *Suppose* $k(k-1)$ *and* $k'(k'-1)$ *are the lowest eigenvalues of* $\hat{K}^{(r)}_{\mathcal{I}}$ *in the* L^*_z *and* $L^{*\prime}_z$ *angular momentum sectors respectively, and that* $L^*_z - L^{*\prime}_z = \mathcal{O}(N^0)$. *The difference between the ground state eigenvalues of* $\hat{K}^{(r)}_{\Lambda}$ *in these two sectors is then approximately* $k(k-1) - k'(k'-1)$. *In other words, the projection onto* Λ *does not result in a significant* ***relative*** *change in the ground state energies of neighbouring angular momentum sectors.*

3.6 Summary of the relevant states, spaces and mappings

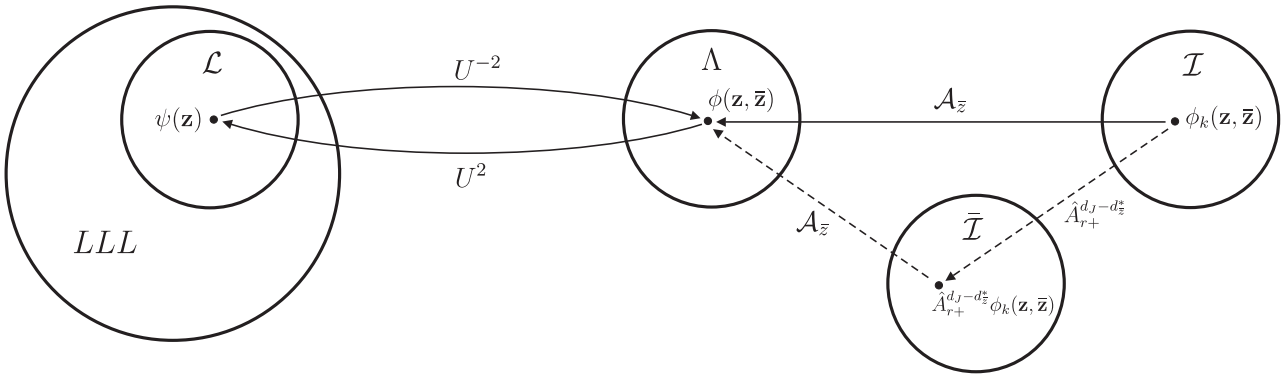

Spaces:

- LLL: the lowest Landau level of the free particle Hamiltonian $\hat{H}_L$ with magnetic field $B\hat{\mathbf{z}}$.
- $\mathcal{L}$: the translationally invariant sector of the LLL.
- Λ: the image of $\mathcal{L}$ under $U^{-2} = \bar{J}/J$.
- $\mathcal{I}$: the space of irreducible/physical states. It is spanned by a subset $B_{\mathcal{I}}$ of $\hat{K}^{(r)}$ eigenstates. It is isomorphic to Λ through the mapping $\mathcal{A}_{\bar{z}}$ and projection $\mathcal{P}_\Lambda$ (not shown).
- $\bar{\mathcal{I}}$: the space obtained by raising the degree of each element of the basis $B_{\mathcal{I}}$ to d_J by applying $\hat{A}_{r+}$ an appropriate number of times.

Representative states:

- $\psi(\mathbf{z}) \in \mathcal{L}$ is an antisymmetric homogeneous polynomial in $\mathbf{z} = (z_1, \ldots, z_N)$ with degree d_z and angular momentum $L_z = d_z$. Its filling fraction ν is determined by $L_z = N^2/(2\nu) + \mathcal{O}(N)$. Furthermore, $\psi(\mathbf{z})$ is factorizable as $\psi(\mathbf{z}) = \sigma(\mathbf{z})J$ where J the Vandermonde polynomial.
- $\phi(\mathbf{z},\bar{\mathbf{z}}) = U^{-2}\psi(\mathbf{z}) = \sigma(\mathbf{z})\bar{J} \in \Lambda$ is a homogeneous polynomial with bidegree $(L_z - d_J, d_J)$ and angular momentum $L_z^* = L_z - 2d_J$. It is generally *not* an eigenstate of $\hat{K}^{(r)}$.
- $\phi_k(\mathbf{z},\bar{\mathbf{z}}) \in \mathcal{I}$ is a lowest weight eigenstate of $\hat{K}^{(r)}$ (and $\hat{H}_L$) with eigenvalue $k(k-1)$ and angular momentum $L_z^* = L_z - 2d_J$. Its filling fraction $\nu^* = n$ is related to that of $\psi(\mathbf{z})$ through $\nu = n/(2n+1)$. It is homogeneous with degrees $d_z^* = k + L_z/2 - N/2$ and $d_{\bar{z}}^* = k - L_z/2 - N/2$. It is mapped onto $\phi(\mathbf{z},\bar{\mathbf{z}})$ as $\phi(\mathbf{z},\bar{\mathbf{z}}) = \mathcal{A}_{\bar{z}}\phi_k(\mathbf{z},\bar{\mathbf{z}}) \propto \bar{J}\phi_k[\mathbf{z},\partial_{\mathbf{z}}]J$.
- $\hat{A}_{r+}^{d_J-d_{\bar{z}}^*}\phi_k(\mathbf{z},\bar{\mathbf{z}}) \in \bar{J}$ is an eigenstate of $\hat{K}^{(r)}$ with eigenvalue $k(k-1)$ and angular momentum $L_z^* = L_z - 2d_J$. It is used in an intermediate step to first define $\mathcal{A}_{\bar{z}}$ on $\bar{\mathcal{I}}$ as the antisymmetriser of the $\bar{\mathbf{z}}$ variables.

CHAPTER 4
The projected interaction

In this chapter we return to the problem of an interacting system in the LLL and establish the connection with the framework developed in Chapters 2 and 3. At the centre of this discussion are three seemingly unrelated operators: the Casimir operator $\hat{K}^{(r)}$, a two- plus three-body interaction and the Chern-Simons Hamiltonian $\hat{H}_{CS}$. These operators are such that their projections onto Λ (for the first) and $\mathcal{L}$ (for the latter two) represent equivalent problems. Any knowledge regarding the spectrum or eigenstates of one can therefore be applied to the other two. The results obtained while studying $\hat{K}^{(r)}_{\Lambda}$ will serve as a starting point for investigating the projections of $\hat{H}_{CS}$ and of the many-body interaction. It is the latter that will ultimately allow us to relate $\hat{K}^{(r)}_{\Lambda}$ to a system of particles interacting in the LLL via a two-body potential.

4.1 The Chern-Simons Hamiltonian

The Hamiltonian[13]

$$\hat{H}_{CS} = \frac{1}{2m_e}\sum_i \Big(\mathbf{p}_i - \frac{e}{c}\alpha\mathbf{A}_i - \frac{e}{c}\boldsymbol{\mathcal{A}}_i\Big)^2 \tag{4.1}$$

is derived from the free particle Landau Hamiltonian of Section 2.1 by weakening the magnetic field by a factor of $\alpha \in [0,1]$ and introducing the Chern-Simons gauge field $\boldsymbol{\mathcal{A}}_i$. The latter is a configuration dependent vector potential of the form

$$\boldsymbol{\mathcal{A}}_i = \hat{\mathbf{z}} \times \frac{2p\phi_0}{2\pi}\sum_{j\neq i}\frac{\mathbf{r}_i - \mathbf{r}_j}{|\mathbf{r}_i - \mathbf{r}_j|^2} \equiv \hat{\mathbf{z}} \times \frac{2p\phi_0}{2\pi\ell}\boldsymbol{\mathcal{E}}(\mathbf{r}_i) \tag{4.2}$$

where $\boldsymbol{\mathcal{E}}(\mathbf{r}_i) \equiv \ell\sum_{j\neq i}(\mathbf{r}_i - \mathbf{r}_j)/|\mathbf{r}_i - \mathbf{r}_j|^2$ is a dimensionless vector field and the parameters p and α are related by $\alpha = 1 - 2p\nu$. Note that, even in the context of the weakened field $\alpha B\hat{\mathbf{z}}$, quantities such as the filling fraction ν, magnetic length and cyclotron frequency will remain defined in terms of the *original* field strength B. The magnetic field corresponding to $\boldsymbol{\mathcal{A}}_i$ is

$$\mathcal{B}(\mathbf{r}) = 2p\phi_0\sum_i \delta(\mathbf{r} - \mathbf{r}_i) \tag{4.3}$$

which amounts to the attachment of a singular flux tube carrying $2p$ fundamental flux quanta to each particle [19]. At an average particle density of $\bar{\rho} = \nu/(2\pi\ell^2)$ the flux density due to

[13] This Hamiltonian is equivalent to $\hat{H}_{MF}$ of Section 1.6.3. We use a different notation to separate our construction from the mean-field approach of 1.6.3. The parameters are related by $\alpha B = B^*$ and $\alpha\mathbf{A}_i = \mathbf{A}^*_i$.

these attachments is $2p\phi_0\bar{\rho} = 2p\nu B$. The relation $\alpha = 1 - 2p\nu$ therefore ensures that the total flux present in $\hat{H}_{CS}$ matches that of the Landau problem with magnetic field $B\hat{\mathbf{z}}$. In this sense the Chern-Simons and Landau Hamiltonians differ by a redistribution of the same nett amount of flux. This becomes apparent when $\hat{H}_{CS}$ is written as

$$\hat{H}_{CS} = \frac{1}{2m_e}\sum_i \left(\mathbf{p}_i - \frac{e}{c}\mathbf{A}_i - \frac{e}{c}\delta\boldsymbol{\mathcal{A}}_i\right)^2 \tag{4.4}$$

with

$$\delta\boldsymbol{\mathcal{A}}_i = \boldsymbol{\mathcal{A}}_i - 2p\nu\mathbf{A}_i = \hat{\mathbf{z}}\times\frac{2p\phi_0}{2\pi\ell}\left[\boldsymbol{\mathcal{E}}(\mathbf{r}_i) - \frac{\nu}{2}\frac{\mathbf{r}_i}{\ell}\right] \equiv \hat{\mathbf{z}}\times\frac{2p\phi_0}{2\pi\ell}\delta\boldsymbol{\mathcal{E}}(\mathbf{r}_i) \tag{4.5}$$

and where $2p\nu\mathbf{A}_i$ is the mean-field average[14] of $\mathcal{A}_i$ for a uniform particle density $\bar{\rho} = \nu/(2\pi\ell^2)$. Since the $\delta\boldsymbol{\mathcal{A}}_i$ term corresponds to the fluctuations of the Chern-Simons gauge field about its mean-field value the average flux density associated with it is zero.

As shown in Section 1.6.3 the Chern-Simons vector potential can also be expressed as the result of a singular gauge transformation [19] of the form

$$\hat{H}_{CS} = \frac{1}{2m_e}\sum_i U^{2p}\left(\mathbf{p}_i - \frac{e}{c}\alpha\mathbf{A}_i\right)^2 U^{-2p} \tag{4.6}$$

where $U = J/|J|$ and $J = \prod_{i<j}(z_i - z_j)$ is the Vandermonde polynomial. For integer p this transformation will preserve the fermion statistics of the electrons and the spectrum of $\hat{H}_{CS}$ will therefore be identical to that of a free particle Landau problem with magnetic field $\alpha B\hat{\mathbf{z}}$. The latter is denoted by $\hat{H}_L^{(\alpha)}$ instead of $\hat{H}_L^{(*)}$ as used previously. We consider the $p = 1$ case with $1/3 \leq \nu < 1/2$ in what follows.

4.2 The LLL projection of $\hat{H}_{CS}$

The aim of this section is to establish a relation between the lowest Landau level projection of $\hat{H}_{CS}$ and the projected Casimir operator $\hat{K}_\Lambda^{(r)} \equiv \mathcal{P}_\Lambda\hat{K}^{(r)}\mathcal{P}_\Lambda$ studied in Chapter 3. Comparing the forms of $\hat{H}_{CS}$ in (4.4) and $\hat{H}_L$ in (2.1) makes it clear that any non-trivial contribution to $\mathcal{P}\hat{H}_{CS}\mathcal{P}$ must be related to fluctuations in the Chern-Simons gauge field.

As defined above $\hat{H}_{CS}$ acts on the full wave function with exponential factor included. To conform to our polynomial state formalism we must determine the action of $\hat{H}_{CS}$ on the polynomial part $\phi(\mathbf{z}, \bar{\mathbf{z}})$ of wave function alone. Applying the same procedure as used in (2.5)

[14] This can be seen using an electrostatic analogy in which $\boldsymbol{\mathcal{E}}(\mathbf{r}_i)$ is the electric field of point charges in two dimensions. The "electric field" $\nu\mathbf{r}_i/(2\ell)$ then corresponds to that of a uniform neutralizing background charge.

yields[15]

$$\hat{H}^{\mathbb{P}}_{CS} = e^{+\sum_i z_i \bar{z}_i/4} \hat{H}_{CS} e^{-\sum_i z_i \bar{z}_i/4} = \hbar\omega_c \sum_i \left[2 \left(\partial_{\bar{z}_i} + \delta\bar{\mathcal{E}}_i \right)^\dagger \left(\partial_{\bar{z}_i} + \delta\bar{\mathcal{E}}_i \right) + \frac{\alpha}{2} \right]. \tag{4.7}$$

Here

$$\mathcal{E}_i = \sum_{j \neq i} \frac{1}{z_i - z_j} \qquad \text{and} \qquad \delta\mathcal{E}_i = \mathcal{E}_i - \frac{\nu}{2} \bar{z}_i \tag{4.8}$$

are the dimensionless complex variables formed using the components of the vectors $\boldsymbol{\mathcal{E}}(\mathbf{r}_i)$ and $\delta\boldsymbol{\mathcal{E}}(\mathbf{r}_i)$. These expressions are generated in (4.7) through

$$U^2 \partial_{\bar{z}_i} U^{-2} = \partial_{\bar{z}_i} + \bar{\mathcal{E}}_i \qquad \text{and} \qquad U^2 \partial_{z_i} U^{-2} = \partial_{z_i} - \mathcal{E}_i. \tag{4.9}$$

In what follows we will deal exclusively with operators acting on polynomial states. To simplify notation we drop the $\mathbb{P}$ superscript in $\hat{H}^{\mathbb{P}}_{CS}$ and take $\hat{H}_{CS}$ to represent the operator on the right-hand side of (4.7).

Since the lowest Landau level of $\hat{H}_L$ consists of polynomials in $\mathbf{z}$ alone it follows that

$$\hat{H}_{CS} \overset{\mathcal{P}}{=} \frac{\hbar\omega_c}{2} \left[4 \sum_i \delta\bar{\mathcal{E}}_i \delta\mathcal{E}_i + \alpha N \right] \overset{\mathcal{P}}{=} \frac{\hbar\omega_c}{2} \left[\frac{1}{\ell^2 B^2} \sum_i |\delta\boldsymbol{\mathcal{A}}_i|^2 + \alpha N \right] \tag{4.10}$$

where $\overset{\mathcal{P}}{=}$ denotes equality under LLL projection. Within the LLL the Chern-Simons Hamiltonian is therefore equal, up to constants, to the square of the fluctuations in the gauge field. As shown above the latter may be expressed either in vector form or in terms of complex coordinates. Note that the relations in (4.10) also hold for projection onto the translationally invariant LLL subspace $\mathcal{L}$. In the next section we will use these equivalent representations of $\mathcal{P}_\mathcal{L} \hat{H}_{CS} \mathcal{P}_\mathcal{L}$ to establish the desired connection with $\hat{K}^{(r)}_\Lambda$.

4.2.1 Relating $\mathcal{P}_\mathcal{L} \hat{H}_{CS} \mathcal{P}_\mathcal{L}$ and $\hat{K}^{(r)}_\Lambda$

The space obtained by applying U^{-2} to $\mathcal{L}$ is denoted by Λ. Since $\delta\bar{\mathcal{E}}_i$ and $\delta\mathcal{E}_i$ do not contain any derivatives they commute with U^2 and $\mathcal{P}_\mathcal{L} \sum_i \delta\bar{\mathcal{E}}_i \delta\mathcal{E}_i \mathcal{P}_\mathcal{L}$ is therefore unitarily equivalent to

[15] Note that the exponential factor involved in this transformation still corresponds to the original magnetic field strength B.

$\mathcal{P}_\Lambda \sum_i \delta\bar{\mathcal{E}}_i\delta\mathcal{E}_i\mathcal{P}_\Lambda$. Noting that $\sum_i z_i\mathcal{E}_i = \sum_i \bar{z}_i\bar{\mathcal{E}}_i = N(N-1)/2$ allows us to write

$$\sum_i \delta\bar{\mathcal{E}}_i\delta\mathcal{E}_i = \sum_i \bar{\mathcal{E}}_i\mathcal{E}_i + \left(\frac{\nu}{2}\right)^2 \sum_i \bar{z}_i z_i - \frac{\nu}{2}N(N-1) \tag{4.11}$$

$$\overset{\mathcal{P}_\Lambda}{=} \sum_i \bar{\mathcal{E}}_i\mathcal{E}_i + \frac{\nu^2}{2}(2\hat{A}_{r0}+1) - \frac{\nu}{2}N(N-1) \tag{4.12}$$

where the second line follows from (2.22) and the fact that $\hat{A}_{c0}$ takes a constant value of $1/2$ on Λ. Furthermore, since the $\bar{\mathbf{z}}$ dependence of states in Λ take the form of a factor of $\bar{J}$ it follows that $\partial_{\bar{z}_i}\phi(\mathbf{z},\bar{\mathbf{z}}) = \bar{\mathcal{E}}_i\phi(\mathbf{z},\bar{\mathbf{z}})$ for all $\phi(\mathbf{z},\bar{\mathbf{z}}) \in \Lambda$. This observation allows us to replace $\bar{\mathcal{E}}_i\mathcal{E}_i$ by $\partial^\dagger_{\bar{z}_i}\partial_{\bar{z}_i}$ and rewrite (4.12) as

$$\sum_i \delta\bar{\mathcal{E}}_i\delta\mathcal{E}_i \overset{\mathcal{P}_\Lambda}{=} \sum_i \partial^\dagger_{\bar{z}_i}\partial_{\bar{z}_i} + \frac{\nu^2}{2}(2\hat{A}_{r0}+1) - \frac{\nu}{2}N(N-1) \tag{4.13}$$

$$\overset{\mathcal{P}_\Lambda}{=} -\hat{A}_{r-} + \frac{\nu^2}{2}(2\hat{A}_{r0}+1) + \frac{\alpha}{4}N(N-1) \tag{4.14}$$

where $\partial^\dagger_{\bar{z}_i} = -\partial_{z_i} + \bar{z}_i/2$ and we used the fact that $\hat{A}_{c-} = 0$ and $\sum_i \bar{z}_i\partial_{\bar{z}_i} = d_J$ on Λ.

The next step is most easily performed by first restricting the discussion to a subspace Λ' of Λ with fixed angular momentum $L_z^* = L_z - 2d_J$. Since $\hat{A}_{r0}$ takes a constant value of $m_r = (L_z + N - 1)/2$ on Λ' it follows that if $\phi(\mathbf{z},\bar{\mathbf{z}}) \in \Lambda'$ then $\hat{A}_{r-}\phi(\mathbf{z},\bar{\mathbf{z}})$ is an eigenstate of $\hat{A}_{r0}$ with eigenvalue $m_r - 1$. This observation and the identity in (2.22) implies that

$$-\hat{A}_{r-} \overset{\mathcal{P}_{\Lambda'}}{=} \frac{\hat{K}^{(r)}}{4m_r - 2} - \frac{m_r(m_r-1)}{4m_r-2}. \tag{4.15}$$

Since none of these operators couple states with different angular momenta this generalises to the full Λ space as

$$-\hat{A}_{r-} \overset{\mathcal{P}_\Lambda}{=} \frac{\hat{K}^{(r)}}{4\hat{A}_{r0} - 2} - \frac{\hat{A}_{r0}(\hat{A}_{r0}-1)}{4\hat{A}_{r0}-2}. \tag{4.16}$$

Returning to $\mathcal{P}_\mathcal{L}\hat{H}_{CS}\mathcal{P}_\mathcal{L}$ in (4.10) and combining these results lead to

$$\frac{\mathcal{P}_\mathcal{L}\hat{H}_{CS}\mathcal{P}_\mathcal{L}}{\hbar\omega_c} = \mathcal{P}_\mathcal{L}\left[2\sum_i \delta\bar{\mathcal{E}}_i\delta\mathcal{E}_i + \frac{\alpha N}{2}\right]\mathcal{P}_\mathcal{L} \overset{U^{-2}}{\Longrightarrow} \mathcal{P}_\Lambda\left[\frac{\hat{K}^{(r)}}{2\hat{A}_{r0}-1} + \hat{C}(\hat{A}_{r0},\nu)\right]\mathcal{P}_\Lambda \tag{4.17}$$

where $\hat{C}(\hat{A}_{r0},\nu) = \Big[\hat{A}_{r0}(1-\hat{A}_{r0})/(2\hat{A}_{r0}-1) + \nu^2(2\hat{A}_{r0}+1) + (1-2\nu)N^2/2\Big]$. Note that since $\hat{A}_{r0}$ is constant within a fixed angular momentum sector of Λ the only non-trivial contribution to the right hand side of (4.17) is $\hat{K}^{(r)}_\Lambda$ itself. This is the desired result which relates the LLL

projections of $\hat{H}_{CS}$ and $\sum_i \delta\bar{\mathcal{E}}_i\delta\mathcal{E}_i$ to the projection of the $su(1,1)$ Casimir operator into Λ. All the results of Chapter 3 can now be applied to the former two problems.

The next step is to investigate how closely $\sum_i \delta\bar{\mathcal{E}}_i\delta\mathcal{E}_i$ resembles a repulsive two-body interaction. This is the topic of Section 4.3. The intermediate subsections contain some clarifying remarks and proofs of claims made in previous chapters.

4.2.2 A remark on extensions and projections

Of course, the fact that operators which differ on the entire Hilbert space may share the same projection within a subspace is not surprising. The usefulness of 4.17 lies in recognising that the various equivalent representations amount to different *extensions* of the same projected operator to a larger Hilbert space. In other words, $\hat{H}_{CS}$, $\sum_i \delta\bar{\mathcal{E}}_i\delta\mathcal{E}_i$ and $\hat{K}^{(r)}$ are all, up to constants, different extensions of the same operator in $\mathcal{L}$ or Λ. While the problem of diagonalizing $\mathcal{P}_{\mathcal{L}}\hat{H}_{CS}\mathcal{P}_{\mathcal{L}}$ is not exactly solvable, determining the eigenstates and eigenvalues of the extensions are almost trivial in comparison. The caveat here is that the spectrum of the extension (or any subset thereof) may bear no resemblance at all to that of the projected operator itself. However, if we could identify an appropriate extension of which the spectrum and eigenstates resemble those of the projected operator in some restricted sense we may be able to make some progress by treating the projection itself as a perturbation. For example, the $\hat{K}^{(r)}$ extension has allowed us to find very accurate (and well motivated) approximations to the low-lying eigenstates of $\mathcal{P}_{\mathcal{L}}\sum_i \delta\bar{\mathcal{E}}_i\delta\mathcal{E}_i\mathcal{P}_{\mathcal{L}}$ and also to formulate a conjecture regarding its low lying spectrum. It seems very unlikely that we would have arrived at those results by considering $\mathcal{P}_{\mathcal{L}}\sum_i \delta\bar{\mathcal{E}}_i\delta\mathcal{E}_i\mathcal{P}_{\mathcal{L}}$ in isolation.

4.2.3 The expectation value of $\hat{k}$ for uniform density states

In Section 3.2 it was claimed that $\langle\hat{k}\rangle = N^2/(4n) + \mathcal{O}(N)$ where $\hat{K}^{(r)} = \hat{k}(\hat{k}-1)$. Using the representations of $\hat{K}^{(r)}_{\Lambda}$ in (4.17) we can now prove the following:

Proposition 4.2.1 *If $\langle\hat{k}\rangle$ is the expectation value of $\hat{k}$ with respect to a low-lying eigenstate of $\hat{K}^{(r)}_{\Lambda}$ then $\langle\hat{k}\rangle = N^2/(4n) + \mathcal{O}(N)$ with $\nu = n/(2n+1)$ the filling fraction of the corresponding $\mathcal{L}$ state.*

Proof: Equation (4.17) provides a relation between the corresponding expectation values $\langle\hat{K}^{(r)}_{\Lambda}\rangle$ and $\langle\sum_i \delta\bar{\mathcal{E}}_i\delta\mathcal{E}_i\rangle$. The latter operator is quadratic in the density fluctuations and therefore expected to scale extensively in the sector of low energy uniform density states. It follows that $\langle 2\sum_i \delta\bar{\mathcal{E}}_i\delta\mathcal{E}_i + \alpha N/2\rangle$ is extensive and, through (4.17), so too $\Theta \equiv \langle\hat{K}^{(r)}/(2\hat{A}_{r0}-1) + \hat{C}(\hat{A}_{r0},\nu)\rangle$.

However, $\langle \hat{A}_{r0} \rangle = (L_z + N - 1)/2 = N^2/(4\nu) + \mathcal{O}(N)$ and therefore a precise cancellation of $\mathcal{O}(N^2)$ terms is necessary to ensure that Θ is linear in N. This constraint will allow us to determine the scaling behaviour of $\langle \hat{K}^{(r)} \rangle$ and $\langle \hat{k} \rangle$.

Since $\langle \hat{A}_{r0} \rangle = N^2/(4\nu) + \mathcal{O}(N)$ we find that $\langle \hat{C}(\hat{A}_{r0}, \nu) \rangle = -(1-2v)^2 N^2/(8v) + \mathcal{O}(N)$ and therefore $\langle \hat{K}^{(r)} \rangle / (2\langle \hat{A}_{r0} \rangle - 1) = (1-2v)^2 N^2/(8v) + \mathcal{O}(N)$ must hold for the $\mathcal{O}(N^2)$ terms in Θ to cancel. Solving for $\langle \hat{K}^{(r)} \rangle$ yields $\langle \hat{K}^{(r)} \rangle = N^4/(16n^2) + \mathcal{O}(N^3)$ and since $\hat{K}^{(r)} = \hat{k}(\hat{k}-1)$ we conclude that $\langle \hat{k} \rangle = N^2/(4n) + \mathcal{O}(N)$. ■

4.2.4 Laughlin's state for $\nu = 1/3$

Next we revisit the claim made in Section 3.4.1.4 and consider the implications of (4.17) for a system at $L_z = 3d_J$ and $\nu = 1/3$. The results of Section 3.4.1 suggest that the ground state of $\hat{K}^{(r)}_\Lambda$ is well approximated by the image of $\phi(\mathbf{z}, \bar{\mathbf{z}}) = J$ under the antisymmetrisation projection $\mathcal{A}_{\bar{z}}$. This yields $\mathcal{A}_{\bar{z}} J \propto J^2 \bar{J}$ which is the Λ counterpart of Laughlin's LLL state $\psi(\mathbf{z}) = J^3$. The latter provides an approximation to the ground state of $\mathcal{P}_\mathcal{L} \hat{H}_{CS} \mathcal{P}_\mathcal{L}$, or equivalently, to the state which minimizes the fluctuations in the Chern-Simons gauge field. It turns out that $L_z = 3d_J$ is a special case where this approximation yields an *exact* eigenstate of the operators appearing in (4.17). To prove this we first note that by (4.12) and (4.17) this statement is equivalent to the claim that $J^2\bar{J}$ is an eigenstate of $\mathcal{P}_\Lambda \sum_i \bar{\mathcal{E}}_i \mathcal{E}_i \mathcal{P}_\Lambda$, i.e. that for all $\sigma(\mathbf{z})\bar{J} \in \Lambda$ it holds that

$$\langle \sigma(\mathbf{z})\bar{J} | \sum_i \bar{\mathcal{E}}_i \mathcal{E}_i | J^2 \bar{J} \rangle = \lambda \langle \sigma(\mathbf{z})\bar{J} | J^2 \bar{J} \rangle. \tag{4.18}$$

Combining the facts that $\partial_{\bar{z}_i} \bar{J} = \bar{\mathcal{E}}_i \bar{J}$, $\partial^\dagger_{\bar{z}_i} = -\partial_{z_i} + \bar{z}_i/2$ and $\sum_i \bar{z}_i \bar{\mathcal{E}}_i = N(N-1)/2$ allows us to rewrite the right hand side of (4.18) as

$$\begin{aligned} \langle \sigma(\mathbf{z})\bar{J} | \sum_i \mathcal{E}_i \bar{\mathcal{E}}_i | J^2 \bar{J} \rangle &= \langle \sigma(\mathbf{z})\bar{J} | \sum_i \partial^\dagger_{\bar{z}_i} \bar{\mathcal{E}}_i | J^2 \bar{J} \rangle & (4.19) \\ &= -2\langle \sigma(\mathbf{z})\bar{J} | \sum_i \mathcal{E}_i \bar{\mathcal{E}}_i | J^2 \bar{J} \rangle + \frac{N(N-1)}{4} \langle \sigma(\mathbf{z})\bar{J} | J^2 \bar{J} \rangle & (4.20) \end{aligned}$$

from which it immediately follows that

$$\langle \sigma(\mathbf{z})\bar{J} | \sum_i \mathcal{E}_i \bar{\mathcal{E}}_i | J^2 \bar{J} \rangle = \frac{N(N-1)}{12} \langle \sigma(\mathbf{z})\bar{J} | J^2 \bar{J} \rangle. \tag{4.21}$$

This translates into an eigenvalue for $\mathcal{P}_\mathcal{L} \sum_i \delta\bar{\mathcal{E}}_i \delta\mathcal{E}_i \mathcal{P}_\mathcal{L}$ of $N/18$ and for $\mathcal{P}_\mathcal{L} \hat{H}^\mathbb{P}_{CS} \mathcal{P}_\mathcal{L}/(\hbar\omega_c)$ of $5N/18$.

To summarize, the Laughlin state $\psi(\mathbf{z}) = J^3$ (together with its Λ counterpart) is an exact eigenstate of the operators appearing in (4.17). In fact, it is expected to be the ground state itself. This is supported by numerical results but a general analytic proof is still lacking. However, if $\psi(\mathbf{z}) = J^3$ is not the true ground state the two would have be orthogonal; a conclusion which is incompatible with numerical results.

4.3 Gauge field fluctuations as an effective two-body interaction

We are interested in studying an interacting system in the LLL, a problem which may appear to have been largely absent from the discussion thus far. In this section we establish the link between the three equivalent operators in (4.17) and a repulsive two-body interaction within the LLL. As starting point we consider $\mathcal{P}_{\mathcal{L}} \sum_i \delta\bar{\mathcal{E}}_i \delta\mathcal{E}_i \mathcal{P}_{\mathcal{L}}$ which contains interaction terms involving up to three particles. The goal is to identify the dominant two-particle interaction present in $\sum_i \delta\bar{\mathcal{E}}_i \delta\mathcal{E}_i$. Separating this contribution from $\sum_i \delta\bar{\mathcal{E}}_i \delta\mathcal{E}_i$ should then allow us to treat whatever remains within a simpler approximation. First we expand $\sum_i \delta\bar{\mathcal{E}}_i \delta\mathcal{E}_i$ as

$$\sum_i \delta\bar{\mathcal{E}}_i \delta\mathcal{E}_i = \sum_i \bar{\mathcal{E}}_i \mathcal{E}_i + \left(\frac{\nu}{2}\right)^2 \sum_i \bar{z}_i z_i - \frac{\nu}{2} N(N-1) \tag{4.22}$$

and then rewrite the first term in vector notation as

$$\sum_i \bar{\mathcal{E}}_i \mathcal{E}_i = \sum_i \boldsymbol{\mathcal{E}}(\mathbf{r}_i) \cdot \boldsymbol{\mathcal{E}}(\mathbf{r}_i) = \ell^2 \sum_i \left[\sum_{j\neq i} \mathbf{E}(\mathbf{r}_i - \mathbf{r}_j)\right] \cdot \left[\sum_{k\neq i} \mathbf{E}(\mathbf{r}_i - \mathbf{r}_k)\right] \tag{4.23}$$

where $\mathbf{E}(\mathbf{r}) = \hat{\mathbf{r}}/|\mathbf{r}|$. Separating this expression into two and three-body terms yields

$$\sum_i \bar{\mathcal{E}}_i \mathcal{E}_i \;=\; \sum_{i\neq j} \frac{\ell^2}{|\mathbf{r}_i - \mathbf{r}_j|^2} + \ell^2 \sum_{i\neq j\neq k} \mathbf{E}(\mathbf{r}_i - \mathbf{r}_j) \cdot \mathbf{E}(\mathbf{r}_i - \mathbf{r}_k) \tag{4.24}$$

where the first term represents a repulsive two-body interaction. The interpretation of the second term is less straightforward and to allow for a sensible comparison with the first we must approximate it by an effective two-body interaction $V_{\text{eff}}(r)$. The details of this construction appear in Section C of the appendix. In short, it is based on a mean-field approximation which incorporates basic features of the interparticle correlations. The construction is very robust and the form of $V_{\text{eff}}(r)$ is insensitive to the details of the approximations. Figures 4.1 (a) and (b) compare the interactions $V_{\text{eff}}(r)$ and $1/r^2$ as functions of r and in terms of their pseudopotentials. $V_{\text{eff}}(r)$ is found to be repulsive and approximately logarithmic at large distances while at short distances it is bounded and varies slowly. This suggests that the strongly repulsive $1/r^2$

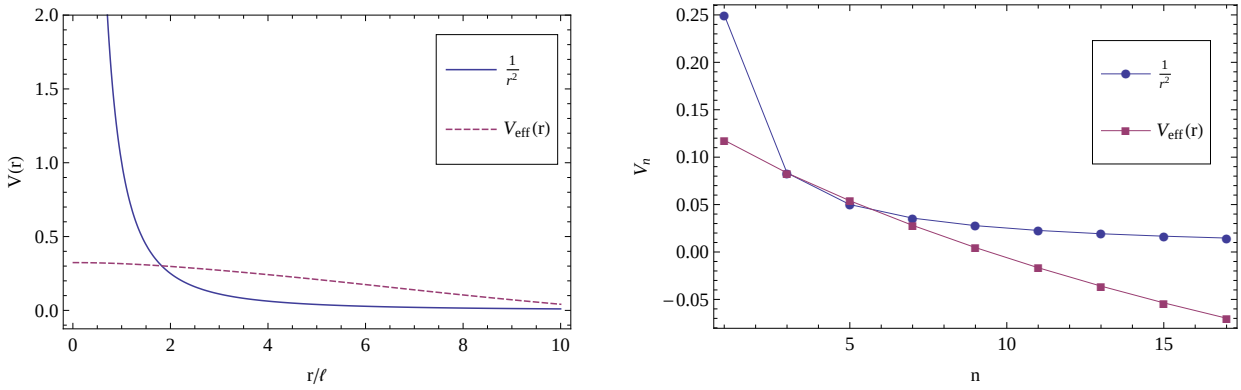

(a) (b)

Figure 4.1: (a) The $1/r^2$ interaction together with the weakly repulsive effective two-body interaction $V_{\text{eff}}(r)$ derived from the three-body term in (4.24). (b) The pseudopotentials of the $1/r^2$ and $V_{\text{eff}}(r)$ interactions. In both figures the curve for the effective interaction has been shifted by a constant to aid illustration.

term in (4.24) will dominate the low energy physics and is responsible for the wave functions exhibiting a large number of zeros at the particle coordinates. These zeros are contained in the Vandermonde factors appearing in (3.24). The energy cost associated with reducing the number of zeros at a particle coordinate will be much greater for a $1/r^2$ potential than for a "soft" potential such as $V_{\text{eff}}(r)$. We therefore expect the contribution of the three-body term to the total energy to be approximately constant within the low energy sector and that its contribution to the excitation gap at incompressibility is minimal. This is clearly reflected by the numerical results presented later.

Returning to the expansion in (4.22) we see that the second term amounts to a quadratic external potential, similar to that generated by a neutralizing background charge. Its function is to counteract the repulsive nature of the $\sum_i \bar{\mathcal{E}}_i \mathcal{E}_i$ term and ensure that an average density of $\bar{\rho} = \nu/(2\pi\ell^2)$ is the most energetically favourable. We must now identify the background potential corresponding to the dominant $1/r^2$ interaction identified earlier. We take this potential to be generated by a neutralizing background charge of $\bar{\rho} = \nu/(2\pi\ell^2)$ uniformly distributed on a disk of radius $R = \ell\sqrt{2N/\nu}$ where charges interact via a $1/r^2$-potential. In terms of $\delta\hat{\rho}(\mathbf{r}) = \hat{\rho}(\mathbf{r}) - \bar{\rho}\Theta(R-r)$ the full potential energy takes the usual form

$$V_{1/r^2} = \frac{1}{2}\int \mathrm{d}\mathbf{r}\,\mathrm{d}\mathbf{r}'\delta\hat{\rho}(\mathbf{r})\delta\hat{\rho}(\mathbf{r}')\frac{\ell^2}{|\mathbf{r}-\mathbf{r}'|^2} = \sum_{i<j}\frac{\ell^2}{|\mathbf{r}_i-\mathbf{r}_j|^2} - \sum_i V_{bg}(\mathbf{r}_i) + V_{bg-bg} \tag{4.25}$$

where

$$V_{bg}(\mathbf{r}_i) = \bar{\rho}\int_{r\leq R}\mathrm{d}\mathbf{r}\frac{\ell^2}{|\mathbf{r}_i-\mathbf{r}|^2} \qquad \text{and} \qquad V_{bg-bg} = \frac{\bar{\rho}}{2}\int_{r\leq R}\mathrm{d}\mathbf{r}V_{bg}(\mathbf{r}) \tag{4.26}$$

represent the particle-background and background-background interactions respectively. Note that all these quantities are dimensionless. The singular nature of the $1/r^2$ interaction results in a divergent integral for $V_{bg}(\mathbf{r}_i)$ and necessitates a regularisation of the interaction at short distances. Regularisation schemes which only modify $V(r) = 1/r^2$ within a range $r_{reg} \sim \ell$ of $r = 0$ will produce background potentials which differ in the bulk by at most an additive constant. It is only within the edge region ($|r - R| < r_{reg}$) where the shape of $V_{bg}(\mathbf{r}_i)$ will be sensitive to precisely how the interaction has been regularised. We make the following choice

$$V_{bg}(\mathbf{r}_i) = \bar{\rho} \int_{r \leq R} \mathrm{d}\mathbf{r} \frac{(1 - e^{-|\mathbf{r}_i - \mathbf{r}|^2/r_e^2})\ell^2}{|\mathbf{r}_i - \mathbf{r}|^2} = \frac{\nu}{2\pi} \int_{x \leq 1} \mathrm{d}\mathbf{x} \frac{1 - e^{-|\mathbf{x}_i - \mathbf{x}|^2 R^2/r_e^2}}{|\mathbf{x}_i - \mathbf{x}|^2} \equiv \frac{\nu}{2\pi} F(\mathbf{r}_i/R) \quad (4.27)$$

where $\mathbf{x} = \mathbf{r}/R$ and $r_e = \ell\sqrt{2/\nu}$. This background potential appears in Figure 4.2 (a).

We can now separate $\sum_i \delta\bar{\mathcal{E}}_i \delta\mathcal{E}_i$ into two terms as

$$\sum_i \delta\bar{\mathcal{E}}_i \delta\mathcal{E}_i = 2V_{1/r^2} + 2V_{3B} \quad (4.28)$$

with V_{1/r^2} as defined in (4.25) and where $2V_{3B}$ contains the weakly repulsive three-body term. In other words, we subtract from $\sum_i \delta\bar{\mathcal{E}}_i \delta\mathcal{E}_i$ the strongly repulsive V_{1/r^2} interaction and denote whatever remains by $2V_{3B}$. It has already been argued that the three-body term present in V_{3B} can be modelled as an effective two-body interaction which is long ranged but weakly repulsive at short distances. We expect the low energy physics to be dominated by V_{1/r^2} and that, up to a constant shift, the spectrum of $\mathcal{P}_\mathcal{L} \sum_i \delta\bar{\mathcal{E}}_i \delta\mathcal{E}_i \mathcal{P}_\mathcal{L}$ should resemble that of $\mathcal{P}_\mathcal{L} 2V_{1/r^2} \mathcal{P}_\mathcal{L}$. We therefore simply approximate $2V_{3B}$ by its ground state expectation value. This approximation can be tested numerically for small system sizes. Figure 4.2 (b) shows the lowest two eigenvalues of $\mathcal{P}_\mathcal{L} \sum_i \delta\bar{\mathcal{E}}_i \delta\mathcal{E}_i \mathcal{P}_\mathcal{L}$ and $\mathcal{P}_\mathcal{L} 2V_{1/r^2} \mathcal{P}_\mathcal{L}$ for each angular momentum sector where $L_z^{(c)} = 0$ and $N = 6$. For $L_z \leq 45$ the two spectra are indeed similar up to a constant shift. At $L_z > 45$ the eigenvalues of $\mathcal{P} 2V_{1/r^2} \mathcal{P}$ exhibit a downward trend which reflects the fact that particles are "falling off" the disk which provides the neutralizing background charge. It should be kept in mind that the filling fraction under consideration enters as a parameter in both V_{1/r^2} and $\sum_i \delta\bar{\mathcal{E}}_i \delta\mathcal{E}_i$ and these kinds of comparisons is only sensible for the range of angular momenta corresponding to the particular filling. In the context of Figure 4.2 (b) this restricts L_z to a region around 45.

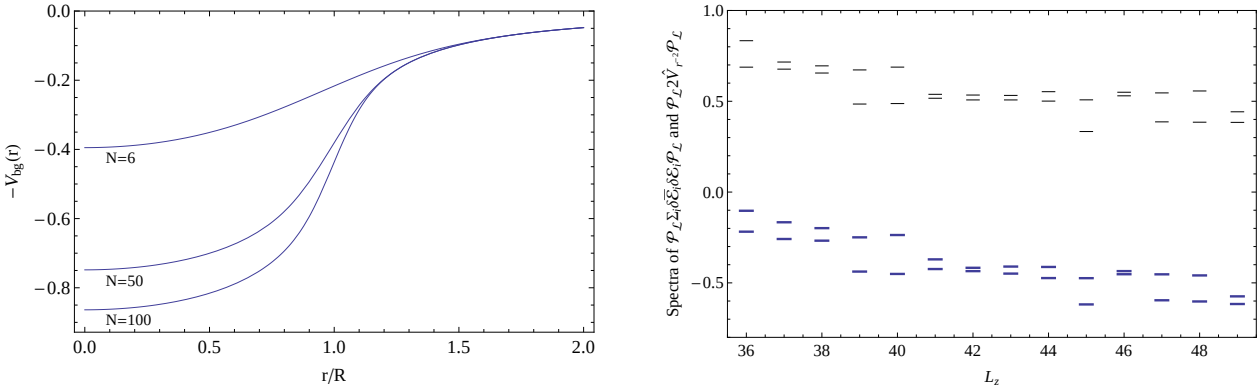

(a) (b)

Figure 4.2: (a) The background potential appearing in (4.27) for $\nu = 1/3$. The vast majority of particles are found at $r < R$. (b) The lowest two eigenvalues of $\mathcal{P}_{\mathcal{L}}2V_{1/r^2}\mathcal{P}_{\mathcal{L}}$ (shown in bold) and $\mathcal{P}_{\mathcal{L}}\sum_i \delta\bar{\mathcal{E}}_i\delta\mathcal{E}_i\mathcal{P}_{\mathcal{L}}$ for a range of L_z. Here $N = 6$ and $\nu = 1/3$.

4.4 Relating the spectra of $\mathcal{P}_{\mathcal{L}}\hat{H}_{CS}\mathcal{P}_{\mathcal{L}}$ and $\hat{K}^{(r)}_{\Lambda}$

In Section 3.5 we introduced the following conjecture regarding the spectrum of $\hat{K}^{(r)}_{\Lambda}$:

Conjecture: *Suppose $k(k-1)$ and $k'(k'-1)$ are the lowest eigenvalues of $\hat{K}^{(r)}_{\mathcal{I}}$ in the L^*_z and $L^{*\prime}_z$ angular momentum sectors respectively, and that $L^*_z - L^{*\prime}_z = \mathcal{O}(N^0)$. The difference between the ground state eigenvalues of $\hat{K}^{(r)}_{\Lambda}$ in these two sectors is then approximately $k(k-1) - k'(k'-1)$. In other words, the projection onto Λ does not result in a significant **relative** change in the ground state energies of neighbouring angular momentum sectors.*

The relation between $\hat{K}^{(r)}_{\Lambda}$ and $\mathcal{P}_{\mathcal{L}}\hat{H}_{CS}\mathcal{P}_{\mathcal{L}}$ expressed in (4.17) allows us to reformulate this conjecture into one regarding the spectrum of $\mathcal{P}_{\mathcal{L}}\hat{H}_{CS}\mathcal{P}_{\mathcal{L}}$. Let E_0 and E'_0 denote the ground state eigenvalues of $\mathcal{P}_{\mathcal{L}}\hat{H}_{CS}\mathcal{P}_{\mathcal{L}}$ in the $L_z = L^*_z + 2d_J$ and $L'_z = L^{*\prime}_z + 2d_J$ sectors respectively. From (2.54) and the result of Proposition 4.2.1 we know that

$$L_z \sim L'_z \sim N^2/(2\nu) + \mathcal{O}(N) \qquad \text{and} \qquad k \sim k' \sim N^2/(4n) + \mathcal{O}(N) \tag{4.29}$$

where $\nu = n/(2n+1)$. Combining the conjecture above with (4.17) allows the expression for $E_0 - E'_0$ in terms of the corresponding eigenvalues of $\hat{K}^{(r)}_{\Lambda}$ to be expanded in orders of $1/N$ to obtain

$$E_0 - E'_0 \approx \alpha\hbar\omega_c(k - k' - (L_z - L'_z)/2) + \mathcal{O}(1/N) \tag{4.30}$$

where $\alpha = 1 - 2\nu$. In its present form this expression may appear quite cryptic, but it can be simplified significantly by relating k and L_z to the bidegree of the $\mathcal{I}$ states which they

label. Recall from Section 3.3 that the elements of $\mathcal{I}_k$ are homogeneous lowest weight states of which the bidegree $(d_z, d_{\bar{z}})$ fixes both $k = (d_z + d_{\bar{z}} + N - 1)/2$ and the angular momentum $L_z^* = L_z - 2d_J = d_z - d_{\bar{z}}$. These states are automatically eigenstates of the Landau problem with $d_{\bar{z}}$ units of cyclotron energy above the ground state. Inserting these expressions into (4.30) produces

$$E_0 - E_0' \approx \alpha\hbar\omega_c(d_{\bar{z}} - d_{\bar{z}}') + \mathcal{O}(1/N) \tag{4.31}$$

which is precisely the energy difference between k and k' states with respect to $\hat{H}_L^{(\alpha)}$, the Landau problem with a weakened magnetic field αB. Furthermore, since $\hat{H}_{CS}$ is unitarily equivalent to $\hat{H}_L^{(\alpha)}$ so this is *also* the gap expected for the *unprojected* Chern-Simons Hamiltonian $\hat{H}_{CS}$. *The low-lying spectrum of $\mathcal{P}_\mathcal{L}\hat{H}_{CS}\mathcal{P}_\mathcal{L}$ therefore resembles that of $\hat{H}_{CS}$ (and $\hat{H}_L^{(\alpha)}$); at least in the restricted sense we are dealing with here.* This result is not entirely unexpected since it follows from the related assumption that the low-lying spectra of $\hat{K}_\mathcal{I}^{(r)}$ and $\hat{K}_\Lambda^{(r)}$ are also similar. The original conjecture therefore translates into the present context as follows:
Conjecture: *The difference between the ground state energies of $\mathcal{P}_\mathcal{L}\hat{H}_{CS}\mathcal{P}_\mathcal{L}$ in the L_z and L_z' sectors is approximately the same as for $\hat{H}_{CS}$ itself when $L_z - L_z' = \mathcal{O}(N^0)$. For a system at a filling fraction ν this energy gap is characterised by the cyclotron energy $\alpha\hbar\omega_c = (1 - 2\nu)\hbar\omega_c$.*

Numerical evidence supporting this conjecture can be found by transforming the content of Figures 3.2 (a) and (b) to apply to $\hat{H}_{CS}$ instead of $\hat{K}^{(r)}$. In Figure 4.3 (a) we show the low lying eigenvalues of $\mathcal{P}_\mathcal{L}\hat{H}_{CS}\mathcal{P}_\mathcal{L}$ in each angular momentum sector. The states at the bottom of the first two bands, as defined in Section 3.5, appear in bold and are connected. This is to be compared with the spectrum of $\hat{H}_L^{(\alpha)}$ in $\mathcal{I}$ appearing in Figure 4.3 (b). We again observe a striking similarity, in particular with respect to the relative energies of the ground states of neighbouring angular momentum sectors.[16]

4.5 Question 4: The duality between the free particle and interacting problems

In Section 1.7 we posed the question: *Can the mapping between the interacting and free particle problems be performed on the level of the microscopic Hamiltonian itself? Can such a construction provide analytic approximations to both the wave functions and excitation gaps?*

[16]The peculiar spike observed at $L_z = 46$ reflects that fact that the true ground state in this sector is not translationally invariant. This is equivalent to noting that the lowest eigenspace of $\hat{K}_\mathcal{I}^{(r)}$ with $L_z^* = 16$ already has $d_{\bar{z}} = 1$, i.e. it is impossible to construct a translationally invariant LLL state with angular momentum $L_z^* = 16$.

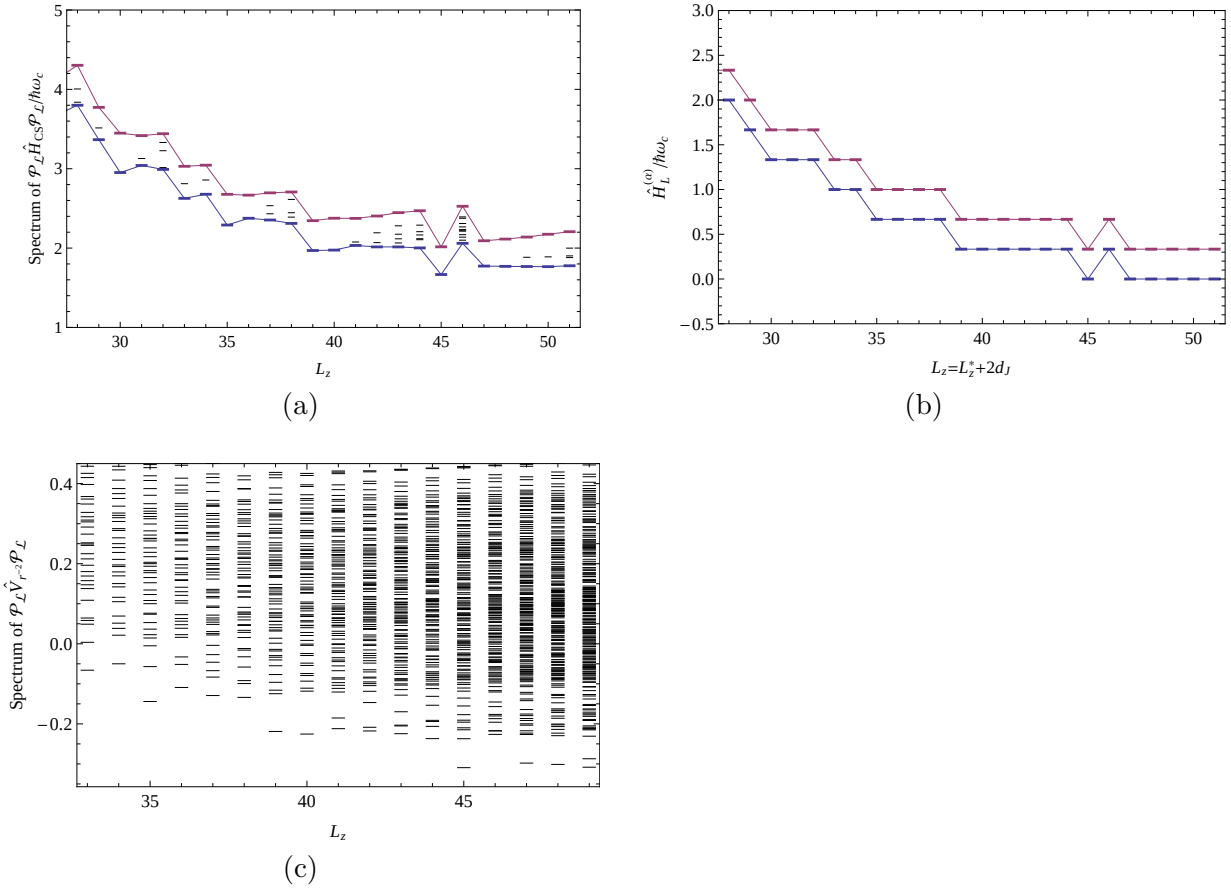

Figure 4.3: In all four figures $N = 6$, $\alpha = 1/3$ and $L_z^{(c)} = 0$. (a) The first $\mathrm{Dim}(\mathcal{I}_{k^*}) + 1$ eigenvalues of $\mathcal{P}_\mathcal{L}\hat{H}_{CS}\mathcal{P}_\mathcal{L}$ in each angular momentum sector. Of those shown the largest and smallest eigenvalue appear in bold. (b) The first two eigenvalues of $\hat{H}_L^{(\alpha)}/\hbar\omega_c$ ($\hat{H}_{CS}/\hbar\omega_c$) per L_z sector. Energies are shown relative to the global ground state. (c) A subset of the exact spectrum of $\mathcal{P}_\mathcal{L}V_{1/r^2}\mathcal{P}_\mathcal{L}$.

The relation derived in Section 4.2.1 can be summarized as

$$\frac{\mathcal{P}_\mathcal{L}\hat{H}_{CS}\mathcal{P}_\mathcal{L}}{\hbar\omega_c} \cong \mathcal{P}_\Lambda\hat{K}^{(r)}\mathcal{P}_\Lambda \cong \mathcal{P}_\mathcal{L}V_{1/r^2}\mathcal{P}_\mathcal{L} \tag{4.32}$$

where $\cong$ indicates approximate equivalence up to trivial constants or similarity transformations. The central notion of the composite fermion framework is that a strongly interacting system of electrons can be mapped onto a system of weakly interacting composite fermions. The relations above hint at such a duality since both $\hat{H}_{CS}$ and $\hat{K}^{(r)}$ have single particle characters. The important caveat is that a single particle problem will not generally retain its non-interacting character under projection, and therefore the relations in (4.32) are only useful if, *in some restricted sense*, projecting $\hat{K}^{(r)}$ and $\hat{H}_{CS}$ does not erase all traces of their single particle nature. This has motived our study of the relation between the eigenstates and spectra of $\hat{K}_\Lambda^{(r)}$ and $\hat{K}_\mathcal{I}^{(r)}$.

A simple mapping between the low-lying states of $\hat{K}_{\mathcal{I}}^{(r)}$ and $\hat{K}_{\Lambda}^{(r)}$ was constructed and found to automatically generate the desired Jastrow type correlation in the wave functions. Through (4.32) these results are immediately applicable to the interacting problem and also explains the success of the Jastrow-Slater wave function ansatz in the composite fermion picture. Numerical results also suggest a simple relation between the low-lying spectra of $\hat{K}_{\mathcal{I}}^{(r)}$ and $\hat{K}_{\Lambda}^{(r)}$ which we formulated as a postulate in Section 3.5. Again, these insights now apply directly to the spectra of $\mathcal{P}_{\mathcal{L}}\hat{H}_{CS}\mathcal{P}_{\mathcal{L}}$ and $\mathcal{P}_{\mathcal{L}}V_{1/r^2}\mathcal{P}_{\mathcal{L}}$ and reveal that the low-lying spectrum indeed resembles that of a free particle Landau problem. In the next section we extend these results to the Coulomb interaction.

4.6 Excitation gaps for interacting quantum Hall systems

4.6.1 Background

In Section 1.6.5 we alluded to the wide array of different excitations [22] exhibited by systems in the FQHE regime. Of particular interest are excitations involving the creation of a well separated quasiparticle-quasihole pair. The corresponding energy cost Δ is known as the activation energy or transport gap and can be determined experimentally by investigating the temperature dependence of the diagonal resistivity. A comparison of experimental and theoretical results appears in Section 4.6.2. Here we briefly review some theoretical approaches to calculating the transport gap.

In the spherical geometry the quasi-particle pair can be realised as a composite fermion exciton. For example, consider the case $\nu = 2/5$ where the composite fermions fill $\nu^* = 2$ effective Landau levels. Moving a composite fermion from the one end of the filled second level to the other end of the empty third level generates a quasiparticle-hole excitation in the spherical analogue of the electron wave function Ψ_ν of (1.20). The two quasiparticles sit at opposite poles of the sphere and become infinitely separated in the large N limit. This eliminates the interaction between them and allows the gap Δ to be identified with the energy required to create the quasiparticles. This construction yields a trial wave function with which the expectation value of the interaction can be calculated using Monte Carlo methods. The calculation is repeated for a range of particle numbers and the results are then extrapolated to the thermodynamic limit. Direct diagonalisation techniques, which do not require a trial wave function as input, have also been used. Larger particle numbers require increasingly sophisticated numerical methods, and the extrapolation to the thermodynamic limit and the handling of finite size corrections also require particular care.

The requirement that the quasiparticles are well separated and essentially non-interacting suggests that Δ may be interpreted as the effective cyclotron gap of free composite fermions [32]. One is tempted to identify Δ with $\hbar\omega_c^{CF}$ where $\omega_c^{CF} = |e|B^*/(m^{CF}c)$ with $B^* = \alpha B$ the weakened field strength and m^{CF} an effective composite fermion mass. However, as seen in Section 1.6.6, the expression $\omega_c^{CF} = |e|B^*/(m^{CF}c)$ will not exhibit the correct scaling behaviour in B *unless* the composite fermion mass m^{CF} itself depends on both B and the coupling constants of the interaction. These requirements have led to postulates [32] regarding the possible forms of m^{CF} and ω_c^{CF}. We will revisit this point later.

4.6.2 Theory versus experiment

At finite temperatures the diagonal resistivity displays Arrhenius behaviour $\rho_{xx} \sim \exp[-\Delta/2kT]$ from which the gap can be determined experimentally. On the theory side a large number of numerical studies have provided estimates of the excitation gap in the thermodynamic limit. However, the theoretical estimates are found to be larger than the experimental values by about a factor of two. This discrepancy is the result of neglecting certain effects in the "full" Hamiltonian (1.6) or in the subsequent derivation of the projected interaction. Specifically, in (1.6) the system was assumed to be free of disorder and perfectly two dimensional with no transverse thickness. Taking the strong magnetic field limit also eliminated the effects of interaction induced Landau level mixing and spin flips. The role of finite thickness corrections have been studied theoretically and found to account for at most half of the discrepancy between the theoretical and experimental results. Landau level mixing and spin flip excitations are also believed to only bring about a minimal reduction in the predicted gap. It therefore appears that disorder plays a significant role and must be taken into account if the experimental and theoretical results are to be reconciled. This remains a significant challenge since little is known regarding the correct theoretical treatment of disorder in this system. More detailed discussions of these points appear in [11, 23].

4.6.3 Outline of calculation

Our approach to calculating the gap is based on the shared characteristics of the low-lying interacting spectrum and that of the free particle Landau problem identified in Section 4.4. It was shown how the postulate regarding the spectrum of $\hat{K}_\Lambda^{(r)}$ can be used to relate the spectra of $\mathcal{P}_\mathcal{L}\hat{H}_{CS}\mathcal{P}_\mathcal{L}$ and its unprojected counterpart $\hat{H}_{CS}$. In particular, the relative values of the ground state energy in neighbouring angular momentum sectors was found to be the same for $\mathcal{P}_\mathcal{L}\hat{H}_{CS}\mathcal{P}_\mathcal{L}$ as for $\hat{H}_{CS}$. Furthermore, $\hat{H}_{CS}$ is unitarily equivalent to $\hat{H}_L^{(\alpha)}$ and an eigenstate

of the former with angular momentum L_z maps onto an eigenstate of the latter with angular momentum $L_z^* = L_z - 2d_J$. In Figure 1.2 (b) we saw that the ground state energy of $\hat{H}_L^{(\alpha)}$ can jump by $\alpha\hbar\omega_c$ as L_z^* is lowered and particles are forced into higher Landau levels. These jumps are then also observed in the spectra of $\hat{H}_{CS}$ *and* $\mathcal{P}_\mathcal{L}\hat{H}_{CS}\mathcal{P}_\mathcal{L}$ at the corresponding L_z angular momenta. Through this chain of equivalences we can conclude that when the ground state energy of $\hat{H}_L^{(\alpha)}$ exhibits a jump of $\alpha\hbar\omega$ at $L_z^* = L_z - 2d_j$ we will observe a corresponding jump of α in the spectrum of $\mathcal{P}_\mathcal{L}\hat{H}_{CS}\mathcal{P}_\mathcal{L}/(\hbar\omega)$. In keeping with the free quasiparticle picture we identify this jump of α with the (dimensionless) effective cyclotron energy of the quasiparticles of $\mathcal{P}_\mathcal{L}\hat{H}_{CS}\mathcal{P}_\mathcal{L}/(\hbar\omega)$ which we can then relate to the gap Δ associated with the interaction $\mathcal{P}_\mathcal{L}V_{1/r^2}\mathcal{P}_\mathcal{L}$.

It is well known [13] that the cusps observed in the spectrum of $\hat{H}_L^{(\alpha)}$ also manifest themselves in the spectrum of the projected interaction. This is also seen in our data in Figure 4.3 (c) where a clear gap is visible at $L_z = 45$ in the spectrum of $\mathcal{P}_\mathcal{L}V_{1/r^2}\mathcal{P}_\mathcal{L}$. The jump in ground state energy as we move to $L_z < 45$ then mimics the jump at $L_z^* = 45 - 2d_J = 15$ in the spectrum of the Landau problem shown in 1.2 (b).

The apparent mismatch between the energy scales of the interacting and free particle problems was first raised in Section 1.6.6. This issue does not appear in our construction since we only deal with relations between *dimensionless* operators. Although the Landau problem features prominently in our construction only a single global energy scale is relevant, namely that of the interaction. Let us make this simple observation more precise. Suppose the electrons really were interacting via an inverse quadratic potential. The full Hamiltonian would then, together with the kinetic term, contain a term of the form $V_0 \sum_{i<j} \frac{\ell^2}{r_{ij}^2}$ where V_0 is some coupling constant with the dimension of energy. In this model Hamiltonian we are free to change V_0 independently of the cyclotron frequency and any attempt to equate $\mathcal{P}_\mathcal{L}V_0 \sum_{i<j} \frac{\ell^2}{r_{ij}^2}\mathcal{P}_\mathcal{L}$ directly with a Landau problem would result in the same problematic mismatch in scales. This is avoided by instead relating the two dimensionless operators $\mathcal{P}_\mathcal{L} \sum_{i<j} \frac{\ell^2}{r_{ij}^2}\mathcal{P}_\mathcal{L}$ and $\mathcal{P}_\mathcal{L}\hat{H}_{CS}\mathcal{P}_\mathcal{L}/(\hbar\omega_c)$. If such a comparison yields information regarding the spectrum of the $\mathcal{P}_\mathcal{L} \sum_{i<j} \frac{\ell^2}{r_{ij}^2}\mathcal{P}_\mathcal{L}$ then simply multiplying all the energies by V_0 restores the dimension and energy scale associated with the interaction. For these reasons we will only consider dimensionless interactions in what follows.

4.6.4 Gaps for the inverse quadratic interaction

Based on (4.17) and (4.28) we arrive at

$$\frac{\hat{H}_{CS}}{\hbar\omega_c} \overset{\mathcal{P}_{\mathcal{L}}}{\approx} 4V_{1/r^2} + (\text{Constants}). \tag{4.33}$$

This relation, together with the hypothesis that relates the spectra of $\mathcal{P}_{\mathcal{L}}\hat{H}_{CS}\mathcal{P}_{\mathcal{L}}$ and $\hat{H}_{CS}$ leads us to conclude that at the filling fractions $\nu = 1/3, 2/5, 3/7, \ldots$ the projected $1/r^2$ interaction will exhibit an excitation gap of $\Delta_{1/r^2} = \alpha/4$ where $\alpha = 1 - 2\nu$. This simple result can be verified through comparison with the Monte-Carlo results obtained by PMJ[33] and which appear in Table 4.1. For the filling fractions $\nu = 1/3$ and $\nu = 4/9$ the two sets of results agree to within the uncertainty of the Monte-Carlo calculations. For $\nu = 2/5$ and $\nu = 3/7$ our results are found to be about 20% smaller than those of PMJ. However, it was pointed out by MDD[23] that the extrapolation procedure used in PMJ and JK[34] to obtain results in the thermodynamic limit may lead to such an overestimation of the gap. This will also be seen in the case of the Coulomb interaction where the predictions of PMJ and JK are in some cases significantly larger than those obtained in later studies.

ν	1/3	2/5	3/7	4/9
$\Delta_{1/r^2} = \alpha/4$	0.0833	0.05	0.0357	0.0278
PMJ[33]	0.0842(11)	0.0609(27)	0.0424(45)	0.0257(77)

Table 4.1: Excitation gaps for the inverse squared interaction from (4.35) and [33].

ν	1/3	2/5	3/7	4/9	5/11
$\Delta_{1/r}$ (4.36)	0.10206	0.0559	0.0385	0.0295	0.0238
MDD [23]	0.1012	0.05	0.035	0.027	–
CFT [35]	0.1005	0.0549	0.0371	0.0276	0.0219
JK [34]	0.1063	0.0585	0.0474	0.0356	0.023

ν	5/11	6/13	7/15
$\Delta_{1/r}$ (4.36)	0.0238	0.02	0.0173
SLJ [36]	0.0219(30)	0.0225(41)	0.018(11)

Table 4.2: Excitation gaps for the Coulomb interaction from (4.36) and [23, 35, 36, 34].

4.6.5 The Coulomb interaction

A simple argument now allows the results for the $1/r^2$ potential to be generalised to any potential which is short ranged and strongly repulsive. For such interactions we expect the low energy states to exhibit strong short range correlations which are the result of higher order zeros (i.e. vortices) appearing at the particle coordinates in the wave function. As outlined in Section 1.6.5 excited states are the result of these zeros being cancelled by powers of $(\bar{z}_i - \bar{z}_j)$ present in $\phi(\mathbf{z}, \bar{\mathbf{z}}) \in \mathcal{I}$ prior to projection. The excitation gap is therefore governed by the energy cost associated with reducing the average number of zeros at each particle coordinate. As set out in the context of the two-body problem in Section 1.4 such a decrease in the number of zeros results in a lower relative angular momentum and interparticle distance. For a strongly repulsive short-range interaction $V(r)$ this energy cost will only be appreciable if the particles were already in close proximity, i.e. at a distance of about $r_e = \ell\sqrt{2/\nu}$, the radius of the correlation hole around each particle. This suggests that the excitation gap is determined by the gradient of the interparticle potential at $r = r_e$. We are led to introduce the following ansatz for the excitation gap Δ_V:

$$\Delta_V = |V'(r_e)| D(\nu) \tag{4.34}$$

where the function $D(\nu)$ depends on the filling fraction but is independent of the specific interaction. Here both Δ_V and $V(r)$ are dimensionless. Fixing the universal function $D(\nu)$ simply requires comparison with the known result $\Delta_{1/r^2} = \alpha/4$. This yields $D(\nu) = \alpha r_e/(4\nu)$ and we conclude that

$$\Delta_V = |V'(r_e)| \frac{\alpha r_e}{4\nu} \tag{4.35}$$

where $r_e = \ell\sqrt{2/\nu}$ and $\alpha = 1 - 2\nu$. For the Coulomb interaction we set $V(r) = \ell/r$ and (4.35) then reduces to

$$\Delta_{1/r} = \frac{1 - 2\nu}{\sqrt{32\nu}}. \tag{4.36}$$

We can now compare the predictions of equation (4.36) with the results obtained through various other schemes. These include direct numerical diagonalisation as in MDD [23] and the composite fermion trial wave function methods used by PMJ [33], JK [34] and SLJ [36]. The numerical values quoted for PMJ are estimates based on the graphs in [33]. Also shown are the predictions of composite fermion theory (CFT) [37, 35, 32] which suggest that the gap for

the Coulomb interaction has the form

$$\Delta_{CFT} \approx \frac{\pi}{2} \frac{1}{(2n+1)(\log(2n+1)+C)} \tag{4.37}$$

where $\nu = n/(2n+1)$. The constant C cannot be determined within the theory itself [35]. Following [23] we choose $C = 4.11$ to fit the gap at $\nu = 1/3$. Results from the various studies are summarized in Table 4.2 for filling fractions ranging from $\nu = 1/3$ up to $\nu = 7/15$. Figure 4.4 also compares $\Delta_{1/r}$ (4.36) and Δ_{CFT} (4.37) as functions of n. It is clear that there exists good agreement between the results based on (4.36) and those obtained using numerical methods and composite fermion theory. We note that for some fillings the gaps found in JK (which match those of PMJ) are significantly larger than those obtained by MDD. It was pointed out in MDD that this may be due to the method used for extrapolating results to the large N limit. If the gaps for the $1/r^2$ interaction are similarly affected this may explain the discrepancies between our results and those of PMJ appearing in Table 4.1. Table 4.3 shows the excitation gaps for the Yukawa potential $V_Y(r) = \exp[-r/\ell]/r$ which was obtained numerically in PMJ together with those given by (4.35). Agreement was again found to within about 10%.

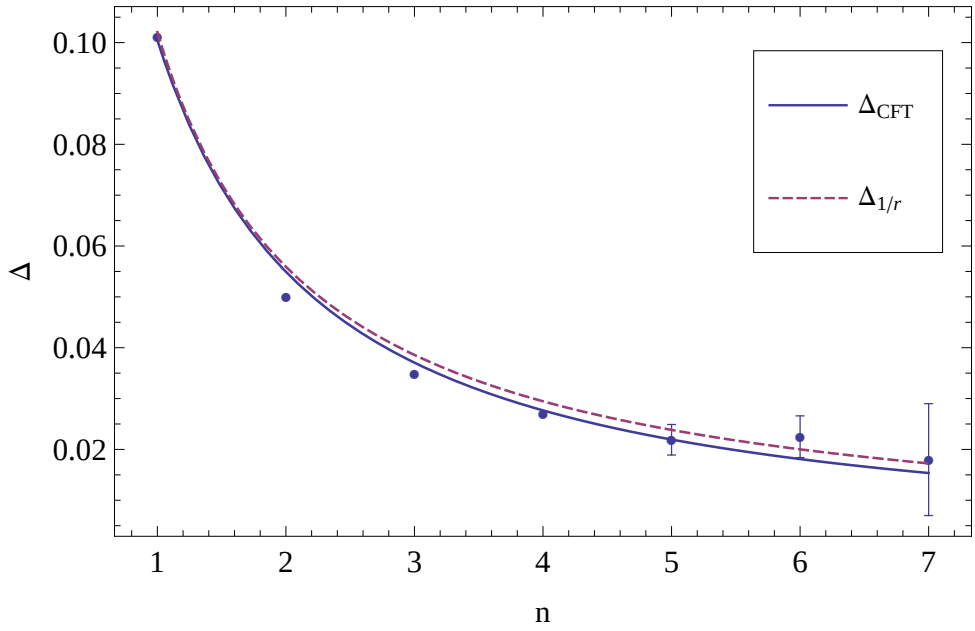

Figure 4.4: $\Delta_{1/r}$ **of (4.35) and** Δ_{CFT} **of (4.37) as function of** n**. The dots at** $n = 1, 2, 3, 4$ **are the numerical results of MDD [23] obtained using direct diagonalisation. The Monte-Carlo results of SLJ [36] appear as dots at** $n = 5, 6, 7$**.**

ν	1/3	2/5	3/7	4/9
Δ_Y (4.35)	0.0304	0.01933	0.01406	0.011
PMJ [33]	0.0271(4)	0.0215(9)	0.0143(15)	0.0102(24)

Table 4.3: Excitation gaps for the Yukawa interactions from (4.35) and [33].

4.7 Wave functions for the interacting quantum Hall system

The $\mathcal{A}_{\bar{z}}$ projection procedure introduced in Section 3.4.1 was shown to yield very accurate approximations to the low-lying eigenstates of $\hat{K}_\Lambda^{(r)}$. Transforming these states using U^2 produces LLL states of the form $\psi(\mathbf{z}) = J\phi[\mathbf{z}, \partial_{\mathbf{z}}]J$ where $\phi(\mathbf{z}, \bar{\mathbf{z}}) \in \mathcal{I}$ is an eigenstate of the free particle Landau problem. These LLL states provide equally accurate approximation to the low-lying eigenstates of $\mathcal{P}_\mathcal{L}\hat{H}_{CS}\mathcal{P}_\mathcal{L}$ and $\mathcal{P}_\mathcal{L}\sum_i \delta\bar{\mathcal{E}}_i\delta\mathcal{E}_i\mathcal{P}_\mathcal{L}$ and, through the arguments of Section 4.3, also of the projected interaction $\mathcal{P}_\mathcal{L}V_{1/r^2}\mathcal{P}_\mathcal{L}$. As with the composite fermion states of Jain the Vandermonde polynomial J appearing in $\psi(\mathbf{z}) = J\phi[\mathbf{z}, \partial_{\mathbf{z}}]J$ result in strong interparticle correlations which keep particles well separated. This makes these states ideal approximations to the low energy states of any strongly repulsive interaction in the LLL. Table 4.4 summarizes the results of numerical tests for gauging the accuracy with which the $\psi(\mathbf{z}) = J\phi[\mathbf{z}, \partial_{\mathbf{z}}]J$ states reproduce the ground state of the Coulomb interaction. Only the interparticle potential has been included here. The algorithm used to obtain this data is outlined in Section 3.4.4. We again observe excellent agreement with both the exact results and those of the composite fermion construction.

			GSEV Percentage Error			Overlap with exact GS		
L_z	Dim(Λ)	Dim($\mathcal{I}_{k^*}$)	$\mathcal{A}_{\bar{z}}$	CF	$\mathcal{P}_\Lambda$	$\mathcal{A}_{\bar{z}}$	CF	$\mathcal{P}_\Lambda$
19	5	1	0.0363	0	0.0008	0.99539	1.00000	0.99990
20	7	1	0.0889	0.0001	0.0013	0.98949	0.99999	0.99985
21	11	1	0.0519	0.0031	0.0004	0.99452	0.99968	0.99996
22	14	3	0.0288	0	0.0069	0.99636	1.00000	0.99925
23	20	2	0.0391	0.0008	0.0143	0.99523	0.99989	0.99832
24	26	1	0.0814	0.0179	0.0252	0.98717	0.99774	0.99643
25	35	1	0.0751	0.0284	0.0467	0.98936	0.99689	0.99439
26	44	3	0.0236	0.0073	0.0651	0.99706	0.99909	0.99086
27	58	2	0.0443	0.0027	0.0357	0.99367	0.99975	0.99438
28	71	5	0.0887	0.0383	0.0766	0.97646	0.98766	0.97560
29	90	2	0.0475	0.0324	0.0795	0.99249	0.99453	0.98513
30	110	1	0.0629	0.0275	0.0605	0.99108	0.99610	0.99216
31	136	3	0.0609	0.0573	0.4039	0.99152	0.99274	0.94745
32	163	7	0.0221	0.0292	0.1295	0.99750	0.99660	0.96708
33	199	2	0.0135	0.0143	0.1584	0.99829	0.99830	0.97803
34	235	4	0.1052	0.0569	0.2425	0.98483	0.99141	0.97224
35	282	1	0.0751	0.0769	0.3172	0.98933	0.98889	0.96048
36	331	2	0.1461	0.1500	0.6723	0.98021	0.97984	0.91174
37	391	5	0.0705	0.0754	0.4261	0.98924	0.98861	0.91857
38	454	9	0.0537	0.0512	0.2658	0.99250	0.99299	0.96480
39	532	1	0.0608	0.0608	0.4302	0.99315	0.99315	0.95371
40	612	2	0.1280	0.1280	0.6400	0.98594	0.98594	0.94116
41	709	4	0.1739	0.1739	0.6173	0.95662	0.95662	0.90813
42	811	7	0.0766	0.0766	0.4911	0.99030	0.99030	0.92578
43	931	12	0.0500	0.0500	0.3025	0.99257	0.99257	0.94989
44	1057	18	0.0284	0.0284	0.2352	0.99772	0.99772	0.98048
45	1206	1	0.1484	0.1484	0.7065	0.98177	0.98177	0.93416
46	1360	39	0.0355	0.0355	0.1866	0.99637	0.99637	0.98277
47	1540	2	0.1780	0.1780	0.9185	0.97896	0.97896	0.91784
48	1729	3	0.2304	0.2304	0.9690	0.97252	0.97252	0.90612
49	1945	5	0.1975	0.1975	0.6240	0.97002	0.97002	0.92317
50	2172	7	0.1605	0.1605	0.6192	0.98235	0.98235	0.94150
51	2432	11	0.0351	0.0351	0.2374	0.99702	0.99702	0.98093

Table 4.4: Comparison of exact diagonalisation results for $N = 6$ particles experiencing a Coulomb interaction with the predictions of the three methods described in the text.

Summary and outlook

We have presented a self-contained treatment of interacting electrons in the lowest Landau level starting from the problem statement and culminating in analytic approximations to the excitation gap and low-lying eigenstates. Our approach is based on a new formulation of the composite fermion picture phrased in terms of the algebraic properties of polynomial states. This section is dedicated to reviewing the construction and summarizing the main results. We conclude by highlighting some open questions and avenues for further study.

We set out to study the Coulomb interaction $V_{1/r}$ within the translationally invariant subspace $\mathcal{L}$ of the lowest Landau level. We were particularly interested in understanding, on a microscopic level, the extent to which this problem allows for a dual description in terms of non-interacting degrees of freedom. In principle this just amounts to applying a transformation that maps $\mathcal{P}_{\mathcal{L}} V_{1/r} \mathcal{P}_{\mathcal{L}}$ onto an equivalent weakly interacting problem. However, this idealised approach is very rarely tractable in practice and here too we find little in the way of a guiding principle for identifying such a transformation. With little hope of success through a direct strategy we instead tried to identify a related problem for which a suitable dual description appeared to be within reach. We would then have to return to this point at a later stage to formalise the connection between this substitute problem and the projected interaction.

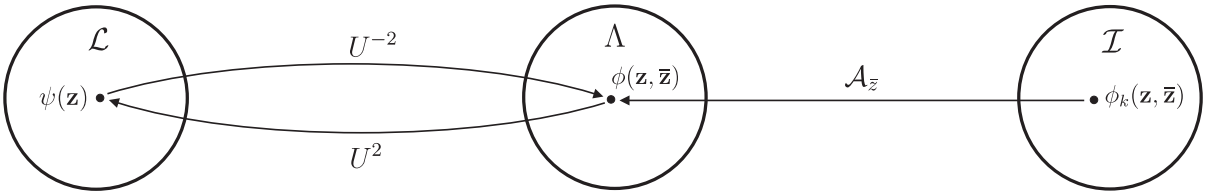

Guided by ideas from the composite fermion picture we shifted our attention to the space Λ which is obtained from $\mathcal{L}$ through the unitary transformation $U^{-2} = \bar{J}/J$. Whereas the states in $\mathcal{L}$ are polynomials in $\mathbf{z}$ alone the elements of Λ contain both $\mathbf{z}$ and $\bar{\mathbf{z}}$ variables to very high degrees. In this regard the $su(1,1)$ representation provided a useful algebraic scheme for labelling and classifying polynomial states. This was particularly appropriate given the central role the generators of $su(1,1)$ played in the investigation of the free particle Landau problem in Chapter 2.

We were led to consider the projection of the $su(1,1)$ Casimir operator $\hat{K}^{(r)}$ to Λ which was written as $\hat{K}^{(r)}_{\Lambda} \equiv \mathcal{P}_{\Lambda}\hat{K}^{(r)}\mathcal{P}_{\Lambda}$. The non-triviality of this problem stemmed from the fact that Λ is not invariant under $\hat{K}^{(r)}$ and is therefore not spanned by a subset of its eigenstates. We observed that this problem appeared to be governed by the properties of states exhibiting a higher filling fraction than the elements of Λ itself and which were naturally associated with a weakened magnetic field. This followed from the fact that the Casimir operator takes a constant value on each irreducible subspace and that all the information relevant to the problem $\hat{K}^{(r)}_{\Lambda}$ was therefore contained equally well in the lowest weight states of the different irreps. These lowest weight states are of a much lower degree than the elements of Λ and resemble low energy states with the respect to a Landau problem with a weakened magnetic field. This suggested that the free particle states relevant to the dual description is a subset of lowest weight states. Based on these insights we introduced the space $\mathcal{I}$ of irreducible states which is spanned by a subset of simultaneous lowest weight eigenstates of $\hat{K}^{(r)}$ and the free particle Landau Hamiltonian. Furthermore, $\mathcal{I}$ was shown to be isomorphic to Λ and, through U^2, also to $\mathcal{L}$. These results led us to identify $\hat{K}^{(r)}_{\mathcal{I}} = \hat{K}^{(r)}|_{\mathcal{I}}$ as a potential approximate dual description of $\hat{K}^{(r)}_{\Lambda}$ and we set about relating the spectra and eigenstates of these two operators.

The symmetry properties that characterise the elements of Λ suggested the bijective mapping $\mathcal{A}_{\bar{z}} : \mathcal{I} \to \Lambda$ which acts on a Landau problem eigenstate $\phi_k(\mathbf{z}, \bar{\mathbf{z}}) \in \mathcal{I}$ as

$$\mathcal{A}_{\bar{z}}\phi_k(\mathbf{z}, \bar{\mathbf{z}}) \propto \bar{J}\phi[\mathbf{z}, \partial_{\mathbf{z}}]J. \tag{4.38}$$

The image of $\phi_k(\mathbf{z}, \bar{\mathbf{z}})$ under $\mathcal{A}_{\bar{z}}$ therefore exhibits two factors of the Vandermonde polynomial J. This is strongly reminiscent of the Jastrow-Slater structure observed in the composite fermions wave function ansatz. However, for this mapping to embody a duality between $\hat{K}^{(r)}_{\mathcal{I}}$ and $\hat{K}^{(r)}_{\Lambda}$ it must preserve, at least approximately, the ordering of eigenstates in the two problems. In particular, $\mathcal{A}_{\bar{z}}$ should map the low-lying eigenstates of $\hat{K}^{(r)}_{\mathcal{I}}$ those of $\hat{K}^{(r)}_{\Lambda}$. This is guaranteed by the fact that $\mathcal{A}_{\bar{z}}$ is a projection with respect to a modified inner product which attaches increasing weights to the higher eigenspaces of $\hat{K}^{(r)}$. The result is a suppression of higher $\hat{K}^{(r)}$-components in $\mathcal{A}_{\bar{z}}\phi_k(\mathbf{z}, \bar{\mathbf{z}})$. Numerical calculations verified that mapping the lowest eigenspace of $\hat{K}^{(r)}_{\mathcal{I}}$ onto Λ using $\mathcal{A}_{\bar{z}}$ indeed produces very accurate approximations to the low-lying eigenstates of $\hat{K}^{(r)}_{\Lambda}$. As a special case this mapping was found to reproduce Laughlin's state for $\nu = 1/3$.

Next we investigated the relation between the spectra of $\hat{K}^{(r)}_{\Lambda}$ and $\hat{K}^{(r)}_{\mathcal{I}}$. These spectra were

certainly not expected to be identical, but numerical evidence did suggest that the low-lying structure is at least qualitatively similar. We formulated these observations as a hypothesis which stated that the "cost of constraint to Λ", i.e. by how much the ground state eigenvalue of $\hat{K}^{(r)}_{\Lambda}$ is greater than that of $\hat{K}^{(r)}_{\mathcal{I}}$, varies slowly from one angular momentum sector to the next.

The fact that the low-lying states of $\hat{K}^{(r)}_{\Lambda}$ was found to exhibit a structure similar to that of the composite fermion ansatz was a strong indication that $\hat{K}^{(r)}_{\Lambda}$ in some sense mimics a repulsive interaction. Chapter 4 was dedicated to establishing this connection and relating the results obtained for $\hat{K}^{(r)}_{\Lambda}$ through its approximate dual $\hat{K}^{(r)}_{\mathcal{I}}$ back to the original problem of the projected interaction. The first step was to show that $\hat{K}^{(r)}_{\Lambda}$ is equivalent, up to constants, to the $\mathcal{L}$-projection of a complicated many-body potential $\sum_i \bar{\mathcal{E}}_i \mathcal{E}_i$. This potential was found to be dominated by a two-particle contribution in the form of a repulsive inverse quadratic interaction. A series of intermediate steps related the results obtained for the eigenstates and eigenvalues of $\hat{K}^{(r)}_{\Lambda}$ to that of the projected interaction $\mathcal{P}_{\mathcal{L}} V_{1/r^2} \mathcal{P}_{\mathcal{L}}$. In particular, we found that the low-lying spectrum of V_{1/r^2} indeed shares characteristics of the free particle Landau problem, as predicted by the composite fermion picture, and we were able to obtain an analytic expression for the excitation gap. Finally, a simple ansatz allowed us to extend this result to the Coulomb interaction and obtain the expression

$$\Delta_{1/r} = \frac{1 - 2\nu}{\sqrt{32\nu}} \tag{4.39}$$

which agreed very well with existing numerical results.

The agreement between our results and those of previous numerical studies supports the validity of the assumptions and approximations used in our construction. However, a number of questions remain unresolved and the construction itself requires further generalisation. In this regard the following four points identify avenues for further study.

- *A simple classification scheme for physical states.* It was found that each $su(1,1)$ irrep contributes at most one physical/irreducible state. It is not understood what properties of an irrep determine whether or not its lowest weight state is irreducible. This issue appears to be governed by the symmetry properties of the various irreps with respect to permutations of the $\bar{\mathbf{z}}$ variables. It would also be interesting to determine whether this question only has a purely mathematical solution or whether the elements of $\mathcal{I}$ can also

be characterized on more physical grounds.

- *Rigorous results relating the spectra of $\hat{K}_{\Lambda}^{(r)}$ and $\hat{K}_{\mathcal{I}}^{(r)}$.* In Section 3.5 we introduced a conjecture relating the spectra of $\hat{K}_{\Lambda}^{(r)}$ and $\hat{K}_{\mathcal{I}}^{(r)}$. Although supported by numerical evidence this result remains unproven. This again appears to be a question which involves the interplay between the representations of $su(1,1)$ and the symmetry group acting on the $\bar{\mathbf{z}}$ variables: the former is labelled by $\hat{K}^{(r)}$ while the latter can be used to characterise the space Λ.

- *Treating a larger class of filling fractions.* We have considered filling fractions in the range $1/3 \leq \nu < 1/2$ with the form $\nu = n/(2n+1)$ for integer n. This represents only a subset of fractions in the sequence $\nu = n/(2pn+1)$ with integer n and p. At these fillings the composite fermion states will exhibit up to $2p$ vortices at each particle coordinate which suggests that the transformation mapping $\mathcal{L}$ onto Λ should be replaced by $U^{-2p} = \bar{J}^p/J^p$. However, this procedure is not guaranteed to produce a polynomial since the LLL states need not contain a factor of J^p when $p > 1$. It is not known whether the $p > 1$ fractions can be treated within the polynomial state formalism presented here.

- *Transferring the construction to the sphere.* The lack of boundaries and the finite degeneracy of each Landau level are two significant technical simplifications provided by the spherical geometry. It is plausible that the preceding questions may be easier to address in this geometry. This would also allow for a more direct comparison of our procedure for calculating the gap and that used in the majority of numerical studies.

These questions represent significant challenges. However, we believe that our approach has provided new insight into the microscopic underpinnings of the composite fermion picture. The mathematical machinery that our formalism has brought to bear on this many-body problem may well lead to further progress in this direction.

APPENDIX A
Constructing expansions in terms of $\hat{K}$ eigenstates

In section 2.2 it was shown that any homogeneous polynomial $\phi(\mathbf{z},\bar{\mathbf{z}})$ with bidegree $(d_z, d_{\bar{z}})$ and $d_z > d_{\bar{z}}$ can be written in terms of the simultaneous eigenstates of $\hat{K}$, $\hat{A}_0$ and $\hat{L}_z$ as

$$\phi(\mathbf{z},\bar{\mathbf{z}}) = \sum_{k=k_0}^{m} \alpha_k \left|k, m-k\right\rangle = \sum_{i=0}^{d_{\bar{z}}} \alpha_{k_i} \left|k_i, d_{\bar{z}}-i\right\rangle = \sum_{i=0}^{d_{\bar{z}}} \alpha_{k_i} d_{k_i,d_{\bar{z}}-i} \hat{A}_+^{d_{\bar{z}}-i} \left|k_i, 0\right\rangle \tag{A.1}$$

where $m = (d_z + d_{\bar{z}} + N)/2$, $k_0 = (d_z - d_{\bar{z}} + N)/2$ and $k_i = k_0 + i$. It follows from (2.18) and (2.19) that applying $\hat{A}_-^{d_{\bar{z}}-j}$ to the i'th term in the expansion produces

$$\alpha_{k_i} d_{k_i,d_{\bar{z}}-i} \hat{A}_-^{d_{\bar{z}}-j} \hat{A}_+^{d_{\bar{z}}-i} \left|k_i, 0\right\rangle = \alpha_{k_i} \Gamma_{ij} \hat{A}_+^{j-i} \left|k_i, 0\right\rangle \tag{A.2}$$

where $\Gamma_{ij} = 0$ if $i > j$ and otherwise

$$\Gamma_{ij} = \frac{d_{k_i,d_{\bar{z}}-i}\, c_{k_i,d_{\bar{z}}-i}}{c_{k_i,j-i}}. \tag{A.3}$$

It then follows that

$$\hat{A}_-^{d_{\bar{z}}-i} \phi(\mathbf{z},\bar{\mathbf{z}}) = \sum_{j=0}^{i} \alpha_{k_j} \Gamma_{ji} \hat{A}_+^{i-j} \left|k_j, 0\right\rangle \tag{A.4}$$

which is equivalent to

$$\alpha_{k_i} \left|k_i, 0\right\rangle = \frac{1}{\Gamma_{ii}} \left[\hat{A}_-^{d_{\bar{z}}-i} \phi(\mathbf{z},\bar{\mathbf{z}}) - \sum_{j=0}^{i-1} \Gamma_{ij} \hat{A}_+^{j-i} \alpha_{k_j} \left|k_j, 0\right\rangle \right]. \tag{A.5}$$

Given a state $\phi(\mathbf{z},\bar{\mathbf{z}})$ we can, at least in principle, calculate $\hat{A}_-^{d_{\bar{z}}-i}\phi(\mathbf{z},\bar{\mathbf{z}})$ for $i = 0, 1, \ldots, d_{\bar{z}}$ and then obtain the terms in expansion (A.1) recursively using equation (A.5) above.

A simpler set of linear equations for the norms of the $\{\alpha_i\}$ coefficients follows from (A.4) by taking the inner product with $\phi(\mathbf{z},\bar{\mathbf{z}})$ on both sides and using (2.18), (2.19) and (2.22) to obtain

$$\sum_{i=0}^{j} \Lambda_{ij} |\alpha_{k_i}|^2 = \langle \phi(\mathbf{z},\bar{\mathbf{z}}) | \hat{A}_-^{d_{\bar{z}}-j} | \phi(\mathbf{z},\bar{\mathbf{z}}) \rangle \qquad \text{for} \qquad j = 0, 1, 2, \ldots, d_{\bar{z}} \tag{A.6}$$

where

$$\Lambda_{ij} = \frac{2^{j-i}}{(j-i)!} \frac{(m-k_i)!}{2^{m-k_i}} \frac{\Gamma(k_j+m)\Gamma(k_i+m)}{\Gamma(k_i+k_j)\Gamma(2m)}. \tag{A.7}$$

If the matrix elements on the right of (A.6) are known we can solve for the $|\alpha_{k_i}|$'s by inverting the Λ matrix.

APPENDIX B
Additional details of proofs in Chapter 3

B.1 Determining the prefactor in Proposition 3.4.2

To obtain the prefactor in (3.14) we expand $\hat{A}_+^{d_J}$ as

$$\hat{A}_+^{d_J} = \sum_{\substack{n_1,\ldots,n_N=0 \\ \sum_i n_i = d_J}}^{d_J} \binom{d_J}{n_1\ n_2\ n_3\ n_4\ \cdots\ n_N} (z_1\bar{z}_1)^{n_1}(z_2\bar{z}_2)^{n_2}\ldots(z_N\bar{z}_N)^{n_N} \tag{B.1}$$

where

$$\binom{d_J}{n_1\ n_2\ n_3\ n_4\ \cdots\ n_N} \equiv \frac{d_J!}{n_1!\,n_2!\,n_3!\cdots n_N!} \tag{B.2}$$

is the multinomial coefficient. When $\mathcal{A}_{\bar{z}}$ is applied to (B.1) only the terms where all the $\bar{z}_i$'s have distinct powers will survive and $n_1, n_2, \ldots, n_N$ must therefore be some permutation of $\{0, 1, 2, \ldots, N-1\}$. Using

$$\mathcal{A}_{\bar{z}}(\bar{z}_1^0\,\bar{z}_2^1\,\bar{z}_3^2\cdots\bar{z}_N^{N-1}) = (-1)^{d_J}\bar{J} \tag{B.3}$$

we see that

$$\begin{aligned}\mathcal{A}_{\bar{z}}\hat{A}_+^{d_J} &= \binom{d_J}{0\ 1\ 2\ 3\ \cdots\ N-1}\mathcal{A}_{\bar{z}}\left[\sum_{\rho\in S_N}(z_{\rho(1)}\bar{z}_{\rho(1)})^0(z_{\rho(2)}\bar{z}_{\rho(2)})^1\ldots(z_{\rho(N)}\bar{z}_{\rho(N)})^{N-1}\right] \\ &= \frac{1}{N!}\binom{d_J}{0\ 1\ 2\ 3\ \cdots\ N-1}J\bar{J}.\end{aligned} \tag{B.4}$$

■

B.2 Proof of Proposition 3.4.5

Using Proposition 3.4.3 the matrix element on the left may be rewritten as

$$\langle\hat{A}_{r+}^{m_r-k'}\phi_{k'}(\mathbf{z},\bar{\mathbf{z}})|\mathcal{A}_{\bar{z}}|\hat{A}_{r+}^{m_r-k}\phi_k(\mathbf{z},\bar{\mathbf{z}})\rangle = \lambda(d_{\bar{z}})\langle\phi_{k'}(\mathbf{z},\bar{\mathbf{z}})J|\hat{A}_{r+}^{m_r-k'}|\phi_k[\mathbf{z},\partial_{\bar{\mathbf{z}}}]J\rangle. \tag{B.5}$$

We note that $\phi_{k'}(\mathbf{z},\bar{\mathbf{z}})J$ and $\phi_k[\mathbf{z},\partial_{\bar{\mathbf{z}}}]J$ are $\hat{A}_{r0}$ eigenstates with eigenvalues $k' + d_J/2$ and $k - d'_{\bar{z}} + d_J/2$ respectively. Using (2.22) the matrix element of $\hat{A}_{r+}^{m_r-k'}$ above becomes

$$\langle\phi_{k'}(\mathbf{z},\bar{\mathbf{z}})J|\hat{A}_{r+}^{m_r-k'}|\phi_k[\mathbf{z},\partial_{\bar{\mathbf{z}}}]J\rangle = \frac{2^{m_r-k'}\Gamma(2m_r)}{\Gamma(m_r+k')}\langle\phi_{k'}(\mathbf{z},\bar{\mathbf{z}})J|\phi_k[\mathbf{z},\partial_{\bar{\mathbf{z}}}]J\rangle \tag{B.6}$$

where $m_r - k = d_J - d_{\bar{z}}$ and $m_r - k' = d_J - d'_{\bar{z}}$ was used to simplify the arguments of the Γ-functions. We note that $\phi_k[\mathbf{z}, \partial_{\mathbf{z}}]J$ is a bosonic LLL state and so $\phi_{k'}(\mathbf{z}, \bar{\mathbf{z}})J$ may be replaced by its LLL projection $2^{d'_{\bar{z}}}\phi_{k'}[\mathbf{z}, \partial_{\mathbf{z}}]J$ as in (2.37). Combining these steps yield

$$\langle \hat{A}_{r+}^{m_r-k'} \phi_{k'}(\mathbf{z}, \bar{\mathbf{z}}) | \mathcal{A}_{\bar{z}} | \hat{A}_{r+}^{m_r-k} \phi_k(\mathbf{z}, \bar{\mathbf{z}}) \rangle = \lambda(d_{\bar{z}}) \frac{2^{m_r}\Gamma(2m_r)}{\Gamma(m_r + k')} \langle \phi_{k'}[\mathbf{z}, \partial_{\bar{\mathbf{z}}}]J | \phi_k[\mathbf{z}, \partial_{\bar{\mathbf{z}}}]J \rangle. \tag{B.7}$$

Taking the complex conjugate of this equation and exchanging $k \leftrightarrow k'$ and $d_{\bar{z}} \leftrightarrow d'_{\bar{z}}$ produces

$$\langle \hat{A}_{r+}^{m_r-k'} \phi_{k'}(\mathbf{z}, \bar{\mathbf{z}}) | \mathcal{A}_{\bar{z}}^\dagger | \hat{A}_{r+}^{m_r-k} \phi_k(\mathbf{z}, \bar{\mathbf{z}}) \rangle = \lambda(d'_{\bar{z}}) \frac{2^{m_r}\Gamma(2m_r)}{\Gamma(m_r + k)} \langle \phi_{k'}[\mathbf{z}, \partial_{\bar{\mathbf{z}}}]J | \phi_k[\mathbf{z}, \partial_{\bar{\mathbf{z}}}]J \rangle \tag{B.8}$$

which, together with (B.7) leads to the final result. ■

APPENDIX C
Derivation of the effective two-body interaction

The goal of this section is to derive a sensible approximation of the three-body operator

$$\sum_{i\neq j\neq k} \mathbf{E}(\mathbf{r}_i - \mathbf{r}_j)\cdot\mathbf{E}(\mathbf{r}_i - \mathbf{r}_k) = \int \mathrm{d}\mathbf{r}\mathrm{d}\mathbf{r}'\mathrm{d}\mathbf{r}''\hat{\rho}(\mathbf{r})\hat{\rho}(\mathbf{r}')\hat{\rho}(\mathbf{r}'')\mathbf{E}(\mathbf{r}-\mathbf{r}')\cdot\mathbf{E}(\mathbf{r}-\mathbf{r}'') \tag{C.1}$$

is the form of an effective two-body interaction $V^{eff}(r)$. Our main consideration is that this construction must be sufficiently robust to ensure that the form of $V^{eff}(r)$ is insensitive to the details of the approximations that are made. An obvious approach is to reduce the integral expression on the right of (C.1) to a two-body operator by replacing one of the density operators by its expectation value. The standard linear order expansion in fluctuations of the particle density around the average $\rho(\mathbf{r}) \equiv \langle\hat{\rho}(\mathbf{r})\rangle$ then leads to

$$\hat{\rho}(\mathbf{r})\hat{\rho}(\mathbf{r}')\hat{\rho}(\mathbf{r}'') \approx \rho(\mathbf{r})\hat{\rho}(\mathbf{r}')\hat{\rho}(\mathbf{r}'') + \hat{\rho}(\mathbf{r})\rho(\mathbf{r}')\hat{\rho}(\mathbf{r}'') + \hat{\rho}(\mathbf{r})\hat{\rho}(\mathbf{r}')\rho(\mathbf{r}'') - 2\rho(\mathbf{r})\rho(\mathbf{r}')\rho(\mathbf{r}''). \tag{C.2}$$

However, this procedure turns out to be insufficient as it does not take into account the strong correlations present in the low energy states. These correlations will play a crucial role in determining the qualitative form of the effective interaction. To this end we modify the expansion as

$$\begin{aligned}\hat{\rho}(\mathbf{r})\hat{\rho}(\mathbf{r}')\hat{\rho}(\mathbf{r}'') \;\approx\; & \hat{\rho}(\mathbf{r}')\hat{\rho}(\mathbf{r}'')\rho(\mathbf{r})g(\mathbf{r}-\mathbf{r}')g(\mathbf{r}-\mathbf{r}'') \\ & +\hat{\rho}(\mathbf{r})\hat{\rho}(\mathbf{r}'')\rho(\mathbf{r}')g(\mathbf{r}-\mathbf{r}')g(\mathbf{r}''-\mathbf{r}') \\ & +\hat{\rho}(\mathbf{r})\hat{\rho}(\mathbf{r}')\rho(\mathbf{r}'')g(\mathbf{r}-\mathbf{r}'')g(\mathbf{r}'-\mathbf{r}'') \\ & -2\rho(\mathbf{r})\rho(\mathbf{r}')\rho(\mathbf{r}'')g(\mathbf{r}-\mathbf{r}')g(\mathbf{r}-\mathbf{r}'')g(\mathbf{r}'-\mathbf{r}'')\end{aligned} \tag{C.3}$$

where $g(\mathbf{r}-\mathbf{r}')$ is the pair distribution function defined through

$$\langle\hat{\rho}(\mathbf{r})\hat{\rho}(\mathbf{r}')\rangle = \bar{\rho}\delta(\mathbf{r}-\mathbf{r}') + \bar{\rho}^2 g(\mathbf{r}-\mathbf{r}') \tag{C.4}$$

for a *translationally invariant* system with particle density $\bar{\rho}$. The constraint that $i \neq j \neq k$ in the original summation in (C.1) is implicit in the assumption that $\mathbf{r} \neq \mathbf{r}' \neq \mathbf{r}''$ which allows the $\bar{\rho}\delta(\mathbf{r}-\mathbf{r}')$ term to be neglected. For a finite system translational invariance is broken and $\rho(\mathbf{r})$ will not be constant. However, we still expect that the interparticle correlations

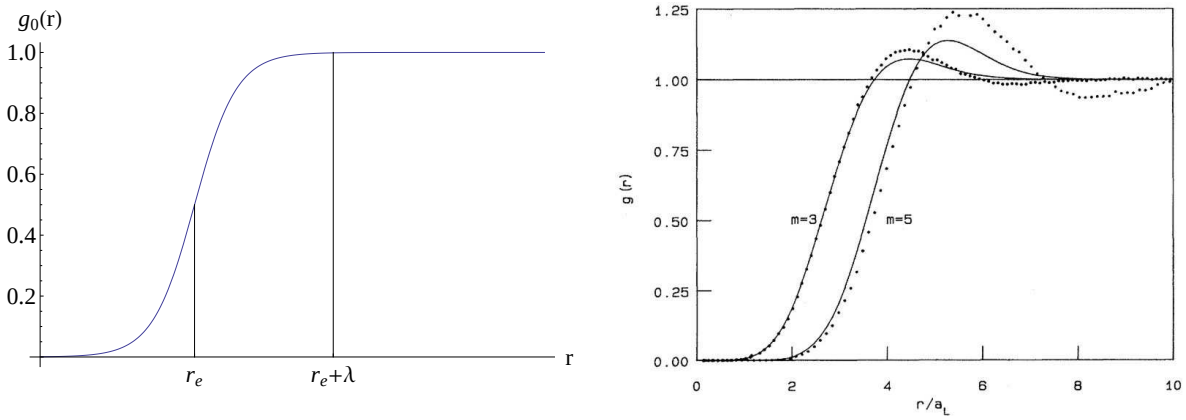

(a) (b)

Figure C.1: (a) The generic form of $g_0(r)$, the approximation to the true pair distribution function $g(r)$. (b) Solid lines correspond to Girvin's analytic approximation [38] for $g(r)$ at $\nu = 1/m$ with $m = 3$ and 5. The dots indicate the Monte-Carlo results of [39]. This figure has been reproduced from [39].

within the bulk will be well approximated by the translationally invariant pair-distribution function defined in the $N \to \infty$ limit. The precise forms of $\rho(\mathbf{r})$ and $g(\mathbf{r}-\mathbf{r}')$ depend on the state under consideration and are, apart from a few special cases, generally unknown. For the purpose of obtaining a qualitative understanding of the effective interaction it is sufficient to replace both $\rho(\mathbf{r})$ and $g(\mathbf{r}-\mathbf{r}')$ by simple approximations which reflect the essential properties of the low energy states. As done in section 2.5.2 we introduce for $\rho(\mathbf{r})$ the approximation $\rho_0(\mathbf{r}) = \bar{\rho}\Theta(r-R)$ with $\bar{\rho} = N/(\pi R^2)$ and $\nu = 2\pi\ell^2\bar{\rho}$. Fermion statistics require that $g(\mathbf{r})$ go to zero at least quadratically in r as $r \to 0$. However, the strong correlations present in the low energy states generally result in $g(r)$ vanishing as a higher power of r. For example, in the case of Laughlin's wave function $\psi(\mathbf{z}) = J^3$ it is clear that $g(r) \sim r^6$ at $r << \ell$. This is reflected by the results of Monte-Carlo calculations which appear in Figure C.1, as well as by Girvin's analytic approximation [38] for $g(r)$. The same generic behaviour is seen in the pair distribution functions obtained in [40] for Jain's composite fermion ground states at the fillings $\nu = n/(2n+1)$ with $n = 1, \ldots, 6$. In general $g(r)$ must satisfy

$$\int \mathrm{d}\mathbf{r}(1-g(r)) = \frac{1}{\bar{\rho}} \tag{C.5}$$

and $r_e = (\pi\bar{\rho})^{-1/2}$ is therefore a measure of the radius of the "excluded area" or correlation hole surrounding each particle[17]. We expect $g(\mathbf{r})$ to increase from zero at $r << r_e$ and saturate to one at $r > r_e + \lambda$ where λ is of the order of a few magnetic lengths. This generic behaviour is

[17] In the literature r_e is also known as the ion disk radius.

illustrated in Figure C.1 (a) and we shall consider a number of different approximations to $g(\mathbf{r})$ which all share this form. However, the resulting effective interaction is found to be largely insensitive to the precise choice of $g_0(\mathbf{r})$.

As a side note we remark that the expansion of $\hat{\rho}(\mathbf{r})\hat{\rho}(\mathbf{r}')\hat{\rho}(\mathbf{r}'')$ in (C.3) is very much in the spirit of the Kirkwood superposition approximation [41] in which the three particle distribution function $g(\mathbf{r},\mathbf{r}',\mathbf{r}'') = \langle\hat{\rho}(\mathbf{r})\hat{\rho}(\mathbf{r}')\hat{\rho}(\mathbf{r}'')\rangle/\bar{\rho}^3$ is approximated by the factorised form $g(\mathbf{r}-\mathbf{r}')g(\mathbf{r}-\mathbf{r}'')g(\mathbf{r}'-\mathbf{r}'')$. Taking the expectation value on both sides of (C.3) indeed produces the Kirkwood approximation when all three points lie within the bulk where it is assumed that the density is constant and that $\langle\hat{\rho}(\mathbf{r})\hat{\rho}(\mathbf{r}')\rangle$ only depends on $|\mathbf{r}-\mathbf{r}'|$. See [42] for a discussion of the shortcomings of the Kirkwood approximation and [43] for an application in the fractional quantum Hall effect. An intuitive understanding of these distribution functions and the approximation involved in (C.3) may be gained from the following two illustrative examples. Figure C.5 compares the exact form of the three particle correlation function to the Kirkwood approximation for the $\psi(\mathbf{z}) = J$ state. In Figure C.6 we show the predictions of the Kirkwood approximation for the $\psi(\mathbf{z}) = J^3$ state where Girvin's analytic approximation for the two particle distribution function was used.

We now return to (C.1) and first insert the expansion in (C.3) and then approximate $g(r)$ by $g_0(r)$ to obtain

$$\sum_{i\neq j\neq k}\mathbf{E}(\mathbf{r}_i-\mathbf{r}_j)\cdot\mathbf{E}(\mathbf{r}_i-\mathbf{r}_k) \approx \bar{\rho}\sum_{i\neq j}V_1^{eff}(\mathbf{r}_i,\mathbf{r}_j) + 2\bar{\rho}\sum_{i\neq j}V_2^{eff}(\mathbf{r}_i,\mathbf{r}_j) + (\text{Constants}) \tag{C.6}$$

where

$$V_1^{eff}(\mathbf{r}_i,\mathbf{r}_j) = \int_{r\leq R}\mathrm{d}\mathbf{r}\, g_0(\mathbf{r}-\mathbf{r}_i)\mathbf{E}(\mathbf{r}-\mathbf{r}_i)\cdot g_0(\mathbf{r}-\mathbf{r}_j)\mathbf{E}(\mathbf{r}-\mathbf{r}_j) \tag{C.7}$$

and

$$V_2^{eff}(\mathbf{r}_i,\mathbf{r}_j) = \mathbf{E}(\mathbf{r}_i-\mathbf{r}_j)\cdot\int_{r\leq R}\mathrm{d}\mathbf{r}\, g_0(\mathbf{r}-\mathbf{r}_i)g_0(\mathbf{r}-\mathbf{r}_j)\mathbf{E}(\mathbf{r}-\mathbf{r}_j). \tag{C.8}$$

These two effective interactions are no longer translationally invariant. However, it will be shown that when summed over i and j the non-invariant contributions to $V_1^{eff}(\mathbf{r}_i,\mathbf{r}_j)$ and $V_2^{eff}(\mathbf{r}_i,\mathbf{r}_j)$ are either constants or may be approximated as such. We only consider the effective interactions within the bulk, i.e. when r_i and r_j are not within $r_e+\lambda$ from the system boundary at $r = R$. In the next two sections we consider $V_1^{eff}(\mathbf{r}_i,\mathbf{r}_j)$ and $V_2^{eff}(\mathbf{r}_i,\mathbf{r}_j)$ separately.

C.1 Simplifying $V_1^{eff}(\mathbf{r}_i, \mathbf{r}_j)$

In a two dimensional electrostatic analogy one may regard $\mathbf{E}(\mathbf{r})$ as the electric field associated with a point charge density $\nabla \cdot \mathbf{E}(\mathbf{r}) = 2\pi\delta(\mathbf{r})$ and logarithmic potential $V(r) = \log(\ell/r)$. Similarly $g(r)\mathbf{E}(\mathbf{r})$ is associated with the modified charge density

$$\rho_g(\mathbf{r}) = \nabla \cdot [g_0(\mathbf{r})\mathbf{E}(\mathbf{r})] = \mathbf{E}(\mathbf{r}) \cdot \nabla g_0(\mathbf{r}) = \frac{1}{r}\frac{\mathrm{d}g_0(r)}{\mathrm{d}r} \tag{C.9}$$

and potential

$$V_g(r) = C - \int_0^r \mathrm{d}r' g_0(r')/r' \tag{C.10}$$

where C is a constant chosen to ensure that $V_g(r) = \log(\ell/r)$ at $r >> r_e + \lambda$. Figures (C.2) (a) and (b) show $V_g(r)$ and $\rho_g(r)$ for typical choices of $g_0(r)$. Note that in both cases the presence of the correlation hole described by $g_0(r)$ has resulted in a regularisation of the functions ($\log(\ell/r)$ and $2\pi\delta(\mathbf{r})$) at the origin. Using integration by parts and the divergence theorem yields

$$V_1^{eff}(\mathbf{r}_i, \mathbf{r}_j) = \int_{r\leq R} \mathrm{d}\mathbf{r}\rho_g(\mathbf{r} - \mathbf{r}_i)V_g(\mathbf{r} - \mathbf{r}_j) - \oint_{r=R} \mathrm{d}\mathbf{a} \cdot [V_g(\mathbf{r} - \mathbf{r}_i)g_0(\mathbf{r} - \mathbf{r}_j)\mathbf{E}(\mathbf{r} - \mathbf{r}_j)]\,. \tag{C.11}$$

Since $\rho_g(\mathbf{r} - \mathbf{r}_i)$ is only non-zero in the region $|\mathbf{r} - \mathbf{r}_i| < r_e + \lambda$ we may extend the integration domain to all of $\mathbb{R}^2$ thereby restoring translational invariance whenever r_i and r_j are in the bulk. The second term only depends on the values of $V_g(\mathbf{r} - \mathbf{r}_j)$ and $\mathbf{E}(\mathbf{r} - \mathbf{r}_i)$ on the boundary where they are slowly varying functions of the particle coordinates $\mathbf{r}_i$ and $\mathbf{r}_j$. We shall approximate this term by its ground state expectation value.

C.2 Simplifying $V_2^{eff}(\mathbf{r}_i, \mathbf{r}_j)$

Introducing the function $\bar{g}_0(\mathbf{r}) \equiv 1 - g_0(\mathbf{r})$ allows $V_2^{eff}(\mathbf{r}_i, \mathbf{r}_j)$ to be written as

$$\begin{aligned} V_2^{eff}(\mathbf{r}_i, \mathbf{r}_j) &= -\mathbf{E}(\mathbf{r}_i - \mathbf{r}_j) \cdot \int_{r\leq R} \mathrm{d}\mathbf{r}\bar{g}_0(\mathbf{r} - \mathbf{r}_i)g_0(\mathbf{r} - \mathbf{r}_j)\mathbf{E}(\mathbf{r} - \mathbf{r}_j) \\ &\quad + \mathbf{E}(\mathbf{r}_i - \mathbf{r}_j) \cdot \int_{r\leq R} \mathrm{d}\mathbf{r} g_0(\mathbf{r} - \mathbf{r}_j)\mathbf{E}(\mathbf{r} - \mathbf{r}_j) \end{aligned} \tag{C.12}$$

where the fact that $\bar{g}_0(\mathbf{r} - \mathbf{r}_i)$ is only non-zero in the region $|\mathbf{r} - \mathbf{r}_i| < r_e + \lambda$ again results in translational invariance being restored. Inside the integral appearing in the second term the factor of $g_0(\mathbf{r} - \mathbf{r}_j)$ may be replaced by one without affecting the result. It then follows from the two dimensional analog of Gauss's law that

$$\int_{r\leq R} \mathrm{d}\mathbf{r}\mathbf{E}(\mathbf{r} - \mathbf{r}_j) = \pi\mathbf{r}_j. \tag{C.13}$$

Since $\sum_{i\neq j}\mathbf{E}(\mathbf{r}_i-\mathbf{r}_j)\cdot\mathbf{r}_j = N(N-1)/2$ the second term (C.12) will reduce to a constant when summed over i and j.

C.3 Combining $V_1^{eff}(\mathbf{r}_i,\mathbf{r}_j)$ and $V_2^{eff}(\mathbf{r}_i,\mathbf{r}_j)$

Taken together these results lead to

$$\ell^2\sum_{i\neq j\neq k}\mathbf{E}(\mathbf{r}_i-\mathbf{r}_j)\cdot\mathbf{E}(\mathbf{r}_i-\mathbf{r}_k)\approx\sum_{i\neq j}V^{eff}(\mathbf{r}_i-\mathbf{r}_j)+(\text{Constants}) \tag{C.14}$$

where $V^{eff}(\mathbf{r}_i-\mathbf{r}_j)$ combines the non-constant translationally invariant components of $V_1^{eff}(\mathbf{r}_i,\mathbf{r}_j)$ and $V_2^{eff}(\mathbf{r}_i,\mathbf{r}_j)$ as

$$V^{eff}(\mathbf{r}_i-\mathbf{r}_j)=\bar\rho\ell^2\int_{\mathbb{R}^2}\mathrm{d}\mathbf{r}\,[\rho_g(\mathbf{r}-\mathbf{r}_i)V_g(\mathbf{r}-\mathbf{r}_j)]-2\bar\rho\ell^2\,\mathbf{E}(\mathbf{r}_i-\mathbf{r}_j)\cdot\int_{\mathbb{R}^2}\mathrm{d}\mathbf{r}\,[\bar g_0(\mathbf{r}-\mathbf{r}_i)g_0(\mathbf{r}-\mathbf{r}_j)\mathbf{E}(\mathbf{r}-\mathbf{r}_j)]\,. \tag{C.15}$$

The first term involves the convolution of $\rho_g(\mathbf{r})$ with the regularised logarithmic potential $V_g(\mathbf{r})$. The result is an interaction which is bounded and approximately constant at short distances. Similarly the second term amounts to a convolution of $\bar g_0(\mathbf{r})$ and the regularised vector field $g_0(\mathbf{r})\mathbf{E}(\mathbf{r})$. This too cannot produce an interaction which is strongly repulsive.

The effective interaction may now be calculated numerically once a choice for the approximation to the distribution function $g(r)$ has been made. We considered the three such approximations:

$$g_0^G(r) = 1-e^{-r^2/2\ell^2}+\left[r^6/(384\ell^6)-r^2/(2\ell^2)\right]e^{-r^2/4\ell^2} \tag{C.16}$$

$$g_0^C(r) = 1-[2r^2/r_e^2-1]e^{-2r^2/r_e^2} \tag{C.17}$$

$$g_0^Q(r) = 1-e^{-r^2/r_e^2} \tag{C.18}$$

The first approximation is Girvin's analytic result [38] for Laughlin's $\nu=1/3$ state. At short distances $g_0^G(r)\sim r^6$ which is a consequence of the wave function exhibiting a third order zero at each particle coordinate. This represents the most strongly correlated state one encounters for filling fractions of the form $\nu=n/(2n+1)$. The second and third approximations to $g_0(x)$ represent weaker correlations and vanish like r^4 (cubically) and r^2 (quadratically) as $r\to 0$. The latter corresponds to the weakest possible correlations allowed by Fermi-statistics. In fact, for $\nu=1$ it is known that $g(r)=1-e^{-r^2/2\ell^2}$ is the exact distribution function for the $\psi(\mathbf{z})=J$

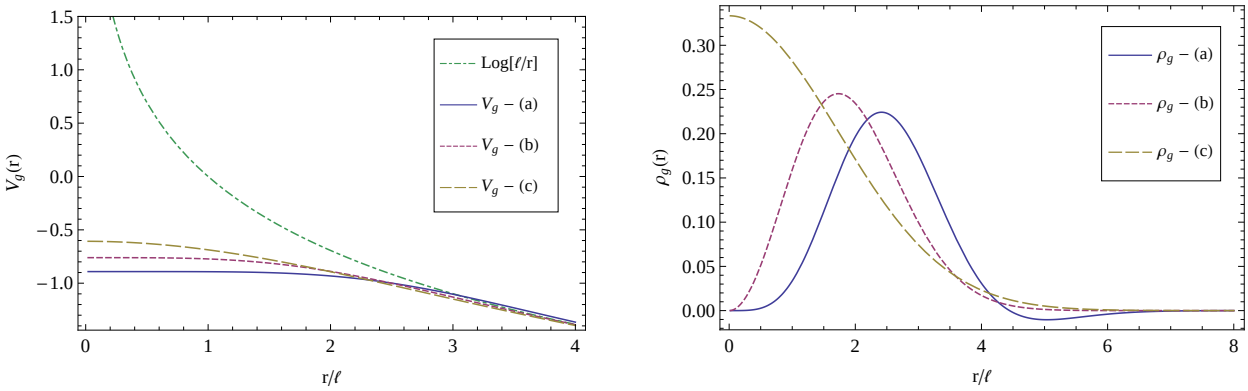

(a) (b)

Figure C.2: (a) The potential $V_g(r)$ for various choices of $g_0(r)$. $V_g(r)$ may be considered as a logarithmic interaction which has been regularised at the origin by the correlations described by $g_0(r)$. Similarly in (b) one may regard $\rho_g(r)$ as a modified point charge density. The curves (a), (b) and (c) correspond to $g_0^G(r)$, $g_0^C(r)$ and $g_0^Q(r)$ respectively. Here $r_e = \sqrt{6}$ was used.

Slater determinant state. The second and third approximations depend on r_e to ensure that $g_0(r)$ obeys (C.5). Figure C.4 shows the result of calculating $V^{eff}(r)$ numerically for different choices of $g_0(r)$. It was found that $V^{eff}(r)$ is virtually independent of the choice of $g_0(r)$ and that it is always a soft, weakly repulsive interaction. The nature of the effective interaction therefore does not depend crucially on the strength of the correlations present in the wave function.

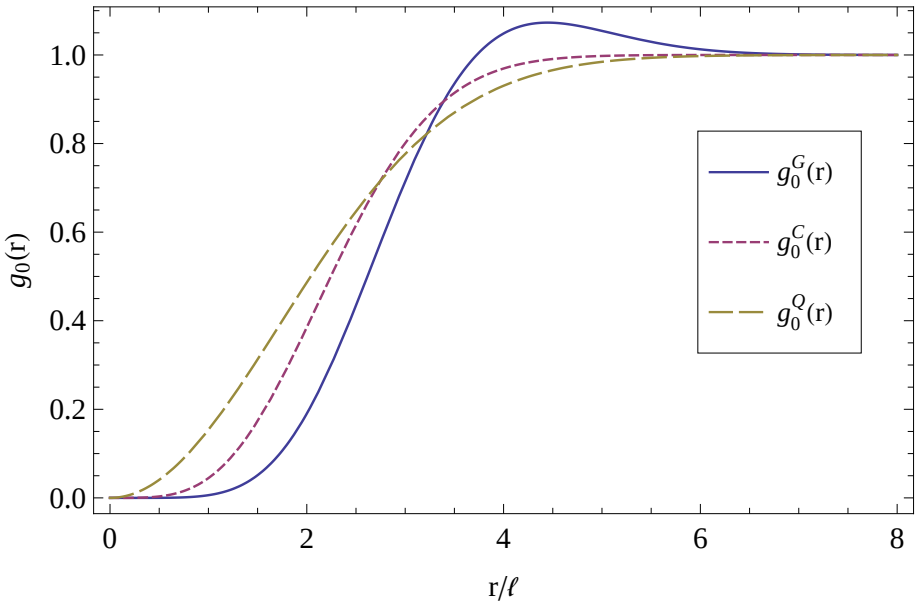

Figure C.3: The various approximations of the two particle distribution function appearing in (C.18). Here $r_e = \sqrt{6}$.

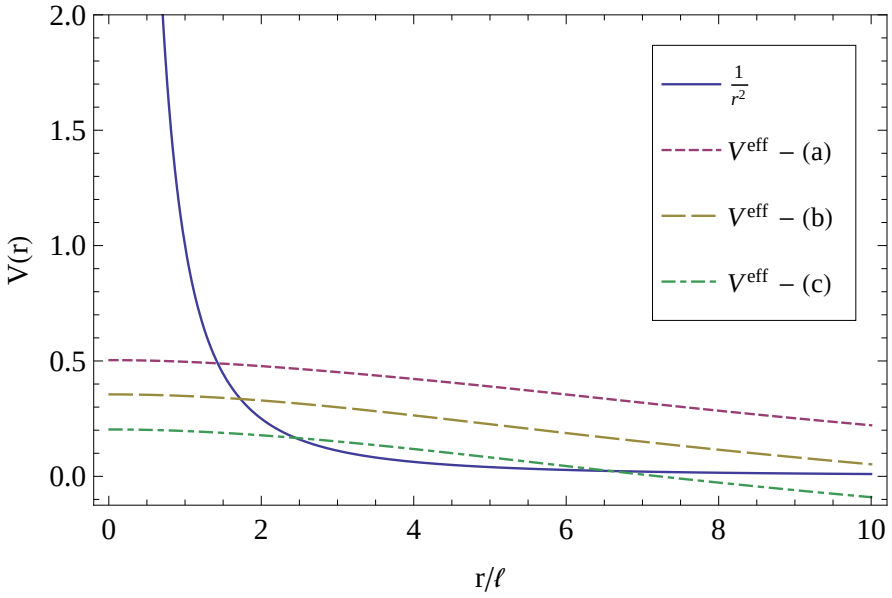

Figure C.4: The effective two-body interactions obtained using different choices of $g_0(r)$. The curves (a), (b) and (c) correspond to $g_0^G(r)$, $g_0^C(r)$ and $g_0^Q(r)$ respectively and have been shifted apart by constants. Here $r_e = \sqrt{6}$.

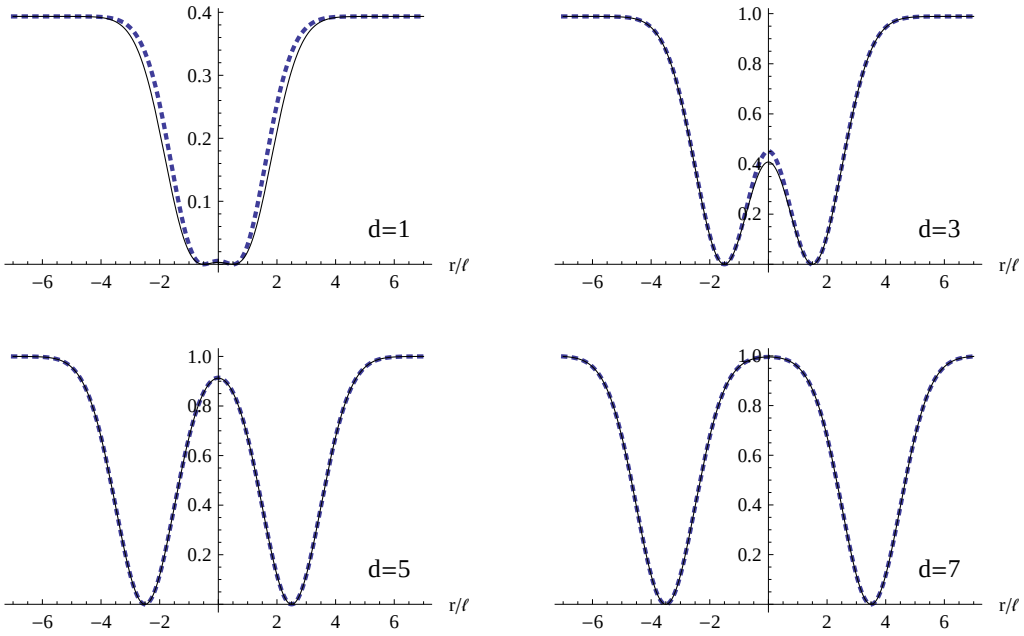

Figure C.5: The three particle distribution function $\langle\hat{\rho}(\mathbf{r}_1)\hat{\rho}(\mathbf{r}_2)\hat{\rho}(\mathbf{r}_3)\rangle$ for the $\nu = 1$ state $\phi(\mathbf{z}) = J$ with $\mathbf{r}_1 = -\mathbf{r}_2 = (d/2, 0)$ and $\mathbf{r}_3 = (r, 0)$. Solids lines represent the exact result while dashed lines correspond to the superposition approximation.

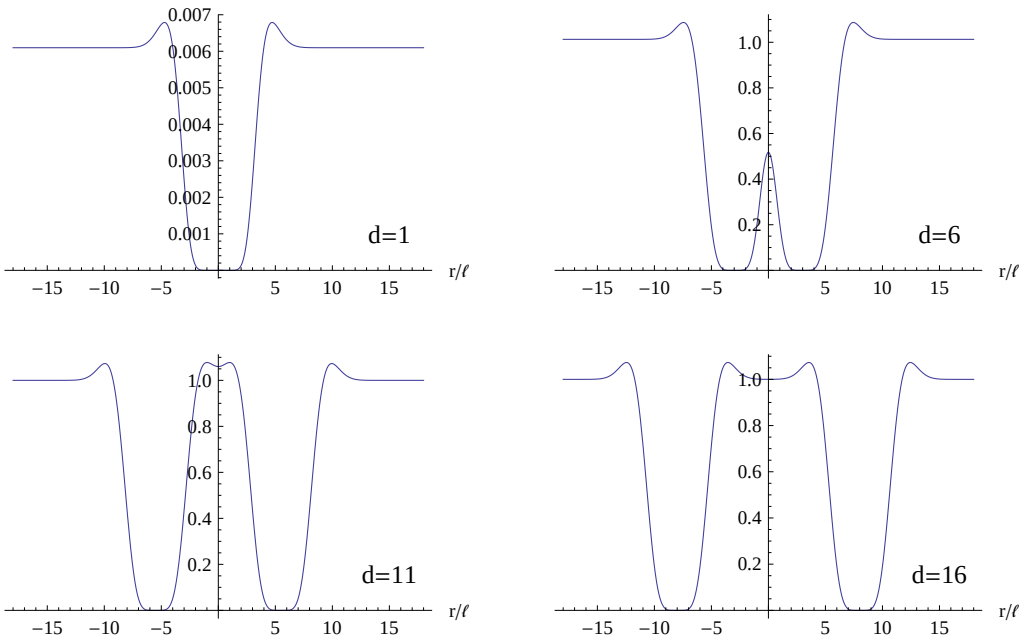

Figure C.6: The three particle distribution function $\langle\hat{\rho}(\mathbf{r}_1)\hat{\rho}(\mathbf{r}_2)\hat{\rho}(\mathbf{r}_3)\rangle$ for the $\nu = 1/3$ state $\phi(\mathbf{z}) = J^3$ using the superposition approximation together with Girvin's analytic approximation (C.18) of $g(r)$. Here $\mathbf{r}_1 = -\mathbf{r}_2 = (d/2, 0)$ and $\mathbf{r}_3 = (r, 0)$.

BIBLIOGRAPHY

[1] E. H. Hall. On a new action of the magnet on electric currents. *American Journal of Mathematics*, 2(3):pp. 287–292, 1879.

[2] P. Fazekas. *Lecture Notes on Electron Correlation and Magnetism*. World Scientific, Singapore, 1999.

[3] K. v. Klitzing, G. Dorda, and M. Pepper. New method for high-accuracy determination of the fine-structure constant based on quantized hall resistance. *Phys. Rev. Lett.*, 45(6):494–497, Aug 1980.

[4] L.D. Landau and E.M. Lifshitz. *Quantum Mechanics*. Addison-Wesley, Reading,Mass, 1965.

[5] H.L. Stormer. Two-dimensional electron correlation in high magnetic fields. *Physica B: Condensed Matter*, 177(1-4):401 – 408, 1992.

[6] D. C. Tsui, H. L. Stormer, and A. C. Gossard. Two-dimensional magnetotransport in the extreme quantum limit. *Phys. Rev. Lett.*, 48(22):1559–1562, May 1982.

[7] A.H. MacDonald. Introduction to the physics of the quantum hall regime. 1994.

[8] S. Girvin. The quantum hall effect: Novel excitations and broken symmetries. In A. Comtet, T. Jolicur, S. Ouvry, and F. David, editors, *Topological aspects of low dimensional systems*, volume 69 of *Les Houches*, pages 53–175. Springer Berlin / Heidelberg, 1999.

[9] B. Douot, B. Duplantier, V. Pasquier, and V. Rivasseau, editors. *The Quantum Hall Effect: Poincar Seminar 2004 (Progress in Mathematical Physics)*. Birkhuser Verlag, Basel, 2005.

[10] D. Yoshioka. *The Quantum Hall Effect (Springer Series in Solid-State Sciences)*. Springer-Verlag, Berlin, 2002.

[11] J.K. Jain. *Composite Fermions*. Cambridge University Press, New York, 2007.

[12] T. Chakraborty and P. Pietiläinen. *The Quantum Hall Effects: Fractional and Integral*. Springer, Berlin, 1995.

[13] J.K. Jain and T. Kawamura. Composite fermions in quantum dots. *Europhys. Lett.*, 29(4):321–326, Feb 1995.

[14] F. D. M. Haldane. Fractional quantization of the hall effect: A hierarchy of incompressible quantum fluid states. *Phys. Rev. Lett.*, 51(7):605–608, Aug 1983.

[15] R. B. Laughlin. Anomalous quantum hall effect: An incompressible quantum fluid with fractionally charged excitations. *Phys. Rev. Lett.*, 50(18):1395–1398, May 1983.

[16] G. Fano, F. Ortolani, and E. Colombo. Configuration-interaction calculations on the fractional quantum hall effect. *Phys. Rev. B*, 34(4):2670–2680, Aug 1986.

[17] J. K. Jain. Composite-fermion approach for the fractional quantum hall effect. *Phys. Rev. Lett.*, 63(2):199–202, Jul 1989.

[18] J. K. Jain. The role of analogy in unraveling the fractional quantum hall effect mystery. *Physica E: Low-dimensional Systems and Nanostructures*, 20(1-2):79 – 88, 2003. Proceedings of the International Symposium "Quantum Hall Effect: Past, Present and Future.

[19] F. Wilczek. Quantum mechanics of fractional-spin particles. *Phys. Rev. Lett.*, 49(14):957–959, Oct 1982.

[20] N. Trivedi and J. K. Jain. Numerical Study of Jastrow-Slater Trial States for the Fractional Quantum Hall Effect. *Modern Physics Letters B*, 5:503–510, 1991.

[21] G. Dev and J. K. Jain. Jastrow-slater trial wave functions for the fractional quantum hall effect: Results for few-particle systems. *Phys. Rev. B*, 45(3):1223–1230, Jan 1992.

[22] J.K. Jain, K. Park, M.R. Peterson, and V.W. Scarola. Composite fermion theory of excitations in the fractional quantum hall effect. *Solid State Communications*, 135(9-10):602 – 609, 2005. Fundamental Optical and Quantum Effects in Condensed Matter.

[23] R. H. Morf, N. d'Ambrumenil, and S. Das Sarma. Excitation gaps in fractional quantum hall states: An exact diagonalization study. *Phys. Rev. B*, 66(7):75408, Aug 2002.

[24] M. Abramowitz and I.A. Stegun. *Handbook of Mathematical Functions*. Dover, New York, fifth edition, 1964.

[25] S. M. Girvin and T. Jach. Formalism for the quantum hall effect: Hilbert space of analytic functions. *Phys. Rev. B*, 29(10):5617–5625, May 1984.

[26] A. Perelomov. *Generalized coherent states and their applications*. Springer-Verlag, Springer, Berlin, 1986.

[27] J. K. Jain. Theory of the fractional quantum hall effect. *Phys. Rev. B*, 41(11):7653–7665, Apr 1990.

[28] J.K. Jain. Microscopic theory of the fractional quantum hall effect. *Advances In Physics*, 41:105–146(42), 1992.

[29] R. Morf and B. I. Halperin. Monte carlo evaluation of trial wave functions for the fractional quantized hall effect: Disk geometry. *Phys. Rev. B*, 33(4):2221–2246, Feb 1986.

[30] O. Ciftja and C. Wexler. Monte carlo simulation method for laughlin-like states in a disk geometry. *Phys. Rev. B*, 67(7):075304, Feb 2003.

[31] I. G. Macdonald. *Symmetric Functions and Hall Polynomials*. Clarendon Press, Oxford, 1979.

[32] B. I. Halperin, P. A. Lee, and N. Read. Theory of the half-filled landau level. *Phys. Rev. B*, 47(12):7312–7343, Mar 1993.

[33] K. Park, N. Meskini, and J. K. Jain. Activation gaps for the fractional quantum hall effect: realistic treatment of transverse thickness. *Journal of Physics: Condensed Matter*, 11(38):7283–7299, 1999.

[34] J. K. Jain and R. K. Kamilla. Quantitative study of large composite-fermion systems. *Phys. Rev. B*, 55(8):R4895–R4898, Feb 1997.

[35] B.I. Halperin. Perspectives in quantum hall effects. In S. das Sarma and A. Pinczuk, editors, *Perspectives in Quantum Hall Effects*, page 225. Wiley, New York, 1996.

[36] V. W. Scarola, S.-Y. Lee, and J. K. Jain. Excitation gaps of incompressible composite fermion states: Approach to the fermi sea. *Phys. Rev. B*, 66(15):155320, Oct 2002.

[37] A. Stern and B. I. Halperin. Singularities in the fermi-liquid description of a partially filled landau level and the energy gaps of fractional quantum hall states. *Phys. Rev. B*, 52(8):5890–5906, Aug 1995.

[38] S. M. Girvin. Anomalous quantum hall effect and two-dimensional classical plasmas: Analytic approximations for correlation functions and ground-state energies. *Phys. Rev. B*, 30(2):558–560, Jul 1984.

[39] D. Levesque, J. J. Weis, and A. H. MacDonald. Crystallization of the incompressible quantum-fluid state of a two-dimensional electron gas in a strong magnetic field. *Phys. Rev. B*, 30(2):1056–1058, Jul 1984.

[40] R. K. Kamilla, J. K. Jain, and S. M. Girvin. Fermi-sea-like correlations in a partially filled landau level. *Phys. Rev. B*, 56(19):12411–12416, Nov 1997.

[41] D.A. McQuarrie. *Statistical Mechanics*. University Science Books, Sausalito, California, 2000.

[42] M. Brownlie and K. A. Benedict. Three-point density correlation functions in the fractional quantum hall regime. *Journal of Physics A: Mathematical and General*, 33(23):4283, 2000.

[43] H. W. Jackson and E. Feenberg. Energy spectrum of elementary excitations in helium ii. *Rev. Mod. Phys.*, 34(4):686–693, Oct 1962.